NTNU
Norwegian University of Science and Technology

Gas Cleaning with Granular Bed Filter

Johnny Ødegård

Master of Science in Energy and Environment

Submission date: August 2009
Supervisor: Johan Einar Hustad, EPT
Co-supervisor: Otto K Sønju, EPT
                        Kavitha Pathmanathan, EPT
                        Kjell Myrland, Technical support

Norwegian University of Science and Technology
Department of Energy and Process Engineering

Problem Description

The Panel Bed Filter (PBF) is currently under development at NTNU. The primary objective of this thesis is to investigate the performance of two Panel Bed Filter rigs. The first one was an earlier tested rig that was re-built for testing on a new area of application. The second was a new rig, built to test a novel louver design.

Assignment given: 04. February 2009
Supervisor: Johan Einar Hustad, EPT

Norwegian University
of Science and Technology
NTNU

Department of Energy
and Process Engineering

EPT-M-2009-80

MASTER THESIS

for

Stud.techn. Johnny Ødegård

Spring 2009

Gas Cleaning with Granular Bed Filter

Gassrensing med granulært filter

Background and objective.

Panel Bed Filter (PBF) is a new alternative for industrial gas cleaning. PBF is a filter consisting of a fixed granular bed. The filter uses sand and other granular materials as a filtration medium. The unbound granular material in the PBF is held together in place by louvers. The louvers are stacked on top of each other into narrow "panels" that creates a vertical wall of granular beds. Several louver designs has been designed and tested. The PBF was patented by Professor A. M. Squires in the United States and has been further developed in Norway at NTNU. One of the most important properties of the PBF is the filter's ability to withstand high temperatures and unburned hot particles. The filter has high filtration efficiency and low pressure drop. The PBF has also the ability to filter particles at high filtration velocity which can reduce the filter size and production cost. The PBF has been demonstrated to perform well in full-scale plants to clean the exhaust gas from biomass combustion. The objective of the present work is to investigate the performance of the PBF at high temperature for a new area of application and to investigate the performance of a novel louvre design.

The following tasks should be considered in the project work:

1. Literature study on filtration theory and currently available gas cleaning technology with an emphasis on cake filtration at high temperature.
2. The candidate shall participate in the investigation of the small scale PBF prototype to clean the exhaust gas from an oil sand extraction pilot plant at high temperature as follows:
   a) Preparation of test rig including testing of the heating elements and the measured temperature distribution.
   b) Calibration of the puff-back system
   c) Modification/upgrading of the existing LabVIEW program.
   d) Start-up and testing of the complete testrig.
   e) The candidate will in the thesis describe the test rig and analyze the obtained data.
3. The candidate shall participate in the investigation of a novel louvre design as follows:
   a) Building of the complete test rig.
   b) Upstart and calibration.
   c) Puff-back and filtration experiments.
   d) Analysis of data.

4. A commercial scale testing shall be conducted at Bjertnæs Sag A/S where the main goal is to clean the exhaust gas from the biomass combustion process (as time allows).
   a) Installation of new equipment and initial testing
   b) Analysis and presentation of results.

Within 14 days of receiving the written text on the diploma thesis, the candidate shall submit a research plan for his project to the department.

When the thesis is evaluated, emphasis is put on processing of the results, and that they are presented in tabular and/or graphic form in a clear manner, and that they are analyzed carefully.

The thesis should be formulated as a research report with summary both in English and Norwegian, conclusion, literature references, table of contents etc. During the preparation of the text, the candidate should make an effort to complete a well presented report. In order to ease the evaluation of the thesis, it is important that the cross references are correct. In the making of the report, strong emphasis should b e placed on both a thorough discussion of the results and an orderly presentation.

The candidate is requested to initiate and keep close contact with his/her specialist teacher and academic supervisor(s) throughout the working period. The candidate must follow the rules and regulations of NTNU as well as passive directions given by the Department of Energy and Process Engineering.

Pursuant to "Regulations concerning the supplementary provisions to the technology study program/Master of Science" at NTNU §20, the Department reserves the permission to utilize all the results for teaching and research purposes as well as in future publications.
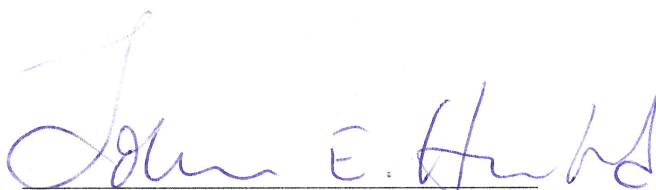
One – 1 complete original of the thesis shall be submitted to the authority that handed out the set subject. (A short summary including the author's name and the title of the thesis should also be submitted, for use as reference in journals (max. 1 page with double spacing)).
Two – 2 – copies of the thesis shall be submitted to the Department. Upon request, additional copies shall be submitted directly to research advisors/companies. A CD-ROM (Word format or corresponding) containing the thesis, and including the short summary, must also be submitted to the Department of Energy and Process Engineering

Department of Energy and Process Engineering, 12. January 2009

_____   _____
Professor Lars Sætran   Johan E. Hustad
Deputy Department Manager   Academic Supervisor

Research Advisors: Professor Otto K. Sønju
                      PhD student Kavitha Pathmanathan
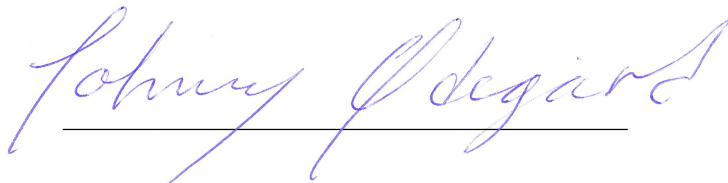   Kjell Myrland

Preface

This master thesis is written and performed at the Norwegian University of Science and Technology at the faculty of Engineering Science and Technology, department of Energy and Process Engineering.

I would like to thank my supervisors Johan E. Hustad, Otto K. Sønju and Kavitha Pathmanathan for their guidance and support through this master thesis.

I would also like to thank the laboratory assistants who have worked so hard to help me get the laboratory work done in a good way.

Trondheim, August 3, 2009

Johnny Ødegård
Student, NTNU

Sammendrag

Den første delen omhandler litteraturstudiet og den andre delen omhandler den eksperimentelle delen. Litteraturstudiet gir en oversikt over filtreringsmekanismer og tilgjengelige gassrensingsteknologier med hovedvekt på varm gass og kakefiltrering. Den eksperimentelle delen beskriver oppsettet og testingen av "filter tray" riggen og L10-56 riggen.

"Filter tray" riggen ble bygget, instrumenteringen tilpasset og programmeringen utført. Puffkalibrering og varmetester ble også utført. Puffkalibreringen viste at denne riggen krevde en betydelig lavere Δp_{min} enn tidligere testede rigger. Varmetestene viste at riggen kunne holde en stabil temperatur på 120 °C. Filtreringstester ble utført med ulike støvkonsentrasjoner (1 og 3 g/m^3) og filtreringshastigheter (10 - 20 cm/s). Resultatene viste at riggen fungerte i samråd med designkriteriene, med en filtreringseffektivitet over 99,5%.

En tidligere brukt L10-56 rigg ble montert på delstrøm fra avløpsgassen til en pilotrigg for oljesandutvinning. En horisontalfiltermediumsrigg (HBU) ble også laget for å finne ut hvilken innvirkning avløpsgassen hadde på filtermediet. Når L10-56 test riggen var ferdig ble det gjennomført puffkalibrering og varmetester ved 350 °C. Resultatene var i samsvarer med tidligere tester gjort på denne riggen. Riggen var klar til å starte filtreringstester, men dette arbeidet ble ikke startet på grunn av tidsbegrensninger og forsinkelser ved pilotriggen for oljesandutvinning.

Sammendrag

Abstract

A literature study is first presented then the practical experiments are described. The literature study provides an overview of filtration mechanisms and available gas cleaning technologies, with an emphasis on hot gas and cake filtration. The experimental chapters describe the setup and testing of the filter tray test rig and the L10-56 test rig.

The filter tray test rig was built, instrumentation was installed and programming performed. Puff-back calibration and heating tests were performed. The puff-back calibration showed that a significantly lower Δp_{min} was obtained with this design compared to previous designs. Filtration tests were conducted at an elevated temperature (120 °C) with different dust concentrations (1 and 3 g/m^3) and filtration velocities (10 - 20 cm/s). The results showed that the rig was working in accordance with the design criteria, with a filtration efficiency above 99,5%.

A previously used filter test rig, the L10-56 test rig, was installed at the slipstream of the exhaust of a oil sand extraction pilot plant at 350 °C. A horizontal bed unit (HBU) was also developed to investigate the impacts of the exhaust gas on the granular filter media. Once completed, the rig was re-tested and the puff-back calibration and heating tests that were performed achieved results corresponding with the previous testis performed on this test rig. The test rig was ready to start filtration tests but they were not initiated due to time limitations and unpredicted halt of the oil sand extraction pilot plant.

Abstract

Contents

CONTENTS

Nomenclature

List of abbreviations

N/A	Not applicable
BAT	Best Available Technique
DAQmx	National Instruments acquisitions system
EEA	European Economic Area
EU	European Union
FieldPoint	National Instruments acquisitions system
HBU	Horizontal Bed Unit
ITPC	International Pollution Control
L10-56	A louver design
NTNU	Norwegian University of Science and Technology
PBF	Panel Ped Filter
PID	Proportional Integral Derivative
SFT	Norwegian Pollution Control Authority

List of symbols

$\%O_2$	Recalculated to a % content of O_2	
Δp	Pressure difference	[Pa]
Δp_{cake}	Pressure difference over the filter cake	[Pa]
Δp_{media}	Pressure difference over the filter media	[Pa]
Δp_{min}	Minimum pressure difference to create spill	[Pa]
Δp_{peak}	Maximum pressure difference during puff-back	[Pa]
η	Dynamic viscosity	$[kg/ms]$
ρ_G	Granular media density	$[g/m^3]$

$A_\%$	Max allowable regulator output	[%]
A_F	Filter area	$[m^2]$
d_G	Nominal diameter of granular media	[m]
I_p	Specific impulse	
k^*	Permeability	$[m^2]$
L_f	Filter thickness	[m]
R_Ω	Electrical resistance	$[\Omega]$
t'	Max allowable regulator output per cycle time	[s]
T_0	Initial temperature	[°C]
t_1	Time when Δp increases above Δp_{min}	[ms]
t_2	Time when Δp decreases below Δp_{min}	[ms]
t_a	Time between t_1 and t_2	$[ms]$
t_C	Time cycle	[s]
T_{set}	Temperature set point	[°C]
U_0	Velocity	[m/s]
U_Ω	Voltage	[V]
N	Number of layers of granular material	[-]
P	Effect	[W]
Ramp	Allowable increase of temperature per hour	
Spill	The spill of granuar media	
T	Temperature	[°C]
t	Time	[s]

List of Figures

List of Tables

Chapter 1

Introduction

This chapter is a brief introduction of the thesis. It describes the background, the objectives, the structure and limitations of the thesis.

1.1   Background

Growing concern for pollution and other environmental impacts are reasons for stricter emission regulations. This creates a constant demand for improving gas cleaning technologies.

The Panel Bed Filter (PBF) is a new alternative, concerning hot gas particle filtration in the industry. The filter utilizes sand, or other granular materials held together by louvers, creating a filter bed [9].

Professor A. M. Squires [21] was the first to patent the PBF filter, and it is presently further developed at NTNU. The filter has performed well in full-scale testing on the exhaust gas from biomass combustion.

The objective of the current studies of the filter is to investigate high temperature filtration for new applications, and testing of the novel filter design.

1.2   Objectives

The primary objective of this thesis is to investigate high temperature filtration for new applications, and to test the novel filter design. The main objectives for this thesis are listed below:

- Literature study on filtration theory and currently available gas cleaning technology with an emphasis on cake filtration at high temperature.

- Participation in the investigation of the small scale PBF prototype to clean the exhaust gas from oil sand extraction pilot plant at high temperature as follows:

    - Preparation of test rig including testing of the heating elements and the measured temperature distribution.
    - Calibration of the puff-back system.

- – Modification/upgrading of the existing LabView program.
- – Start-up and testing of the complete test rig.
- – Describe the test rig and analyze the obtained data.

- • Participation in the investigation of a novel louver design as follows:

  - – Building of the complete test rig.
  - – Upstart and calibration.
  - – Puff-back and filtration experiments.
  - – Analysis of data.

- • A commercial scale testing rig shall be conducted at Bjertnæs Sag A/S where the main goal is to clean the exhaust gas from the biomass combustion process (as time allows):

  - – Installation of new equipment and initial testing.
  - – Analysis and presentation of results.

All but one of the objectives are of an experimental nature, which means a considerable number of hours spent in the laboratory. The time and effort put into laboratory experiments have resulted in a large amount of experimental test data and knowledge.

1.3   Structure and limitations

The small scale PBF prototype test rig will, due to the name of the louver design, be identified as the L10-56 test rig, while the novel louver design, called the filter tray design, will be identified as the filter tray test rig in this thesis.

Chapter 2 presents the literature study performed on filtration theory and available gas cleaning technology with an emphasis on cake filtration at high temperature.

Chapter 3 describes the LabView programs and the modifications of them along with how the rigs are constructed and how the tests on the rigs are performed.

Chapter 4 presents and discusses the results for each of the two filters from the tests described in chapter 3.

Chapter 5 presents the conclusion.

Chapter 6 suggests further work.

Bjertnæs Sag A/S was unable to perform any tests with the full scale rig within the defined time plan. Secondly it was not possible to perform filtration tests with the small scale PBF prototype rig, identified as the L10-56 test rig. This was due to the unpredicted halt in the oil sand extraction pilot plant and other limitations. Thus no results or discussions regarding these tests have been included.

Chapter 2

Filtration theory and gas cleaning technologies

Chapter two presents a literature study concerning filtration theory and gas cleaning technologies with an emphasis on cake filtration and high temperature. Within filtration theory for instance attraction forces, collection mechanisms and influence of velocity and temperature are described. The high temperature cake filters studied are bag filters, candle filters and panel bed filters.

2.1   Forces between particles

Two of the most important descriptions of interaction forces are adhesion and autohesion. Adhesion is defined as the ability of two dissimilar particles to cling together while autohesion is for similar particles. Adhesion and autohesion is caused by Van der Waals Columb and Capillary forces [8]. Van der Waals attraction forces acts where the distance between the particles is short (not longer than a few molecular diameters). The attraction force depends on particle dimensions and contact area. The van der Waals force has a relation to dipole charge in the particles where one of the poles in a particle is attracted to the opposite pole of another particle [2]. Coulomb forces are created by pre-charged particles coming in contact with each other. The amount of charge, size and material of the particles, and contact time are the most important characteristics [8]. Capillary forces arise when liquid matter is present. The surface tension of the liquid is holding the two bodies together. For smaller particles the capillary forces arise when the relative humidity rises above 65%. The capillary force increases with the surface tension of the liquid, size of the particle and the wetability of the liquid. It is not dependent on the amount of liquid present as long as a full bridge is formed between the surfaces of the particles [2].

There are many factors which might affect the adhesion forces. In addition to particle size, contact area and the gap between the particles, the surface of the particles and the particle shape amongst others influence the adhesion [8].
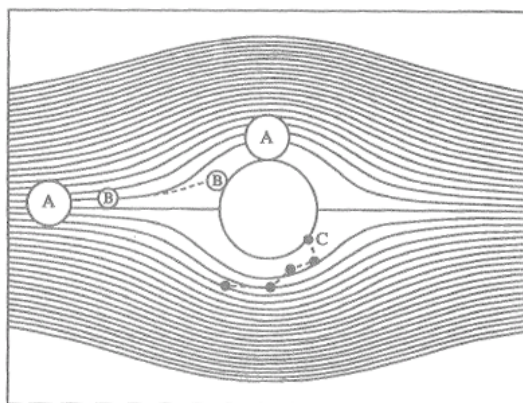
Figure 2.1: Particle capture mechanisms: A, particle capture by interception; B, particle capture by inertial impaction; C, particle capture by diffusion deposition [2].

2.2 Filtration mechanisms

The term filtration is based on a capture of substance from a gas or a fluid. The substance is removed from the gas by adding forces or obstructions, forcing the particles to settle. There are several filtration principles used today. Only the obstruction principle where filter cake formation can occur, is described in this work. Several mechanisms are contributing to the settlement of particles on the media. To describe filtration mechanisms the single fiber theory, where the filtration mechanisms are investigated around a single fiber, is used [2] [9] [8].

2.2.1 Direct interception

By direct interception the particles are captured because they come into contact with the filtration material while following the gas flow. As shown in figure 2.1 particle A is following the stream line and is captured. The direct interception is an ideal mechanism applying to particles which totally follow the stream lines of the flow. Therefore the most important characteristics in this mechanism are the projected areas of the particle and filter media. Larger particles come in contact with each other at a greater distance then smaller particles and thereby enhance interception between larger particles. Larger particles are therefore more influenced by direct interception and will be collected by this at greater areas then small particles [2].

2.2.2 Inertial impaction

When the flow turns and flow around an obstacle the particle continue straight ahead and end up impacting the obstacle. This phenomenon is called inertial impaction. When the flow is exposed to changes it results in multi dimensional acceleration of the flow. Usually particles have a resistance to follow the accelerations or inertia which give the particle another direction or speed than the flow itself. When the inertia is zero the particle follow the flow perfectly. If the inertia is infinite the
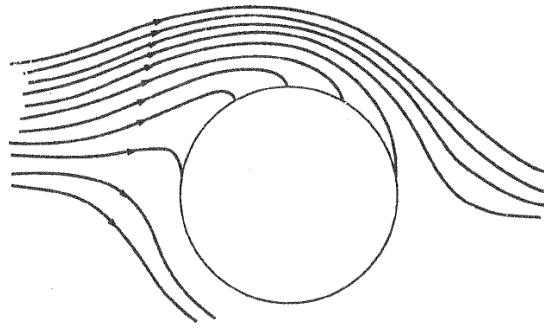
Figure 2.2: Gravitational settlement in horizontal flow [2].

particles do not respond to the changing flow at all. In filter technology this is a good characteristic because the filter material is obstructing the flow and it is forced to accelerate. The particles that resist this acceleration will continue straight and hit the obstacle of the flow and end up captured by the filter media. This phenomena is shown in figure 2.1 as particle B [2].

2.2.3 Brownian diffusion

Particle C in figure 2.1 shows a typical Brownian motion, or Brownian diffusion, which looks like a random movement of particles. The diffusion is a complex motion which is not emphasized in this work. Smaller particles are more affected by the Brownian diffusion then the large particles. Temperature also increases the Brownian diffusion, moving more and larger particles. All the particles in contact, or in near proximity to the filtration media will be captured, due to the adhesion and autohesion forces [2].

2.2.4 Gravity

The gravitational force is working perpendicular at a horizontal flow, and thereby influences the particle trajectory. The new trajectory of the particles in a horizontal flow is highly dependent on the mass of the particle. Figure 2.2 shows how the gravitational force influence a particle. The particles are most influenced at low velocities [2].

2.2.5 Electrostatic forces

Electrostatic forces can enhance the filtration efficiency. Filter media such as fabric filters can be electrically charged to enhance performance. Charged particles will then have an extra force attracting them towards the filter media [2].

2.2.6 Bouncing and re-entrainment

In constant flow, adhesion forces are usually strong enough to hold on to a particle if the particle initially was captured. However there are circumstances where particles do not stay attached to the filter media. Bouncing and re-entrainment are two

conditions where the adhesion forces between the particle and the filter media are overcome by other forces [2].

Bouncing is often observed after inertial impaction. This is because the velocity of the particle, and therefore the kinetic energy, is higher than in other conditions. For direct interception on the other hand, the flow velocity and therefore the particle velocity is low at proximity to the filter media where the direct interception occurs. This results small chances for bouncing of the particle [2].

Re-entrainment of a particle means that the particle leaves the filter media after it has settled. In a steady flow this is not likely to happen, but if the flow alters or other particles or larger clusters of particles are hitting already deposited particles re-entrainment can occur. If this happens the particles receive enough energy from the altering flow or transfer energy from other particles to annul the adhesion forces and the deposited particle is able to re-enter the flow [2].

2.2.7 Formation of filter cake

The forces and mechanisms mentioned earlier in this chapter create filtration by capturing free particles in a flow and deposit them on a filter media. The media itself usually have a good ability to capture particles. Particles from the gas are captured in the pores of the filter media, which creates smaller openings for penetration and even better filtration efficiency. After a while the particles start gathering on the top of the filter and a filter cake is formed. Figure 2.3 shows the formation of a filter cake step by step. With the increase of the filter cake thickness the pressure difference over the filter also increases. The pressure difference contributes to the forces causing re-entrainment. When these forces are sufficiently strong particles will re-enter the flow, often in larger lumps creating a hole in the filter cake. Such holes are called pinholes and are often hard to close when first opened [9].

2.2.8 Penetration

During particle filtration there will always be some particles that penetrate the filter. However, the filters can be optimized to create as little penetration as possible, and thereby increase the filtration efficiency, if the mechanisms of the penetration are known.

Straight through penetration is present when particles are able to penetrate freely, without even getting attached to the filter media. This type of penetration happens mostly when the filter is clean and the porous in the filter is still not filled with particles. Figure 2.4 shows a decrease of this type of penetration as the deposited filter cake gets thicker. The increase in straight through penetration later on is because of the creation of pinholes [9].

Seepage or bleeding penetration includes all the particles which at one point are deposited in the filter but somehow manages to escape from the filter. Both bouncing and re-entrainment mechanisms are present. It is called a bleeding penetration because there are bleeding particles from the filter evenly during the filtration. The seepage penetration is most present when the straight through penetration is low. This mechanism is most important in filters where the adhesion forces are weak [9].
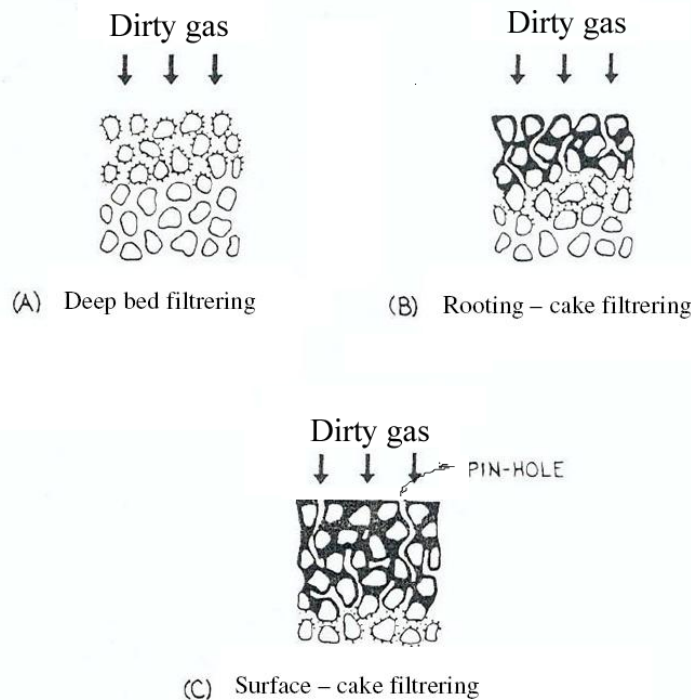
Figure 2.3: Filter cake phases [9].

Pinhole plug penetration occurs when the force of the pressure difference over the filter overcome adhesion forces at weak points of the filter cake. The pinhole plug penetration itself is described as a plug of particles penetrating the filter cake. This creates small holes in the filter cake, shown in figure 2.3, allowing straight through penetration. Because it is so hard to fill the pin holes the straight through penetration can go on for a long time after the pinhole plug has penetrated the filter. As seen in figure 2.4 the pinhole plug penetration is the most important penetration mechanism when the filter cake reaches about 10 micrometer in thickness [9].

Minimizing penetration is highly important in order to maximize filtration efficiency. By looking at figure 2.4 it is clear that the importance of the different mechanisms change over time. When a clean filter is used the straight through penetration is high. To minimize the straight through penetration at the start of each filtration cycle the filter should never be totally clean. This would prevent large amounts of straight through penetration. When the pinhole plug penetration becomes a big problem the filtration cycle should be finished and the filter cleaned. Using materials with higher adhesion forces better the ability to collect and hold on to the particles. This would also help increase the filtration efficiency [9].

2.3   Effects on the filter

Velocity and temperature are both important parameters affecting filtration in general. In this section some of these effects are described.
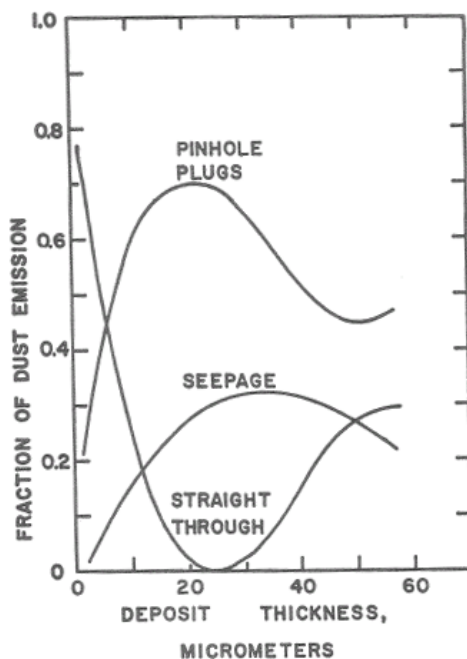
Figure 2.4: Penetration mechanisms [9].

2.3.1 Velocity effect on the filter cake

The filtration velocity influences the filter cake creation by altering the force each particle has when reaching the filter. During deep bed penetration, higher velocities create deeper penetration and deeper roots. Deeper penetration complicates the regeneration of the filter [9]. During surface filtration and cake filtration, higher velocities pack the particles closer and harder together at the filter, creating a denser filter cake than at lower velocities. Regeneration of filters operating at a high filtration velocity is therefore overall more complicated. Higher velocity also tends to create pinhole penetration more frequently than at low velocity. However, the filtration efficiency increases with a dense filter cake and thereby at high velocity [19]. Low velocities such as $0,01m/s$ to $0,06m/s$ is used because of the regeneration issues. The loose and porous filter cake is easier to clean [12].

The filtration area required is highly dependent of the filtration velocity. Higher velocities require less filtration area and thereby a smaller plant. Smaller plants tend to be less expensive and space consuming [12].

Brownian diffusion mechanisms are most important at low velocity and at low particle size [8]. During filtration of smaller particles such as FeSi fumes, decreasing the filtration velocity will also increase the filtration efficiency due to Brownian diffusion [19].

2.3.2 Temperature effect on the filter cake

A study of the temperature influence on particle separation by W. Peukert and F. Löffler [15] shows that temperature influences many aspects of filtration mechanisms.

Fuel	Plant size (MW)	Limits (mg/Nm^3)
Solid	>500	50
	<500	100
Liquid	All	50
Gaseous	All	5 as a rule
		10 for blast furnace gas
		50 for gases produced by the
		steel industry which can be used elsewhere

Table 2.1: Particle emission limits in EU [13].

With increasing temperatures the Brownian motion increases, this influence the smaller particles, up to about $0,5\mu m$. The increasing movement of these particles increases the possibility of the particles to come into contact with the filter media thus they are captured. Larger particles, mainly captured by inertial impaction, are more influenced by the drag forces, therefore the filtration efficiency for larger particles decreases with increasing temperature. Particle adhesion forces are improving with increasing temperatures, thus the filter media have greater forces to capture and hold the particles preventing penetration. This means that penetration of larger particles increase at a higher rate than the smaller particles [15].

2.4 Emission limits in the European Union (EU) and Norway

Pollution from large combustion plants are regulated by the government in a given country. Pollution law and regulations varies from region to region. In this section the regulation rules for the EU and for Norway are presented.

2.4.1 European Union (EU)

Particle emission limits in the EU are regulated by the large combustion plants directive [13]. Emission limits for dust, in particular, are given in table 2.1. For new plants authorized after 27 November 2002 stricter regulation apply. Except of gas turbines the new regulations are given in table 2.2. For larger plants using solid or liquid fuels, this require a decrease in emissions from 50 or 100 mg/Nm^3 to 30 mg/Nm^3 [13].

2.4.2 Norway

Norway is a part of the European Economic Area (EEA) which meanes that the directive regulating particle pollution in the EU also applies for plants in Norway. This means that Norwegian regulations must fullfill the EU regulations; however Norwegian regulations can be stricter. The recommended regulations in Norway are stated in the 1995 directive: *Guidelines for environmental inspectors* [1], produced

Fuel	Plant size (MW)	Limits (mg/Nm^3)
Solid ($6\%O_2$)	50 to 100	50
	>100	30
Liquid ($3\%O_2$)	50 to 100	50
	>100	30
Gaseous ($3\%O_2$)	All	5 as a rule
		10 for blast furnace gas
		30 for gases produced by the
		steel industry which can be used elsewhere

Table 2.2: Emission limits for new combustion plants [13].

Fuel	Plant size (MW)	Limits (mg/Nm^3) dry, $3\%O_2$
Gas	<8	-
	$8-50$	5^1
Oil	<5	100^2
	$5-50$	50
Coal (1% S)	<0,5	150 (dry, $7\%O_2$)
	$0,5-10$	150 (dry, $7\%O_2$)
	$10-50$	50 (dry, $7\%O_2$)
Biomass	$0,02-0,5$	200
	$0,5-4$	150
	$4-15$	100
	$15-50$	50

1) $10 mg/Nm^3$ for plants with blast furnace gas emissions
   $50 mg/Nm^3$ for gas from the steel industry if it is used for useful purposes
2) $30 mg/Nm^3$ is recommended for lighter oils

Table 2.3: Recommended particle emission limits in Norway [1].

by the Norwegian pollution control authority (SFT), see table 2.3, and *The regulation to limit emissions in Norway* [5].

Every new application sent to SFT is individually considered according to different criteria. The local authority handles the air quality issue for the given location, according to Norwegian regulations. SFT and the county governor (fylkesmannen) have the responsibility to evaluate the application according to other regulations such as the EU directives and other national and international regulations. For large plants above 50 MW special regulations such as the Best Available Technique (BAT) requirements, which is regulated by the International Pollution Control (ITPC) directives, applies.

2.5 Important filtration parameters

This section will present parameters affecting hot gas cake filtration. These parameters will be used to describe three types of hot gas cake filters in section 2.6, 2.7 and 2.8.

2.5.1 Materials and construction

The handbook of filter media [17] state a definition of filter media:

> A filter medium is any material that, under operating conditions of the filter, is permeable to one or more components of a mixture, solution or suspension, and is impermeable to the remaining components.

Everything that removes a component from a flow deliberately can be considered as a filter media. There are therefore a wide range of materials and constructions of materials which are considered as filter medias. The shape, construction and distribution of the filter are just as important as the material itself. The materials can be woven systematically or unorganized, molded with pores, membrane shaped or created by loose granular materials among others. There are several advantages and disadvantages for each construction which make it difficult to choose the right type for a specific filtration process.

The most commonly used filter materials are the fabric materials. Fabric filters are made up by fabrics described as soft and flexible and they can be woven or non-woven. The woven ones are most commonly used in the industry and are made from natural or artificial fibers which are spun into threads. These threads are then woven or knitted to a cloth or bag.

Ceramic and metal materials are also used as a filter media because of the good temperature resistance and strength. These materials can be spun into threads and woven as the fabric filters, or they can be sintered and molded creating a rigid, porous material. Metal, ceramic, sand and other materials which can be created as spheres can also be used in a bed creating a filter with loose granular media.

A filter's material and construction gives is it certain characteristics. This information is used to choose the right material and composition for a given filtration situation [16].

2.5.2 Particle deposition

Particles settle differently on different media and are influenced by pore size, shape of the filters and the particles to be filtered. Four different mechanisms of particle deposition are described. More than one can occur in a single filtration media [16]. Surface straining occurs when the particle deposited is too large to penetrate into the material and is settling on the top of the filter. These particles have a tendency to block pores hindering smaller particles to penetrate the top layer of the filter. This can be the start of a filter cake formation. Depth straining is when a particle manages to penetrate the top layers of the filter media and is captured by a closing of the pore it is travelling in. This makes penetration even harder for arriving particles.

Depth filtration is possible because of the forces between the particles and capture mechanisms. The particles are captured even if the pore size is large enough to let the particle through. Cake filtration occurs when a layer or a cake is formed on top of the filter caused by one or several of the mechanisms mentioned above. Because of this layer the pore size is reduced and more particles are captured which increase the total efficiency of the filter [16].

2.5.3   Pressure drop

To create a filter which has 100 % efficiency is not difficult, but at the cost of a very high pressure drop. The pressure drop over the filter determines the operation cost by the pumping effect needed to overcome this pressure drop. The difficulties lie in creating an efficient low pressure drop filter. Due to economical importance, the pressure drop over a filter can be just as important as the filtration efficiency [12].

At low velocity, incompressible and Newtonian flow, which is usually present in industrial filters, Darcy's law applies. Darcy's law correlates the permeability of the filtration media with the pressure drop by equation 2.1 [12].

$$\Delta p = \frac{1}{k^*} \eta U_0 L_f \tag{2.1}$$

Where k^* is the permeability of the filter media. During cake filtration also the cake contributes to increased pressure drop. The total pressure drop can therefore be written as equation.

$$\Delta p = \Delta p_{media} + \Delta p_{cake} \tag{2.2}$$

Where Δp_{media} is the pressure drop over the filter with no filter cake attached and Δp_{cake} is the pressure drop over the filter cake alone [6] [10].

2.5.4   Temperature resistance

More focus has been offered to hot gas filtration the last decades. There are several positive effects achieved by elevated temperature filtration. Utilization of energy is one of the main goals when hot gas filtration is considered. If the exhaust gas still is hot after cleaning, it is easier to utilize the energy in downstream equipment. The protection of downstream instrumentation is another positive achievement. High temperature filtration eliminates the need to cool and process the gas before filtration. Equipment for clean gas processing is less expensive and requires less maintenance. At high temperatures, tars and oils still in the exhaust gas are held above condensation temperature making it easier to clean particles without clogging particle filters. The tars and oils can thereby be separated gradually without the problems of particle interference in separators.

As a consequence of the focus on high temperature filtration, the demand for better temperature resistant filter materials increase. Materials such as quarts which can withstand 900 °C, and specially designed ceramic and metal filters which can withstand 1000 °C are under development and testing [10].

2.5.5 Filtration velocity

The filtration velocity is determined by the filter media, regeneration method, particle size and set up of the filter. A higher filtration velocity reduces the area needed for the filtration and therefore also reduces the investment cost and required space. Higher filtration velocity also increases how deep the particles are penetrating into the filter media and how dense the filter cake ends up being. The denser the filter cake and the deeper the filtration is, the harder it is to clean the filter properly [10].

2.5.6 Regeneration

Particles gathering at a filter, create an increasing flow resistance. At high flow resistance a high pressure drop over the filter and more pumping power is required to push or pull the gas through the filter. It is an economical factor deciding the point of maximum pressure drop, filtration efficiency and cleaning cost. When this maximum pressure drop over the filter is reached, the filter needs to be cleaned. This problem can be solved in many different ways depending on cleaning frequency, how deep the penetration is, how clean the filter should be and cost. For small filters with small dust loads which seldom need to be cleaned, total replacement or manual cleaning by washing or shaking could be sufficient. Larger industrial filters often need automatic cleaning systems because of the size of the filter and the cost of manual cleaning or replacement. Mechanical shaking of the filter to detach the deposited particles can be sufficient. The particles are then collected at the bottom of the filter and removed. Another method is the back blow cleaning where a steady stream of air or gas is passed through the opposite direction of the filter to force particles of the filter surface. This method requires offline time because of the slow speed back flow, often 2 to 5 minutes. These two techniques can also be combined for better performance. Later the pulse jet has been developed, which is a pulse of compressed gas forced through the filter in the opposite direction of the normal flow. This pulse is created to decrease offline time [12].

2.6 Bag filter

The bag filter is a common type of filters which has been around since the 1850's. It has been in use as large industrial, automatic cleaning, filters since the 1920's. The bag filter is usually used at low temperatures, but if it is made by certain materials it can be used at high temperatures as well [20].

2.6.1 Working principle

The bag filters are built of a fiber filter media and shaped as a bag or an envelope. The filter is fitted into blocks where the dirty gas enters at an inlet, passes through the filter and exits at a clean outlet. The particles deposit at the surface of the filter, or within the filter.

There are different types of bag filters in use at present time and figure 2.5(a) and (b) shows two of them. The first one is a small scale filter where the bags are

formed as long cylinders. The second one is a large scale filter which uses envelope shaped bags, which is shown in figure 2.5(c).
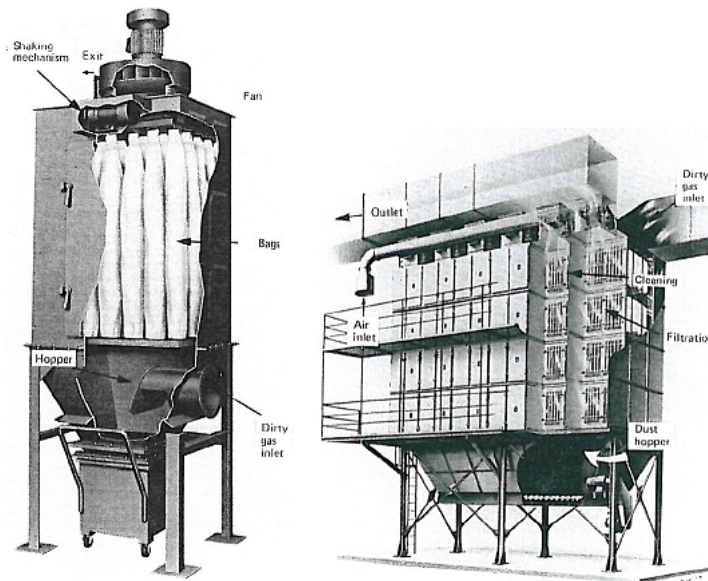
(a) Small bag filter re-generated by mechanical shaking.

(b) Industrial envelope bag filter.
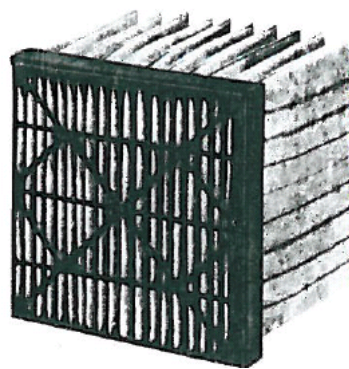
(c) Envelope shaped bag filter.

Figure 2.5: Bag filter [12].

2.6.2   Regeneration

Regeneration of a bag filter depends on the application and shape of the filter. Deep bed filters are washed or replaced when the pressure drop reaches the predetermined limit. For industrial high concentration (from $0,02-0,03$ g/m^3 to $100g/m^3$) surface filters are used. They are regenerated in different ways depending on particle and fabric properties. The size and design of the bags also influence the choice of regeneration mechanism [12]. In figure 2.5(a) the bags are formed as pipes hanging down from the top of the filter. Here the filter is mechanically shaken to detach the dust cakes from the filter and make them fall down into the collector bin.

Regeneration by jet pulse or back flow is also used in bag filters. The flexibility of the filter media allows the pulse or flow to alter the shape of the bag activating a detachment of the filter cake.

P. W. Riley introduced a regeneration method which combines shaking and back flow [12].

2.6.3 Operating conditions

Temperature

Temperature is dependent on the media used in the filter. The most common used medias can handle $80 - 150\,°C$ but there are materials that can handle as high as $260\,°C$ such as Teflon and glass fiber materials. There are also other factory secret materials which can handle higher temperatures, such as the filter material from 3M which can handle $371\,°C$ [20].

Filtration velocity

Bag filters require low filtration velocity. This is due to problems regenerating the filters with strongly attached particles. Filtration velocities at $0{,}01\,m/s$ are common for shaking and back flow regenerated bag filters. Higher filtration velocities at about $0{,}04\,m/s$ are allowed in jet pulse regenerated bag filters.

Filtration Efficiency

Regarding filtration efficiency the material is the most important parameter. Bag filters are able to achieve great filtration efficiencies depending on the material and construction. The filters can be created to obtain a filtration efficiency of $99{,}99\%$. However, the limits of emission and the allowable pressure drop determines the level of efficiency in real life [20].

2.7 Candle filter

The candle filter got its name because the filter media in these filters are shaped like candles. They are often made of ceramic material or sintered metal which are molded into the characteristic look of the hollow candles. The filters are made by materials that allow them to operate under high temperatures [12].

2.7.1 Working principle

The candles are fitted into a frame where the dirty side is separated from the clean side by the candles. The candles are created to increase the filtration area. A sketch of the working principle is shown in figure 2.6 (a) and (b) [12] [11].

2.7.2 Regeneration

There are different ways to regenerate candle filters. One way is to wash the candles with a solvent then drying it with hot gas. Another approach is to use back flow

(a) A schematic candle filter [12].

(b) Working principle [11].
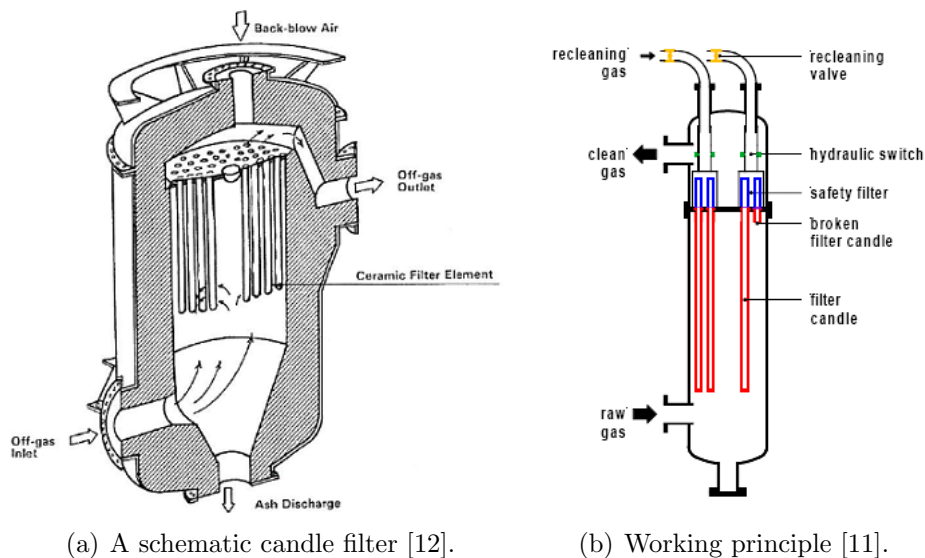
Figure 2.6: Candle filter [12] [11].

or jet pulses. In addition new methods are being investigated such as mechanically cleaning with a scraper [3]. Regeneration is performed on single candles or series of candles at a time. Regeneration in a given sequence provides that a filter is able to operate continuous, preventing a shutdown of the system every time the filter needs to be regenerated [12].

2.7.3 Operating conditions

Temperature

The candle filters are able to withstand high temperatures because the ceramic and metal materials they are made of are highly resistant to high temperatures. Temperatures up to 1000 °C are available with present technology. A patent also claims to be able to create ceramic candles which can withstand operation temperature above 1400 °C [7].

Temperature and filtration velocity have an impact on the pressure drop over the filter. According to Peukert [14] the pressure drop depends on material, temperature and filtration velocity and is shown in figure 2.7. The figure shows a decrease in pressure drop for higher temperature while the pressure drop significantly increases with filtration velocity. Especially the fleece materials have a clear disadvantage with high pressure drop at high velocity flow.

Velocity

Typically a filtration velocity around $0,06 m/s$ is applied on candle filters. The limiting parameter is that the higher velocities, the higher the pressure drop is [20]. Increasing filtration velocity also decreases the adhesion effect and therefore increases the penetration ratio. The bouncing phenomena start to take place at a filtration velocity between $0,05$ and $0,15 cm/s$ [12].

16
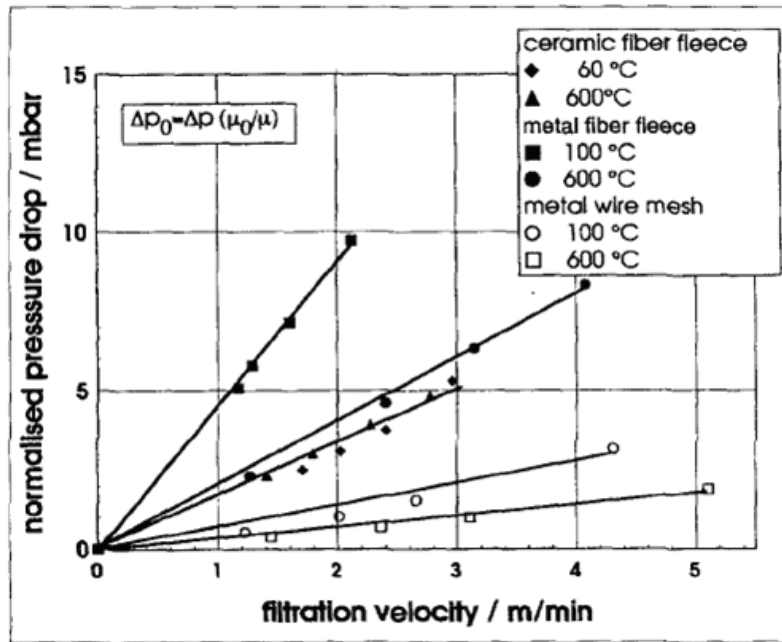
Figure 2.7: Pressure drop dependent on material and temperature [14].

Efficiency

Candle filters normally have a filtration efficiency beyond $99, 9\%$. If a lower efficiency is sufficient it is possible to provide a lower pressure drop, by using other materials or compositions [20].

2.8 Panel Ped Filter (PBF)

The panel bed filter is a filter under development and testing. At present time a new filter tray design is being tested at NTNU. The filter is designed to work at higher filtration velocities and the materials used are made to withstand high temperatures, utilizing high temperature cake filtration [8].

2.8.1 Working principle

The panel bed filter utilizes the effect of small spheres or granular media of different materials to create an obstruction of the flow. The formation of the filter media is called a bed. A panel bed filter is designed with louvers to hold the granular media in place so that the dirty gas can flow through and deposit particles and impurities at, or within, the filter media. There is a wide variation in design and methods of keeping the granular media in place. Figure 2.8 shows the working principle of the PBF [25].

2.8.2 Regeneration

Regeneration of a panel bed filter is performed by a jet pulse of compressed gas which is blown through the filter at opposite direction of the operational flow. This

17
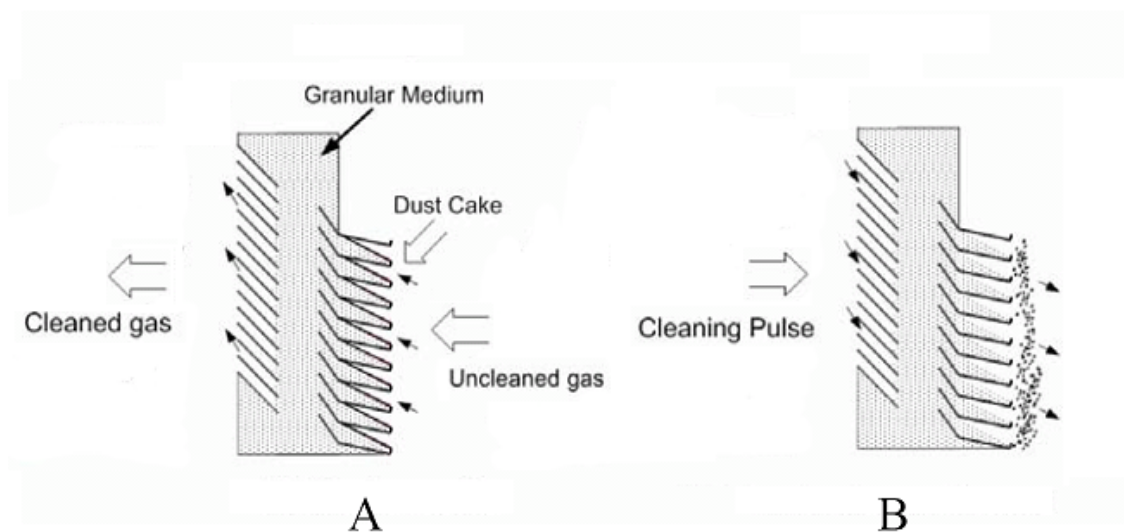
Figure 2.8: Cross-section of the PBF [25].

is called a puff-back pulse.

Puff-back

The pulse jet is released at the outlet of the filter travelling from the clean side to the dirty side of the filter. The pulse creates a motion in the bed. During the movement of the bed the structure fails and a sand spill occur. This sand spill includes the top layers of granular media and the dust cake accumulated during the filtration. Calibrating the puff-back configuration gives the desired sand spill from each louver. The pressure and the length of the pulse are the two parameters which can be regulated. The size of the granular media has little effect on the spill [8].

It is important to avoid too much sand spill to maintain the dust roots formed during the filtration in the lower layers of the bed ($0, 3 - 0, 8 \ g/cm^2$ for sand [18]).

Soil failure mechanism

Soil mechanisms can explain the behavior of the granular media movement. Applying a force to a soil will inflict movement or deformation. The force applied need to annul the forces keeping the soil together. Therefore the force needed, change from soil to soil type, depending on the force keeping it together. During puff-back the force applied is the pressure drop over the filter. The lowest pressure drop needed to create any spill at all is called Δp_{min} [8].

Cake formation on the filter can lower the Δp_{min}. This may be due to that the cake formation is holding the puff-back with no reaction for a longer time, and when it burst a more rapid sand spill are achieved [19]. The movement in the soil is helped by the angled louvers to invoke a sliding motion in the top layers. The filter cake is removed along with the top layers of the bed leaving some of its roots in the bed still in the louver [8].

18
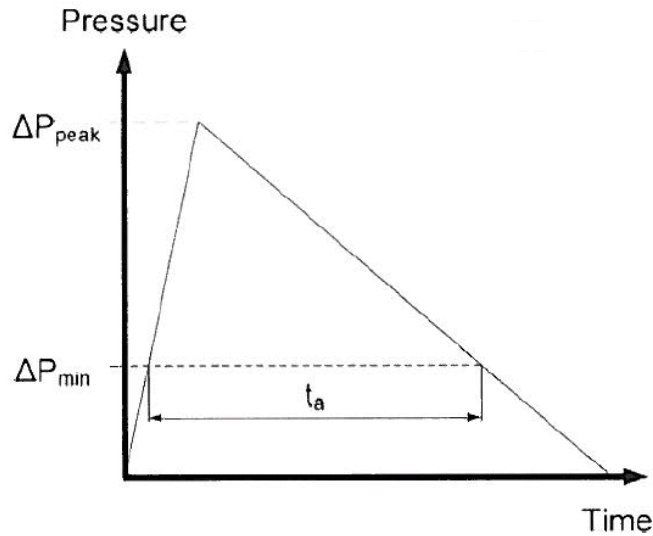
Figure 2.9: Definition of active time [8].

Active time theory

The active time theory state that the only important parameter of the puff-back pulse is the duration of time, t_a, the pulse exceeds Δp_{min} shown in figure 2.9 [8].

Specific impulse theory

Risnes [18] proposes a specific impulse theory. The specific impulse, I_p is correlated to the amount of spill by equation 2.3.

$$I_p = \int_{t_1}^{t_2} (\Delta P - \Delta P_{min}) dt \qquad (2.3)$$

Where t_1 is the time when the pressure drop reaches the ΔP_{min} and t_2 is the time when the pressure drop decreases below the ΔP_{min}. Risnes claims that the specific impulse is the most important parameter opposed to the time t_a.

2.8.3 Operating conditions

Temperature

The granular material can be highly temperature resistant, depending on the material used. Materials such as metal spheres can handle up to 1000 °C as in the candle filters [15]. The highest temperature tested so far is filtration at 550 °C in Güssing in Austria. These tests were successfully performed at these temperatures [24].

Filtration velocity

Depending on the thickness of the bed, type of granular media and the size of granular media high filtration velocities can be applied. $0,20 m/s$ is tested successfully with original design [8] and the filter tray design [4].

Filtration efficiency

Researchers have provided good results measuring filtration efficiency on panel bed filters. The experiments in Güssing had a collection efficiency at above $99,98\%$ [24].

Chapter 3

Experiments

Chapter 3 describes the setup and the executed experiments performed on the filter tray test rig and the L10-56 test rig. First the logging programs created in LabView are presented, and then each of the rigs and their components and the tests performed on them are described.

3.1 LabView

LabView was used to create programs to calculate, visualize and log measured data acquired by National Instrument acquisition boards. The base program was initially created by Håvard Risnes during his PhD [18] and has later been modified to suit further applications in new rigs. The program contains important individual parameters from each rig, therefore the program needed to be modified especially for each rig. The Programs looks something like figure 3.1.
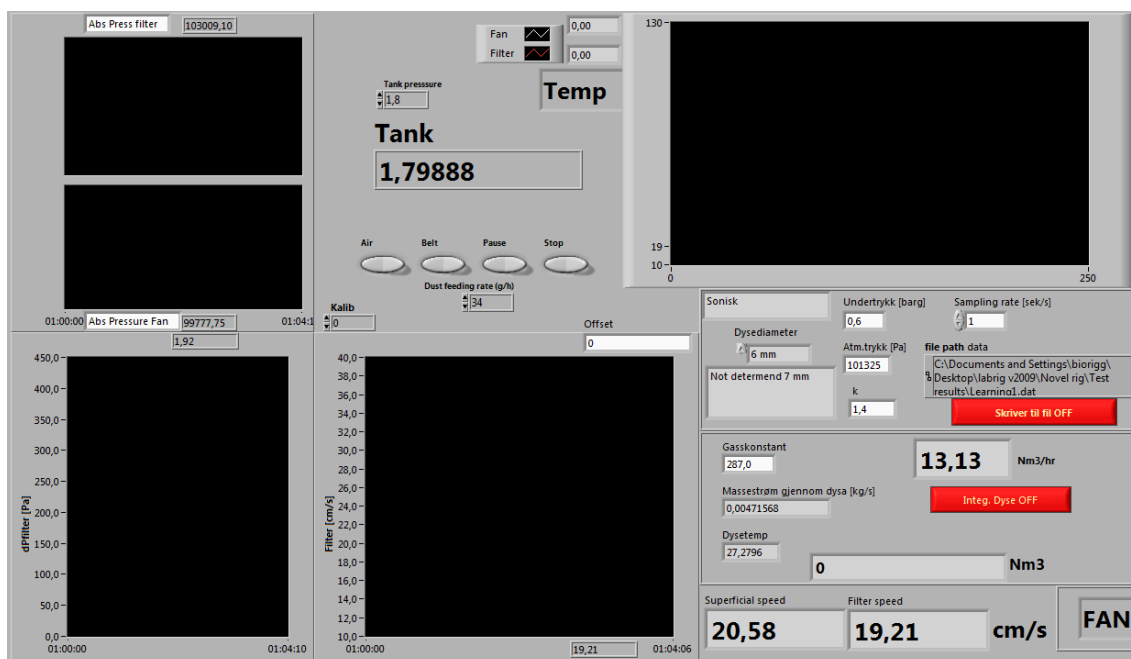

Figure 3.1: LabView program.

3.1.1 Filter tray test rig

The base of the large modifications of the filter tray test rig program was a new acquisition system which enabled different input signals and output signals. The operator was then able to control applications from the computer, thereby making the task easier and more accurate. Each controllable application is commented in the description of the components later in this chapter. Also minor changes were made to the program such as implementation of filtration area and calibration of the flow calculation. The flow diagram in figure 3.2 visualizes the working principle of the programs.

Additional programs were created to be used during the heating and puff-back testing of the rig. The programs were only used during the preparation and construction of the rig and are therefore not described any further.

3.1.2 L10-56 test rig

The L10-56 test rig had already been used several times in other applications. Daniel Stanghelle modified the program during his work [24], therefore the program was only slightly modified. All the physical parameters on the rig were controlled manually because no output module was available. Without the output module figure 3.2 also show the flow diagram for this program.

A small program was created to monitor and log data from the heating calibration test of the L10-56 test rig. The data gathered from the heating tests was therefore logged and available for consideration and analysis. The program was only used for a short period of time and is therefore only mentioned here.

An additional program was created to observe and test an additional unit created to investigate the actual inlet gas of the L10-56 test rig. The temperatures and pressure drop were shown in real time to give information about the rig during the test. The data was also logged to file for further evaluation and analysis.

3.2 Filter tray test rig

This test rig is based on a novel louver design which is based on filter tray design, and is therefore called the filter tray test rig throughout this thesis. The test rig was to be built and tested at 120 °C.

3.2.1 Filter tray test setup

Figure 3.3 shows the setup and the components of the filter tray test rig. The different components and setups are described in this section.

Pressurized air

Pressurized air from the lab was required in several applications on the rig. The air was cleaned and dried in to air filters to meet required specifications for some of the applications.
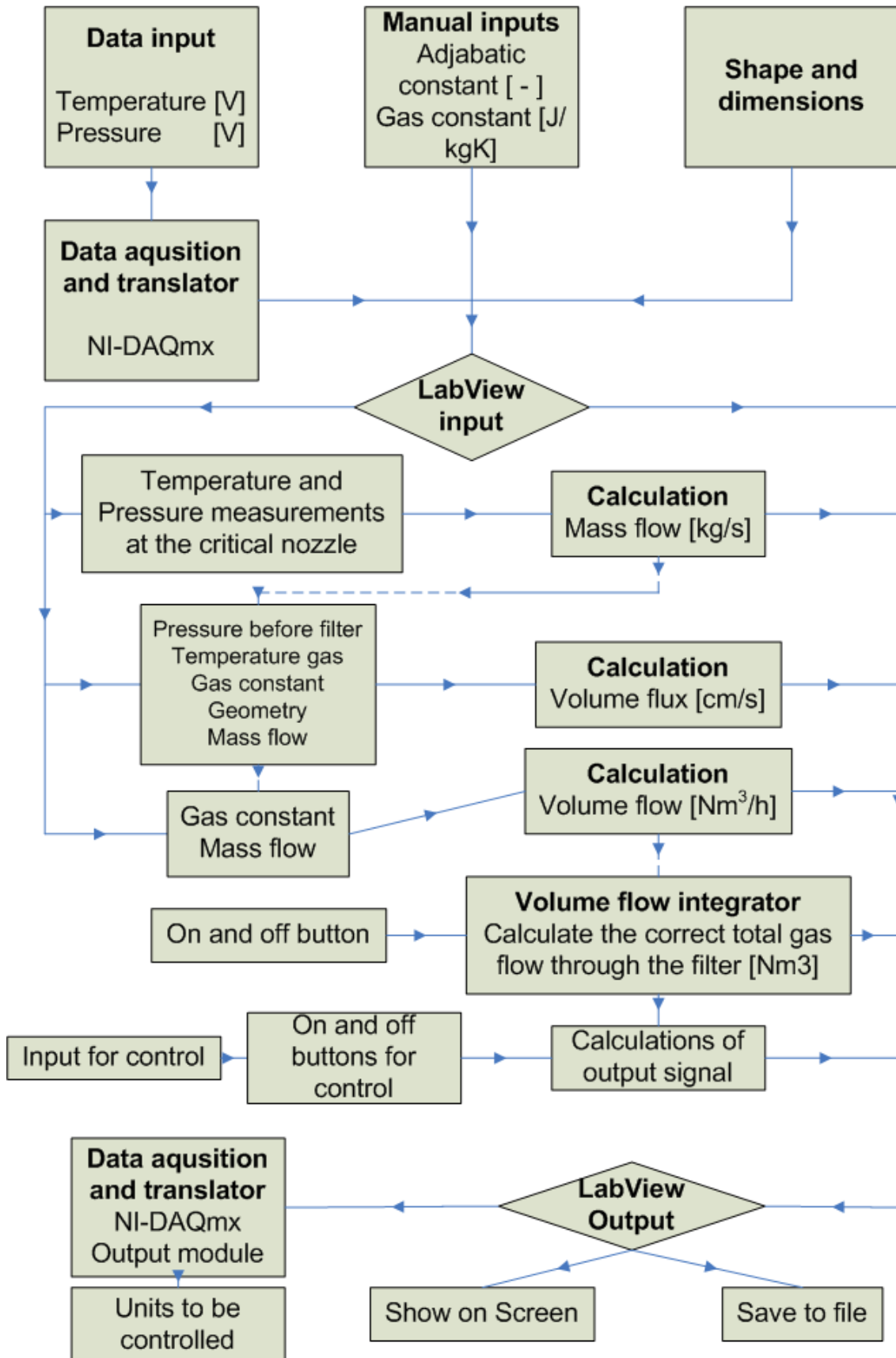
Figure 3.2: Flow diagram for the LabView programs.
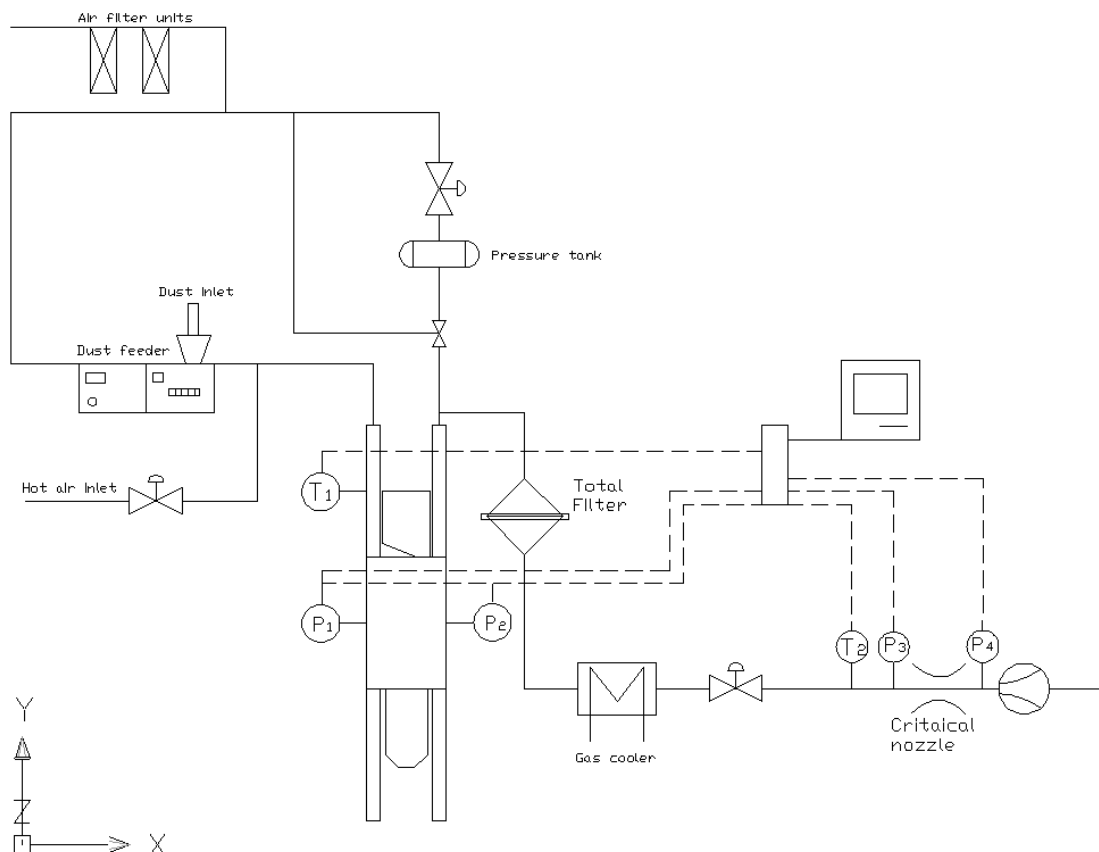
Figure 3.3: Filter tray test rig.

Dust feeder

A dust dispenser was used to supply dust to the filter. Pressurized air create suction in an ejector pulling dust from a belt in the dispenser. The belt speed regulated the amount of dust dispersed through the ejector, mixing with the pressurized air creating an aerosol. The dust dispenser only gave 5 to 10 Nm^3/h, therefore the aerosol needed to be mixed with more air.

Hot air inlet

In order to meet the maximum desired volume flow of 70 Nm^3/h, additional air was supplied before the inlet of the filter. The additional air was heated by a heating battery in the laboratory, and regulated by the temperature at the inlet of the rig. This temperature was decided by the amount of air in relation to amount of aerosol at the inlet. The provided hot air needed to have a temperature much higher than the desired temperature, of 120 °C, because it was going to be mixed with the cold aerosol before entering the filter and they together should obtain the desired temperature.
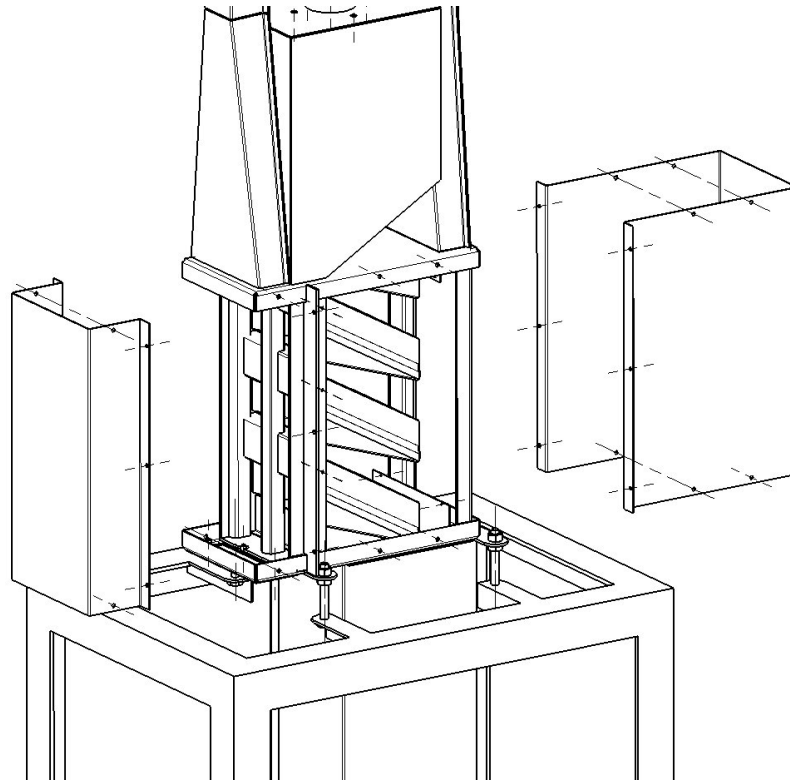
Figure 3.4: Filter tray assembly drawing.

Filter design

The filter tray design has many advantages compared to the other louver designs. Footprint reduction of about 50% and a 75% lower residual pressure drop than the original louver design are the most important improvements [22]. The problem of granular media spilling from the back louvers at high filtration velocities are not longer an issue because of the wire mesh holding the granular media in place. This allows for higher filtration speed, reducing filtration area and there by footprint.

An earlier filter tray design was built and tested by Stanghelle [24] at room temperature. This test rig was the basis of the new novel filter tray test rig investigated in this work. The trays are enlarged and the design has been compressed to a more compact rig with perpendicular inlet and outlet ducts. This is also the first filter tray test rig to be exposed for heating during tests. The main filter part is shown in figure 3.4.

Almost every part of the rig is welded together as one piece with two covers enabling the possibility to look inside before and after testing. The granular media feeding tank and collector tank are a piece of the total rig.

Heating

The rig was heated by flexible heating cables wrapped around the filter, as shown in figure 3.5. Four cables were fitted to improve regulation and give the possibility to disassemble the rig easily. In addition, the rig had four PID regulators, one for each heating cable. The input to each regulator was temperature measurements

Figure 3.5: Filter tray heating cables.

from four PT-100 elements inside the filter. The elements sent signals to a LabView program which transformed them into electrical current signals that were sent to the regulators. From these current signals the regulators calculated the amount of power applied to the heating cables, at any given time. This was done by providing voltage to the heating cables at a fraction (t') of a time cycle t_C. If too much power is applied to heating cables, it tends to get extremely hot and they may burn and cause problems. This was avoided by limiting the maximum output power from the regulators by $A_\%$, which meant that the regulators could at maximum output only apply power in t' equal to $A_\%$ percentage of t_C.

The entire rig, including the heating cables, was insulated and secured to obtain safety regulations and decrease energy consumption.

Absolute filter

The performance of the filter is measured by the amount of particles captured in relation to the total amount of input dust. Therefore an absolute filter was installed downstream of the back cone to capture the particles that were in the outlet gas. The amount of dust captured by the absolute filter was the basis of the calculations of the overall filtration efficiency of the filter. It also prevented dirty gas entering the cooling system and the vacuum pump downstream. The absolute filter is mounted in a casing shown in figure 3.6.
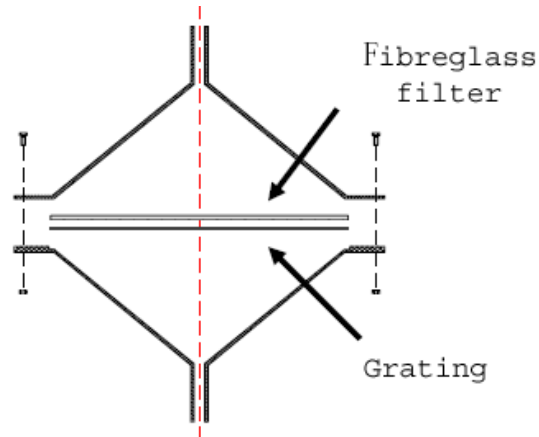
Figure 3.6: Absolute filter [23].
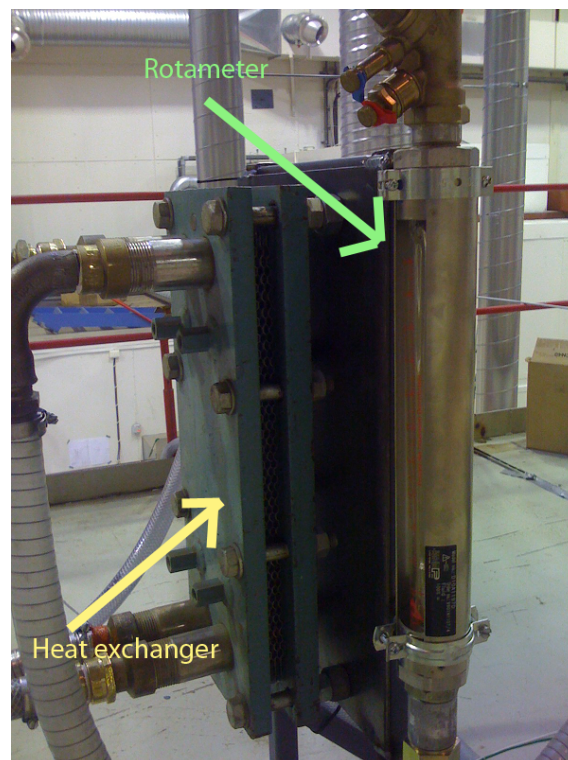
Figure 3.7: Heat exchanger and flow meter.

Heat exchanger

In order to cool the gas before it entered the vacuum pump, a plate type heat exchanger was installed. It used cold water to cool the hot gas from the filter. A picture of the heat exchanger is shown in figure 3.7. In this picture the rotameter shown, which is a flow meter.

27
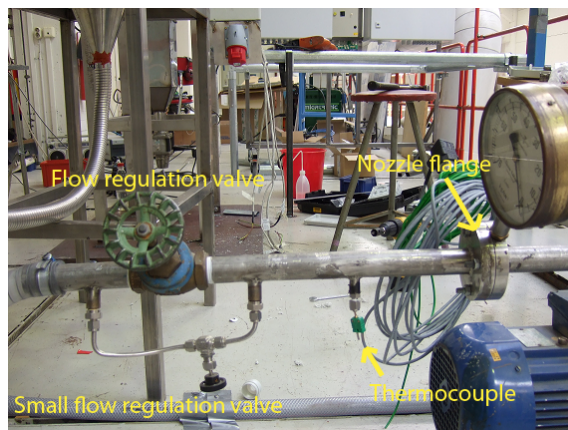
Figure 3.8: Flow regulation and critical nozzle assembly.

Flow regulation

A throttle valve was installed downstream of the heat exchanger. This valve regulated the volume flow allowed trough the system. To fine tune the volume flow a small bypass valve was installed in parallel. The valves are shown in figure 3.8.

Critical nozzle

A critical nozzle fitted with temperature measurements and pressure measurements was used to calculate the mass flow. The nozzle is installed inside the flange on the right hand side of the picture in figure 3.8. To verify and calibrate the new nozzle a rotameter was fitted downstream of the pump. The meter showed, manually, the volume flow on a scale from 0 to 100 where 0 was zero and 100 is 71 m^3/h. The flow meter is shown in figure 3.7.

Vacuum pump

The vacuum pump created a vacuum downstream the nozzle assembly to suck air through the rig. A datasheet for the pump is given in figure C.5 appendix C.

Puff-back system

Pressurized air from the laboratory was used to pressurize a tank. A proportional regulator, regulating the tank, was controlled by the LabView program to sustain the desired pressure. On the outlet of the tank a fast open and shutting valve was fitted. How long the valve was open was also regulated from LabView. A sketch of the puff-back system is shown in figure 3.9.

Instrumentation and acquisition system

Mainly K-thermocouples were used for temperature measurements. K-elements shown in figure 3.10(b) were used to monitor the temperature in the gas and welded K-threads shown in figure 3.10(a) were used to monitor the temperature on the
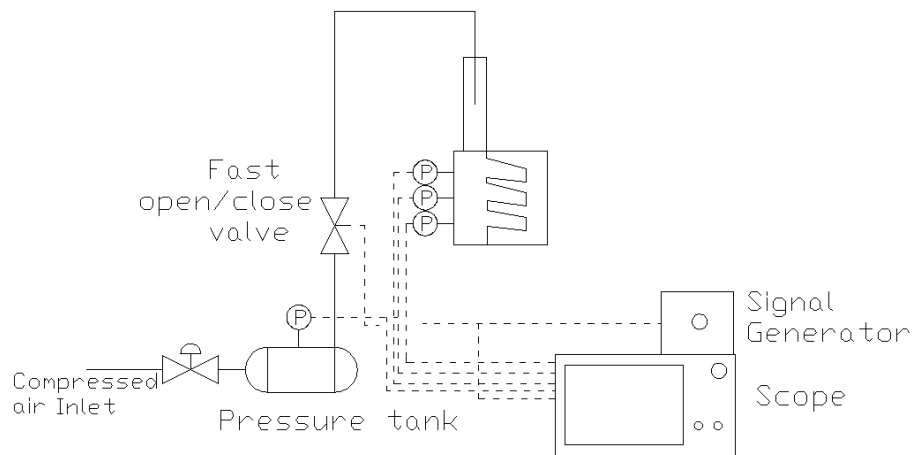
Figure 3.9: Puff-back calibration setup.

filter. Also four pt100 elements were used to obtain the regulation temperatures for the regulators.

(a) A welded thermocouple.

(b) A thermocouple element.
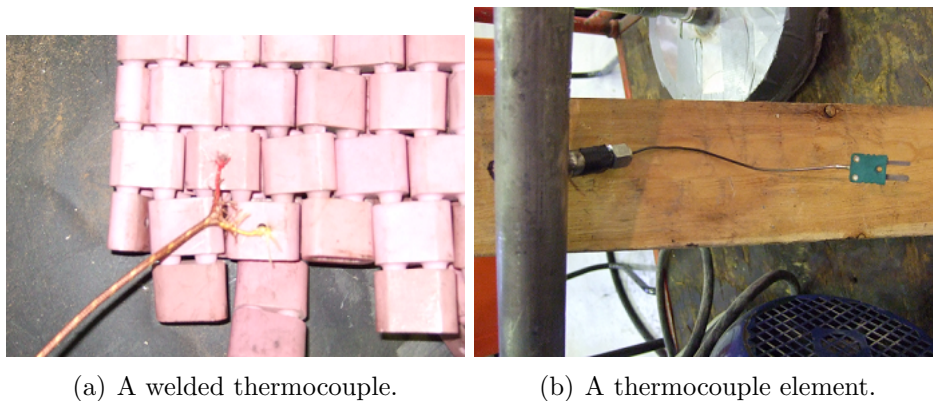
Figure 3.10: Thermocouples.

Different pressure transducers were used to measure pressures and pressure drops on the filter and at the nozzle. Overpressure, pressure difference and absolute pressure measurements were used. Figure B.1 inn appendix B, shows the placement of the instrumentation on the rig. Voltage signals were transmitted from the pressure transducers to a LabView which interpreted the signals and used them to show the pressure drop and calculate velocities.

A new data acquisition system from National Instruments named DAQmx was used for the new filter. The main advantages of the new data acquisition system were more accuracy and new controlling possibilities of the puff-back. It also allowed remote controlling of the valves and the dust feeding, and a more flexible signal input and output range. The new features of the system were integrated into the LabView program, se section 3.1. Documentation regarding the coupling of instrumentation, acquisition and power supply is found in appendix B.

Number of layers (N) (#)	Spill required (g)	Spill required (g/cm^2)
1	86,3	0,135
1,5	129,4	0,203
2	172,6	0,270
3	258,9	0,405
4	345,2	0,540
5	431,5	0,675

Table 3.1: Required amount of granular media removed.

3.2.2 Puff-back calibration

The puff-back test made it possible to both measure spill and pulse. The setup of the puff-back is shown in figure 3.9. ISO standard test dust was used, and alumina spheres was used as granular media, data sheet C.3 and C.2, are both attached in appendix C.

Puff-back spill calibration

A constant equal spill over all of the trays is important to ensure that the same amount of granular media and dust cake is removed from each tray. To ensure this the front cover was replaced with a transparent cover in order to see that the puffing was working properly. A test was performed by collecting granular spill from each tray. The spill was then measured and compared to ensure that it was uniform. When the spill from the three trays was sufficiently uniformly distributed, only the total spill was measured. However, to ensure repeatability three tests were performed for each test setup used. The required spill is calculated from equation 3.1.

$$Spill = N * \rho_G * d_G * A_F \tag{3.1}$$

This formula was used to calculate the amount of spill according to the number of layers (N) desired to remove. The determination of how many layers to remove is based on how deep the particles are penetrating and the amount of dust. The filter cake should be removed while keeping some of the roots to enhance the formation of a new filter cake. Alumina spheres were used as granular media in the filter tray test rig. A data sheet describing the alumina spheres is attached in figure C.2 in appendix C. The amount of spill required to remove the desired number of layers using alumina spheres is shown in table 3.1. Deeper penetration at higher filtration velocities demands more layers to be removed. Several tests were performed with different values for tank pressure and the time the valve was open. The purpose of these tests was to create a tool which allows operators to find the right input values to create the desired spill.

Puff-back pulse calibration

The pressure pulse was obtained to discover the effects behind the puff-back and to find the dependence on the pulse according to the theory. The pressure pulse varied with the time the valve was open, and the pressure in the pressure tank. These measurements were therefore taken while performing the spill calibration. It was obtained by using an oscilloscope and pressure transmitters on the tank and on the filter. The oscilloscope was used to obtain the required reading speed to capture the pressure changes in the filter and the tank. This gave the possibility to acquire the delay time, pulse length, peak pressure and pressure drop in the tank. The pulse was measured by three pressure difference transducers on the clean side of the filter to detect if the pulse varied over trays. To obtain the tank pressure an over pressure transducer was used. The tank pressure was used to calculate the amount of used air per puff. The instrumentation and setup is shown in figure 3.9. A computer based LabView program was created to control the time the valve was open and acquire the tank pressure, see section 3.1.

3.2.3   Heating test

Heating tests were performed to check if it was possible to apply the sufficient power, to optimize the PID regulators and to find possible heat losses and insulation failures. The desired filtration temperature for this application was 120 °C.

The time constant t used for the regulators was set to 8 seconds according to section 3.2.1.

Test #1

The first heating test was performed with the original setup of the regulators. The only limitation was that maximum output $A_\%$ was set to 50%. The rig was already somewhat hot due to a hot air test performed right before the heating test. During the test no hot air was running through the rig. It was a basic test to show that the heating system was working and capable of heating the rig to 120 °C. It was also a question if the insulation was sufficient. In order to examine this, the temperature was monitored at nine points in the rig via LabView and logged to a file for processing and analysis.

Test #2

Some modifications were necessary after the first heating test. The maximum output was altered to 80% for the granular media feeder and 70% for the collector tank. In test two, hot air was sendt through the filter during heating. This was done to shorten the heating time and enhance the uniformity of the temperatures. In addition, the gas cooler was tested to see if it could cool the gas sufficiently.

3.2.4   Filtration test

Start up filtration tests were performed during this work. The tests were mainly performed to control that each component of the rig was performing as it should

and that the filter rig worked. Therefore some components got special attention; the dust feeder, the heating, the gas cooler, the absolute filter and the puff-back system. The dust feeder was tested by adding a certain amount of dust, letting it run and using the time until it was empty to calculate that the feeding rate was correct. The temperatures were constantly monitored manually to control that they were stable, and an alarm was mounted in the LabView program to ensure that the gas cooler was operating below the allowed limit. The puff-back system was controlled by measuring the spill after each puff. Measures were also taken concerning safety issues. Therefore documentation and safety regulation documents were placed in a folder at the rig site. An operator manual and guide was also created to ensure safe and correct usage of the rig. This was also placed in this folder. The operators guide is also attached to this document in appendix B. The startup, running and shutdown procedure is found in this guide.

The filtration tests also provided usable results concerning the rig's ability to perform as a filter. The results obtained were logged in separate data files for processing and analysis. A text file was created for each test to provide any comments about the given test. Another file was created to contain the most important parameters from all of the tests, which were used to obtain filtration efficiency and emission rates.

3.3 L10-56 test rig

The PBF prototype rig is based on the L10-56 louver design and is therefore called the L10-56 test rig in this thesis. The L10-56 test rig was going to be tested at 350 °C on the exhaust gas from an oil extraction pilot plant running in the laboratory. Olivine sand was used as filter media in this rig, a data sheet is attached in C.1 in appendix C. The prototype panel bed filter was built of the L10-56 louvers. The louvers were arranged as in figure A.1 in appendix A.1, mounted between a front and a back cone distributing the inlet and outlet gas to and from the filter. Figure 2.8 shows the layout of the louver part with the granular media in the middle. The front louvers were created to hold up the granular media with an angle so that the filtration area was as large as possible, while the back louvers were designed to keep the granular in place by placing them in an upwards angle. The left figure shows the filter in operation mode, and the right figure shows the filter in cleaning mode.

A slip stream from the oil sand extraction rig at NTNU was used to test the L10-56 filter. The filter rig consisted of a series of components which are described in this section.

3.3.1 Horizontal bed unit (HBU)

Running the exhaust gas with unknown composition through the filter might cause trouble. If the exhaust gas contained sufficient amount of oil or other sticky matters could end up clogging the test rig. The HBU was created with easy access to the filter media to enable investigation of the filter cake created, and to discover potential harmful clogging of the media. A figure of the setup is shown in figure 3.11, and the construction and instrumentation of the rig is described in this section. No
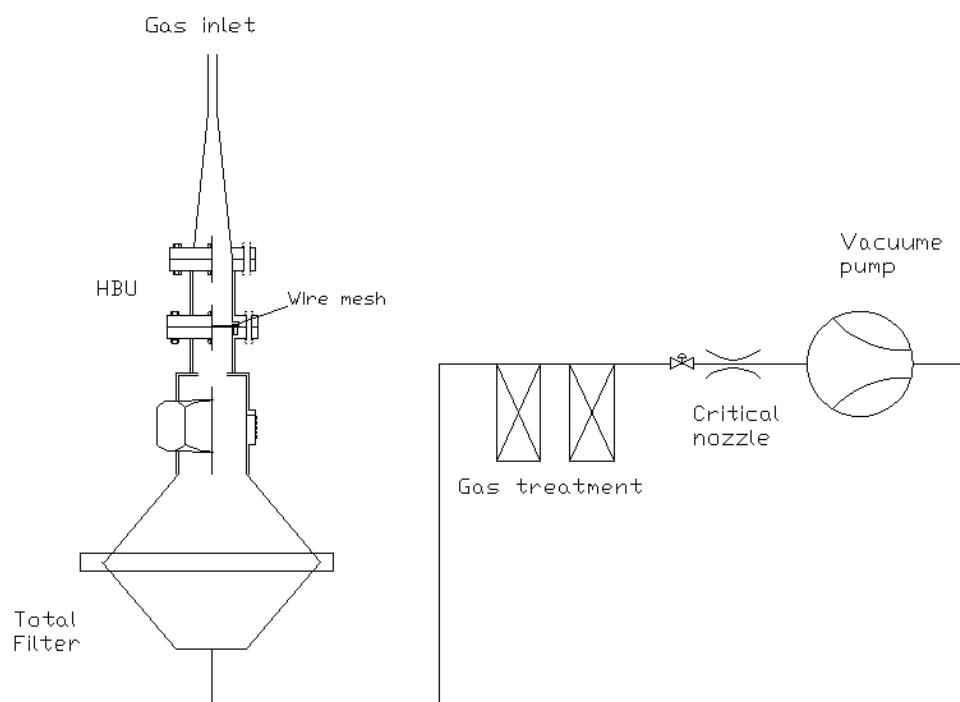
Figure 3.11: HBU test rig setup.

experiments was performed on the HBU due to that the oil extraction facility was not running at the time the HBU was finished.

Description of the HBU

The HBU unit was based on a design earlier used by Risnes [18] and Lee [8] [26] to investigate the formation of the filter cake. A bed filter media was filled in a vertical pipe on top of a wire mesh to allow the gas to flow through the filter media. The dimensions were calculated to fit a flow of $0,3Nm^3$. The filter rig is shown in figure 3.12(a).

Heating

A flexible heating cable of 2 meters and 440 Watts was used to preheat the rig and to maintain a uniform temperature from the inlet through the sand layer. The temperature was regulated by an external manual regulator. The regulator had a temperature input from a K-element and regulated the output power to the heating cable according to this temperature. The heating cable attached to the HBU is shown in figure 3.12(b) and the regulator is included on figure 3.12(c).

(a) Full HBU picture.

(b) Heating cables attached to the HBU.
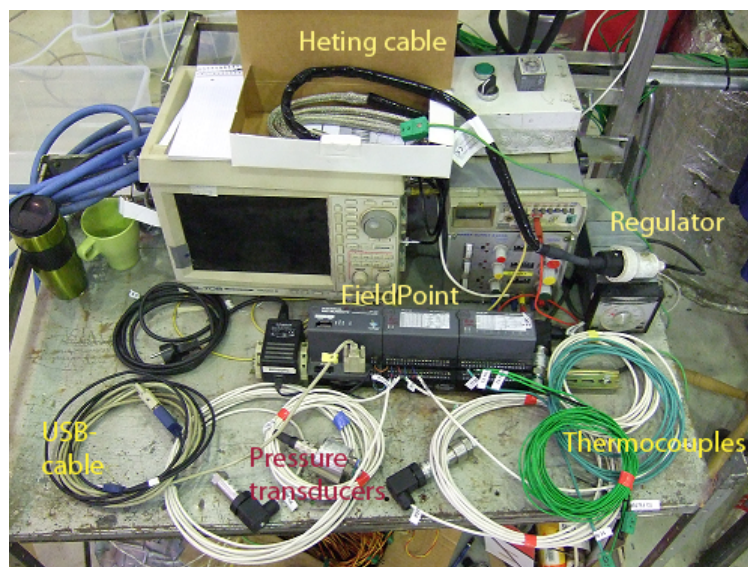
(c) Instrumentation on the HBU.

Figure 3.12: HBU setup and instrumentation.
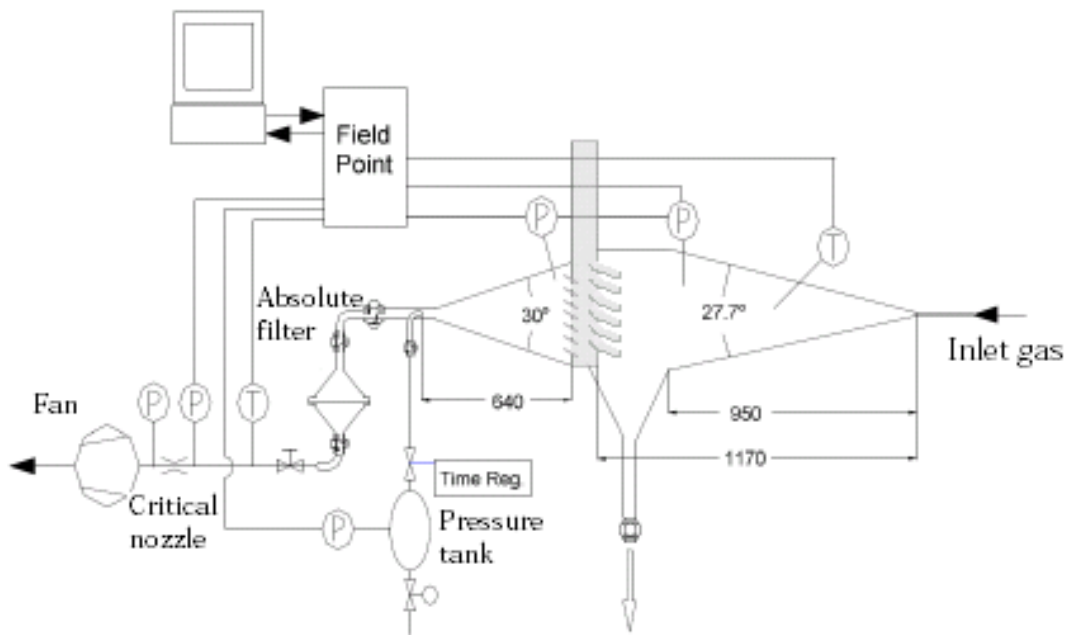
Figure 3.13: L10-56 test rig setup.

Flow measurement

The same flow measurement system was used in the filter tray test rig. The setup is described in section 3.2.1.

Instrumentation and acquisition system

A pressure drop build up over the sand used in the HBU, would indicate that the filter is gathering particles or getting clogged by other contaminants. The pressure drop was monitored by a delta pressure transducer. K-element thermocouples were fitted above and underneath the filter media in order to monitor the temperature in the filter. All the gathered data was processed in a FieldPoint unit which was coupled to a LabView program giving the operator full overview of the rig. In addition to show data in real time, the data was logged to a file for further review and analysis. All the instrumentation is shown in figure 3.12(c).

3.3.2   L10-56 test setup

The test setup is shown in figure 3.13.

Pressurized air

The pressurized air for the L10-56 was provided the same way as for the filter tray test rig. The setup is described in section 3.2.1.

Figure 3.14: L10-56 heating cables.

Heating

Preheating the entire rig was important to be able to start at an elevated temperature of 300 to 350 °C and maintain this temperature during the filtration. Also the granular media had to be at this temperature to avoid cooling of the gas during filtration. Heating cables were fitted inside ceramic elements which were attached to the filter. Figure 3.14 shows the heating elements. The heating cables and ceramic elements were woven into heating pads which were then coupled together in series in four areas. The areas, heating cables and boxes are described in appendix A.2.

The resistance in the cables were 0,5 Ω per meter and 230 V was applied. The heating cables produced an effect according to formula 3.2. More details are given in appendix A.2 where the effect output from each cable is presented.

$$P = \frac{U_\Omega^2}{R_\Omega} \qquad (3.2)$$

The same type of regulators were used in the filter tray test rig. The setup is described in section 3.2.1. However, the regulators in the L10-56 test rig differed from the ones in the filter tray test rig because there were used K-element thermocouples instead of electrical current signals. The L10-56 test rig regulators also differed from the filter tray test rig regulators because they controlled an area instead of a single heating cable.

Insulation

Two layers of insulation were used. The inner layer was a high temperature resistant insulation specially adapted to fit the filter. The insulation was first fitted right on top of the heating elements, and then a second layer of insulation was applied on top of the first one. This was done to ensure total coverage of the filter and to decrease the heat loss from the filter. The first layer of insulation is shown in figure 3.15.

Figure 3.15: Specially fitted insulation.

Puff-back system

The same type of puff-back system as used in the filter tray test rig was used in the L10-56. The difference was that the regulation valve and the opening signal were controlled manually.

Absolute filter

The same principal for the absolute filter was used in the L10-56 filter as in the filter tray test rig described in section 3.2.1.

Instrumentation and acquisition system

The instrumentation for the L10-56 filter was similar to the ones used in the filter tray test rig with small exceptions. Only K-thermocouples were used in the L10-56 filter, the placement of the thermocouples is shown appendix A.3 . The acquisition system used were National Instrument FieldPoints only fitted with thermocouple and voltage input signals.

Flow measurement

The same flow measurement system was used in the filter tray test rig. The setup is described in section 3.2.1.
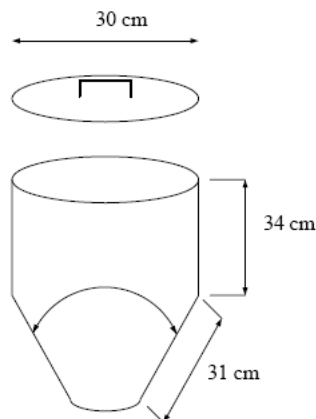
Figure 3.16: Granular media feeding tank [23].
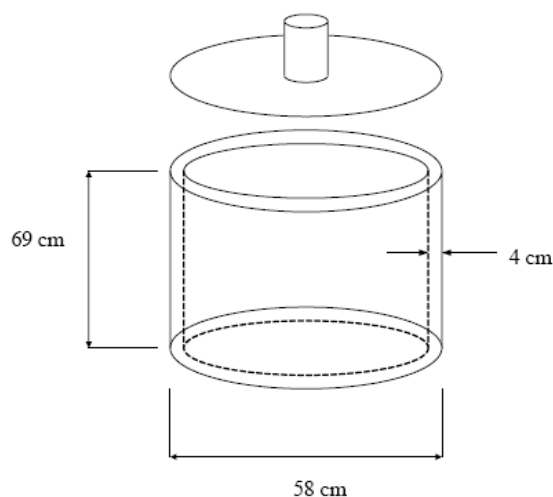
Figure 3.17: Granular collector tank [23].

Granular media feeding tank

The granular media feeding tank contained unused granular media. The tank was mounted on the rig using the gravitational force to feed the granular media into the louvers. Spilled granular media was replaced by new granular media from the tank after each puff. The granular feeding tank is shown in figure 3.16

Collecting tank

At the bottom of the filter a collecting tank was fitted. This tank collected granular media and dust that fell out of the louvers when the back pulse was applied. Figure 3.17 shows a drawing of the container.

3.3.3 Puff-back calibration

A puff-back calibration test was performed on the L10-56 test rig. The setup is explained earlier in this section.

Puff-back spill calibration

Risnes calculated the desired amount of granular media removed to be between 154 and 386 g [18]. Spill above 386 g was therefore not tested during this calibraton. The test procedure was the same as used in the filter tray test rig.

Puff-back pulse calibration

The puff-back pulse was also measured in the same way that was done on the filter tray test rig. The only difference was that that the time the valve was open and the tank pressure was regulated manually. The results were used to calculate the active time.

3.3.4 Heating test

Heating tests were performed to check if it was possible to apply the sufficient power, to optimize the PID regulators and to find possible heat losses and insulation failures. The desired filtration temperature for this application was between 300 and 350 °C, and the heating tests were therefore performed at 350 °C. The heating tests were performed without gas flowing through the filter, no collecting bin attached to the rig and with no granular media in place. The selected temperature inputs and maximum power initially used in this test were defined by looking at earlier heating tests performed on the rig.

The time constant t used for the regulators was set to 4 seconds according to section 3.3.2.

Test #1

The first test was set up to ensure that all the heating cables, thermocouples, software and logging instruments were working. The objective was also to discover where the regulation temperature measurements should be performed on the filter and to investigate if the insulation was sufficient. A picture of the test rig is shown in figure 3.18

Test #2

The second test was performed to improve the performance of the heating. The regulation pattern was altered to a time dependent ramping set point regulation. This made it possible for the operator to better controle the heating time. The ramping was set to increase 80 degrees per hour, which gave a warm up time of approximately 4 hours. Equation 3.3 was used to calculate the warmup time.

$$t = \frac{T_{set}}{Ramp} - T_0 \tag{3.3}$$

The second layer of insulation was fitted for extra insulation. The test time was 7 hours while the logging program was on over night. This was done to be able to discover if any parts of the filter cooled faster and therefore had any insulation failure. A picture of the filter during test two is shown in figure 3.19.

Figure 3.18: Filter during heating test #1, L10-56 test rig.

Figure 3.19: Second layer of insulation at test #2, L10-56 test rig.

Test #3

In the second test there were some problems with regulator number two. The details are explained in the results, section 4.2.3. After the adjustment of the regulator, test three was performed in the same way as test two.

3.3.5   Filtration test

Due to the delay in the L10-56 test rig and the oil sand extraction test rig, the full scale filtration test has been delayed.

Chapter 4

Results and discussion

This chapter presents the results obtained in the tests described in chapter 3. Puff-back calibration, heating tests and filtration tests are described.

4.1   Filter tray test rig

The results from the puff-back, heating and filtration tests on the filter tray test rig are presented in this section.

4.1.1   Puff-back calibration

Puff-back spill calibration

During the first tests the top tray spilled more than the second and the third tray. To improve the distribution of the spill, the top two tray angles were changed. The top one was decreased by $2,2°$ and the middle one by $1,1°$. The results from these tests are shown in table 4.1. The table shows that the new tray angles give a fairly even distribution of spill, with a deviation of 0,3 to 6 g.

When the spill from the three trays was uniformly distributed, only the total spill was measured. To ensure repeatability three tests were performed for each combination of values for tank pressure and the open time of the valve. This gave an average deviation of 6 grams of spill per set of values. The error lay in the

Pressure	Opening time	Top (1)	Middle (2)	Bottom (3)
(bar)	(ms)	(g)	(g)	(g)
1	100	12,6	13,1	13,1
1	100	13,7	13,8	13,8
1	160	33,2	33,7	33,7
1	200	44,4	47,4	47,4
1,4	100	30	29,4	29,4
1,4	160	68,9	67,2	67,2

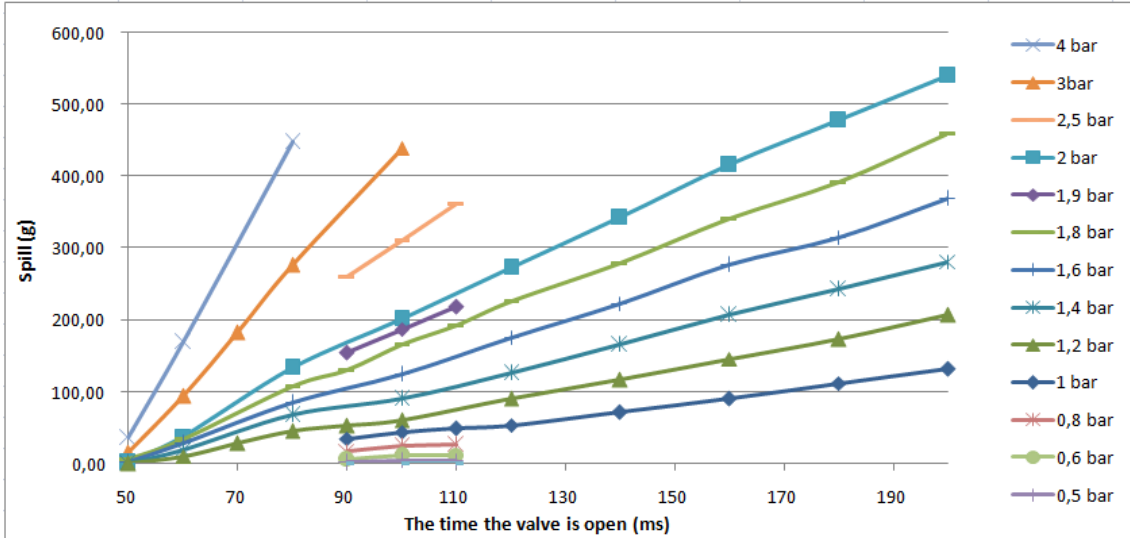Table 4.1: Equal spill over the trays.

Figure 4.1: Puff-back spill calibration.

difficulties of maintaining the accurate pressure in the tank and adjusting the time the valve was in the open position.

The data obtained during the puff-back tests are displayed in figure 4.1 where the time the valve is open and the tank pressure is plotted against the spill. The linearity of the graph makes it easy to find the right tank pressure and how long the valve needs to be open, when desired amount of spill is decided.

By comparing all the spill tests carried out, the shortest time the valve was open, with findings that made it possible to repeat the test with good accuracy, was between 90 and 110 ms. Therefore the time while the valve was open should be chosen to be above 90 ms. At shorter pulses the tank pressure needs to be raised. The results had a wide enough range to spill granular media from 0 to 5 layers, and therefore there was enough data to carry out the further planned tests.

Puff-back pulse calibration

All the results from the pulse tests were obtained from the oscilloscope. An example of a screenshot of the oscilloscope is shown in figure 4.2. The yellow line is the pulse signal controlling the valve. The red line is the tank pressure registered to calculate gas consumption. And the green, pink and blue lines are the registered pulse. The rest of the results can be found in the electronic appendix following the thesis. These pictures are the foundation of the data used to find the results in this section.

The peak pressure from the series of test were plotted in figure 4.3. This figure gives the Δp_{min} of the filter tray test setup. This value is obtained by finding the zero point, which in this figure is at 80 to 120 Pa. This is the lowest pressure drop over the filter which creates any spill at all. This value is very low compared to the earlier designs, where this value is referred to as the threshold value [18]. Risnes found a threshold value of 500 Pa for the L10-56 design with olivine sand. Decreasing this value means that less air and pressure are needed to create spill, which means that the filter tray design is better considering the effect of the cleaning pulse.

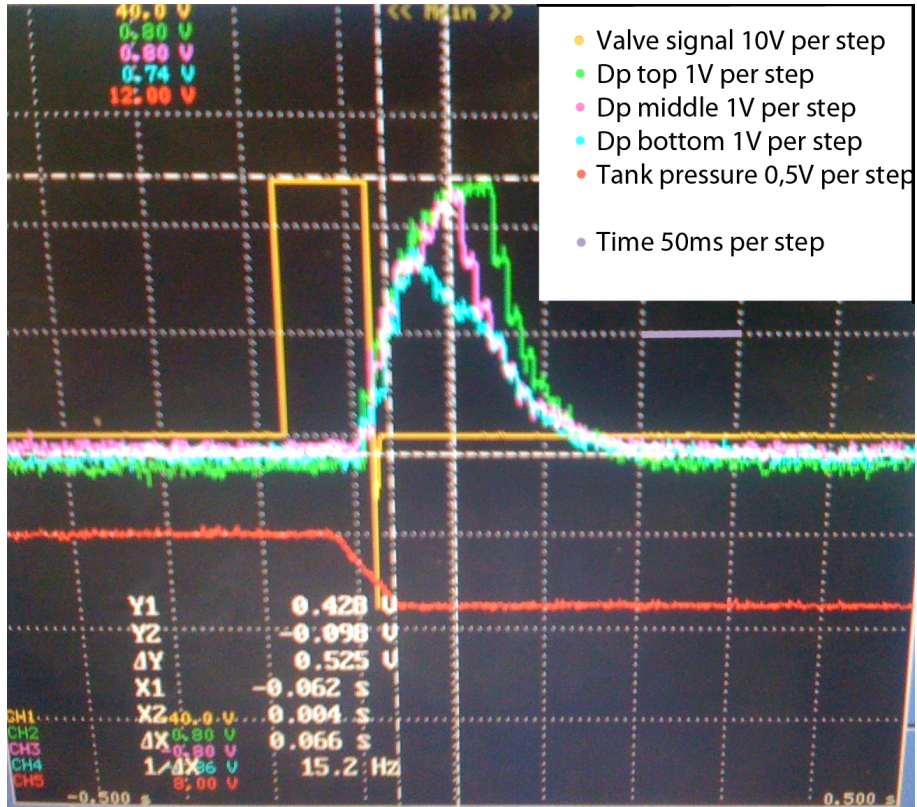The active time is read from the pictures of the oscilloscope using the Δp_{min} as

43

Figure 4.2: Pulse result example.
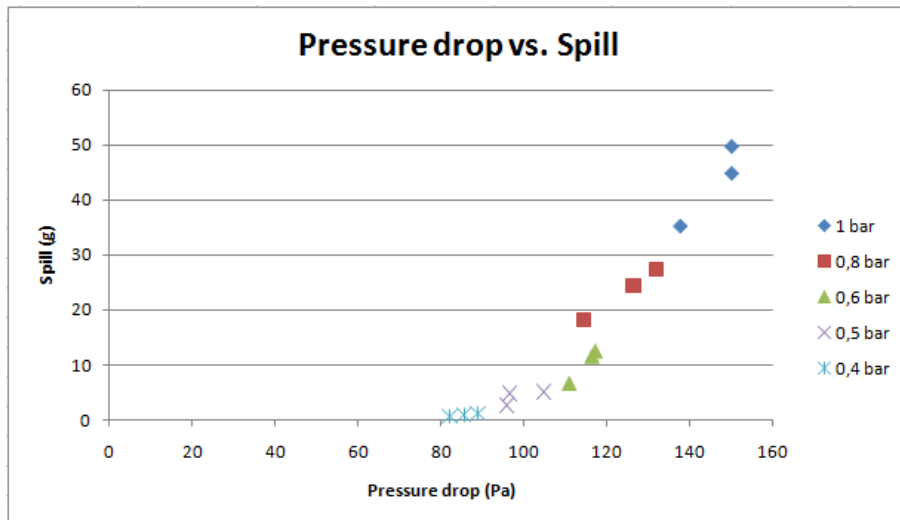
Figure 4.3: Δp_{min} for the filter tray test rig.
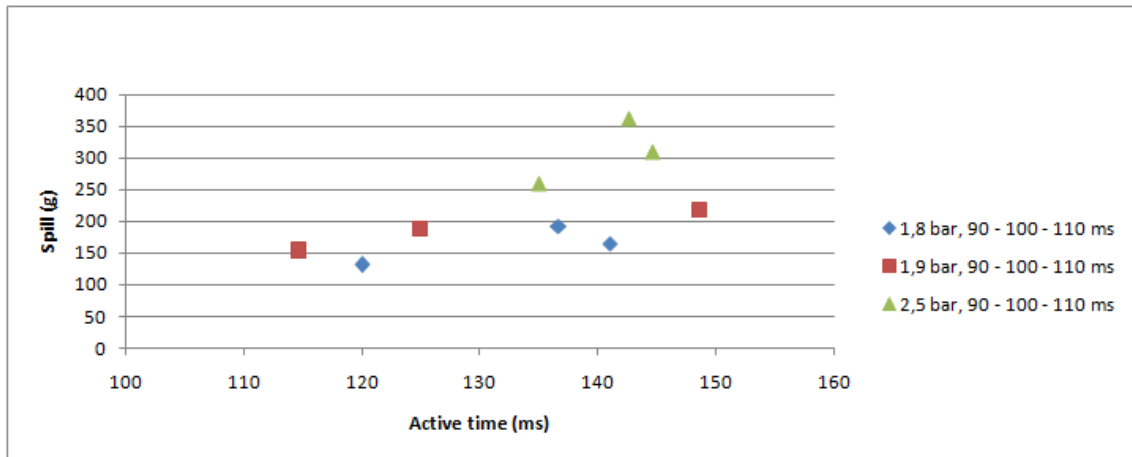
Figure 4.4: Active time for the filter tray test rig.

the starting point. Figure 4.4 shows the active times for all the tests performed. According to the theory the spill should only be dependant on the active time. Ideally the graph should be a straight line underlining the dependency. No such line can be read from this figure. However, a tendency of increasing spill with increasing active time can be observed. Although the results are inconsistent from test to test the figure shows some correlation between spill and active time. A problem might be that the pulse detection system was not accurate or sensitive enough for the test to be repeatable. To obtain better results a more repeatable setup should be used by improving data acquisition and censoring equipment. Another problem could be the travel distance of the pulse. Shortening the travel distance by mounting the pressure tank closer to the filter trays could improve repeatability and also decrease needed tank pressure and time the valve needs to be open.

During the calibration of the pulse, data was also gathered to explore the use of compressed air during the puff. The amount of used air are plotted against spill in figure 4.5. The figure shows that little air is used to create the spill. A spill of 200 g require only 3,2 l of air. It also shows a good relationship between air used and spill. In other facilities where more expensive gases than compressed air are used in the puff-back, a low consumption will reduce costs. However, by shortening the travel distance of the pulse the use of puff-back gas could become even more efficient, because it reduces the pressure drop of the pulse and leakage possibilities.

4.1.2 Heating test

Test #1

The results from heating test one are presented in figure 4.6. The start temperature in this test was between 60 and 70 °C because of the prior run hot air test. The figure shows that the temperature increase on the filter is steadily rising. All the heating cables were working properly and the regulators were regulating at the right temperature point. The main problem of the heating was the wide range of temperatures at the end of the test. The test shows that the temperatures of the regulated areas, one to four, were in a good range. The low temperatures in the
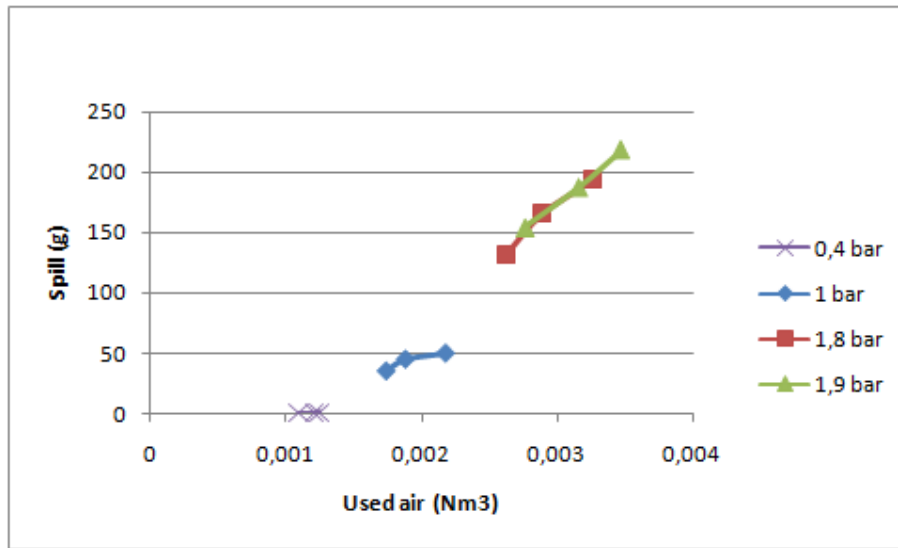
Figure 4.5: Used air against spill in filter tray test rig.
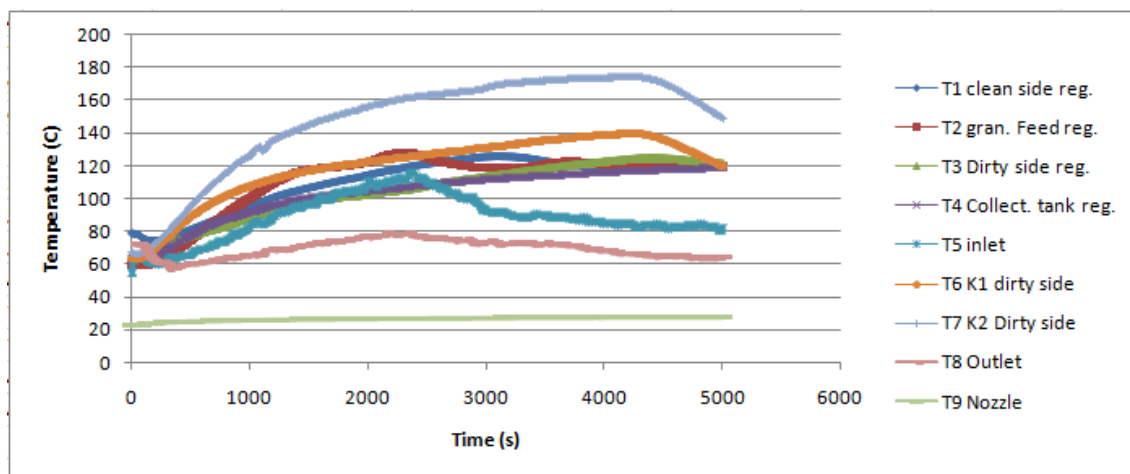
Figure 4.6: Heating test #1.

inlet and outlet are due to that the heating cables was heating the rig and the air inside, but there were no heating cables at the inlet and outlet pipe. At some point all of the insulated temperature points reached above 120 °C which means that the insulation was sufficient to keep the rig at the wanted temperature elevation. It took about 35 minutes to heat the rig to 120 °C. This means that at regular starting temperature, ambient temperature, the heating time would be about an hour. The system was working but some alteration needs to be done to create even temperature distribution. The figure shows a wide range of temperature distribution. All the temperatures should stay stationary at about 120 °C. A solution could be to add a flow of hot air through the filter during heating, which could help stabilizing and sustaining a uniform temperature distribution.
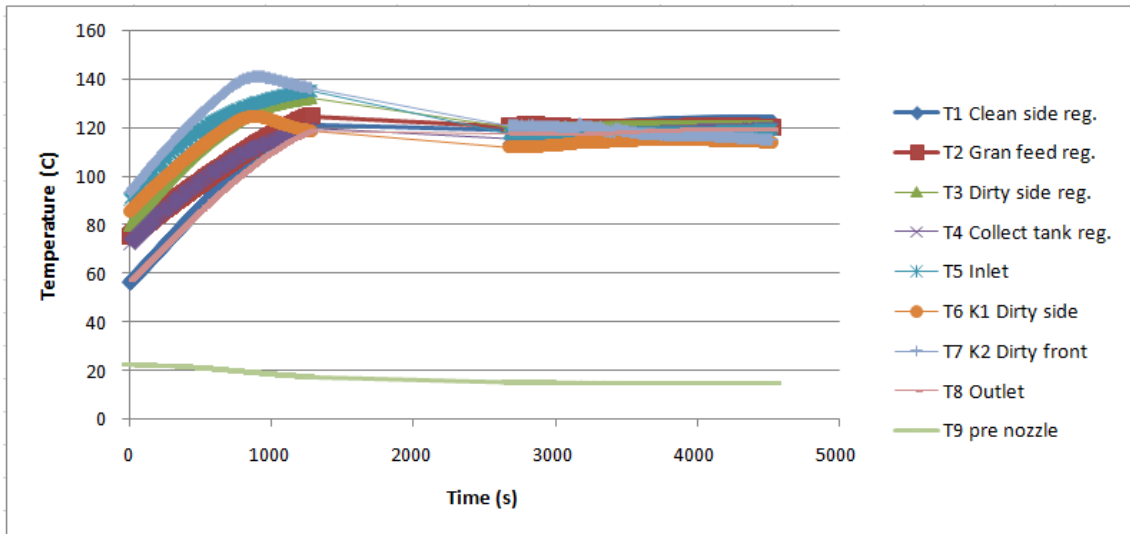
Figure 4.7: Heating test #2.

Test #2

During the second heating test the logging of the temperatures was not started before the temperatures reached about 60 °C. All the temperatures were increasing steadily which is shown in figure 4.7. The hot air passing through the filter during the test created a more stable and uniform temperature all over the filter. It was discovered that the temperature of the inlet air needed to be changed with the volume flow especially when the dust feeder was in operation. With a temperature of 170 °C at the hot air inlet the heating took about 50 minutes from ambient temperature. At the end of this test the regulation temperatures only deviated by 4 °C. All the other temperatures were stable and had acceptable values around 120 °C. The cooler also performed well and kept the temperature at the inlet of the vacuum pump at an acceptable level as shown in the figure (T9 pre nozzle).

These values of regulation and temperatures can be used in full tests. Still it is important to adjust the inlet temperature to give the right amount of heat. The volume flow of hot air and the flow of cold air from the dust feeder are the most important parameters when it comes to adjusting the hot air inlet temperature.

4.1.3 Filtration test

The filtration tests showed that the temperature on the filter was fluctuating. Adding the granular media and the inlet aerosol had more effect on the temperatures than first assumed. The heating calibration was good enough to be used for heating of the rig, but temperature regulation was needed during the test to sustain a good temperature range at all times. The outlet gas was sufficiently cooled by the heat exchanger maintaining an outlet temperature below 19 °C as long as the cold water was running.

No puffs were applied during the first two tests. This was due to the low dust feeding rate at 1 g/m^3. At this rate the pressure drop over the filter did not reach 1500 Pa, which was set as the maximum allowed pressure drop, during a day of

Results and discussion

Test	Velocity	Puff	Dust on absolute	Filtration	Dust flow	Total dust	Emission
(#)	(cm/s)	(Pa)	filter (g)	efficiency (%)	rate (g/h)	used (g)	(mg/Nm^3)
1	10	1500	0,1	99,913	23	115	0,9
2	10	1500	0,2	99,839	23	124,6	1,6
3	10	1500	1,7	99,552	69	379,5	13,4
4	10	1500	1,2	99,783	69	553,2	6,5
5	10	2000	1,8	99,495	69	356,5	15,1
6	10	2000	1,4	99,573	69	327,8	12,8
7	15	1500	1,2	99,652	103,5	345,1	10,4
8	15	2000	3,4	99,456	103,5	621,2	16,4
9	15	2000	2,2	99,528	103,5	465,9	14,2
10	20	1500	0,9	99,837	138	552	5,0

Table 4.2: Results from the filtration tests on the filter tray test rig.

testing. Therefore the dust feeding rate was increased from 1 to 3 g/m^3 from test three. Test three was therefore the first test where a puff-back was performed during filtration. The firs puff-back utilized input values obtained from the puff-back calibration. However, it was soon discovered that the spill from a hot bed with cake formation attached did not give a spill resembling to the calibration data. The puff-back consistently created about double the amount of spill compared to the calibration tests. The puff-back was more dependant of the dust cake settlement and the elevated temperature than anticipated. As described in the theory this is believed to be caused by the dust particles binding the granular media together. The heating of the cold air used in as a pulse could contribute to greater spill. The puff-back input values were therefore adjusted to provide the desired spill. More puff-back tests needed to be performed in order to obtain a sufficient amount of data to re-calibrate under filtration conditions. This was not done because each filtration test provided to few puff-backs. Anyway, the puff-back calibration needs to be performed in relation to the residual pressure measurements. These measurements are only possible to obtain from longer filtration tests.

The filtration tests also showed the ability of the rig to perform as a filter. The results from the tests performed are shown in table 4.2 obtained from the results and the analysis attached in the electronic appendix following the thesis. Comparing the averaged emission from the tests performed at 23 g/h (test 1 and 2) and at 69 g/h (test 3 and 4) all with a maximum allowed pressure drop at 1500 Pa, in table 4.2, provides an increasing emission rate with increasing dust flow rate (three times higher) by 796%. Comparing the first test to the last test in the same way shows an increase by 400% where the inlet dust concentration is three times higher than in the first tests. The highest emission rates were obtained from the tests performed with a maximum allowed pressure drop of 2000 Pa. The results could indicate lower filtration efficiency at higher dust flow rates and maximum pressure drop allowed, or that an alteration needs to be performed with the puff-back system to obtain the same good results as in the tests where low dust flow rate and low maximum pressure drop allowed was used.

Results below the EU regulation limits for emission from gaseous fuels at 5 mg/Nm^3 are obtained from test 1, 2 and 10. This shows that the filter tray test rig already during startup tests obtain good results.
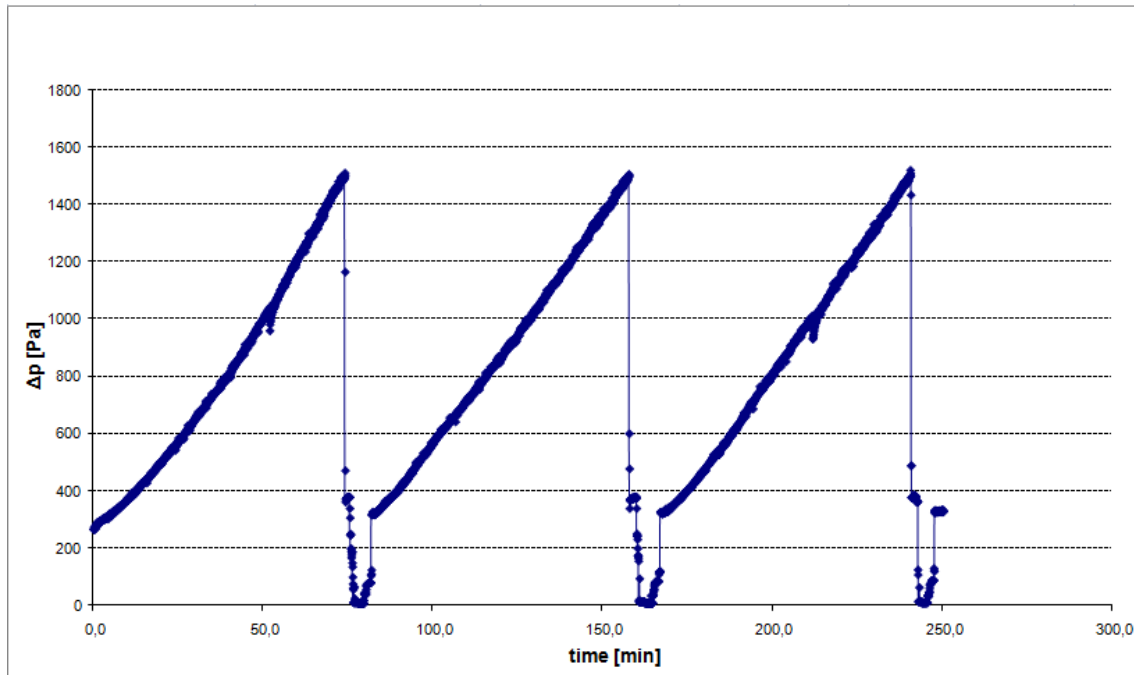
Figure 4.8: Pressure drop from test 10.

Figure 4.8 shows the pressure drop increase in test 10. At a concentration of $3g/Nm^3$ the pressure builds up to 1500 Pa in about 72 minutes. Three puff-backs where applied during this test. The test shows that the buildup is consistent and fairly even. It indicates that the filter is working as it should, collecting dust and forming a filter cake which increases the pressure drop. For each puff-back applied the residual pressure was measured and plotted in figure 4.9. It is preferable that the residual pressure is stable after the first few puffs. This test indicates that the residual pressure slightly increases but seems to stabilize. However, only longer tests would show if the residual pressure stabilizes over time. A stable residual pressure indicates that the right amount of granular media was removed. Therefore a wider analysis and calibration of the pulse should be performed alongside with the residual pressure investigation.

4.2 L10-56 test rig

The results from the puff-back and heating tests on the L10-56 filter test rig are presented in this section.

4.2.1 Horizontal bed unit (HBU)

The HBU was not tested during this work, however, it was built and programmed to be ready for testing at the next opportunity.
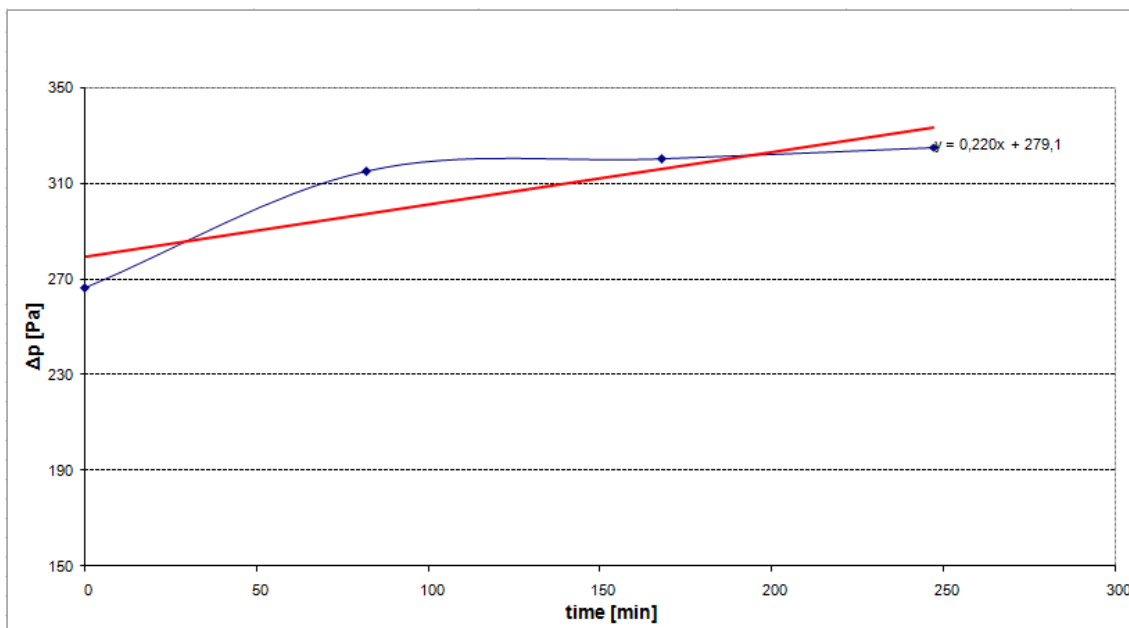
Figure 4.9: Residual pressure evolvment during test 10.

4.2.2 Puff-back calibration

The results and analysis of the results are included in the electronic appendix attached to the thesis.

Puff-back spill calibration

Figure 4.10 shows the spill calibration data. Only results within the ideal spill range are shown. The aim is to have a figure that makes it easy to identify the relationships between tank pressure, how long the valve needs to be in the open position and amount of spill, in order to use it in later tests. The figure shows an approximately linear relation between spill, open position time of the valve and tank over pressure. For over pressure above 0,8 bar tests were only performed with the valve in a open position for 60 ms. This is because it will result in a spill greater than the upper limit of desired spill, which is 386 g.

Testing showed that the valve needed to be in an open position at least 60 ms in order to get repeatable results. Therefore only tests with valve open times starting from 60 ms are plotted into the graph. The figure shows that it is possible to extract the desired amount of spill with an over pressure in the tank of between 0,6 and 0,8 bar. The figure also shows that if the valve is in the open position 80 ms, the upper limit of desired spill is obtained. This means that within the range of 0,6 to 0,8 bar over pressure in the tank, and to keep the valve in an open position from 60 to 80 ms, is a good range that will sufficiently cover the desired amount of spill. The results from these tests show a significantly increasing spill compared to earlier performed spill calibration. This can be due to increased louver angle and granular media size distribution.
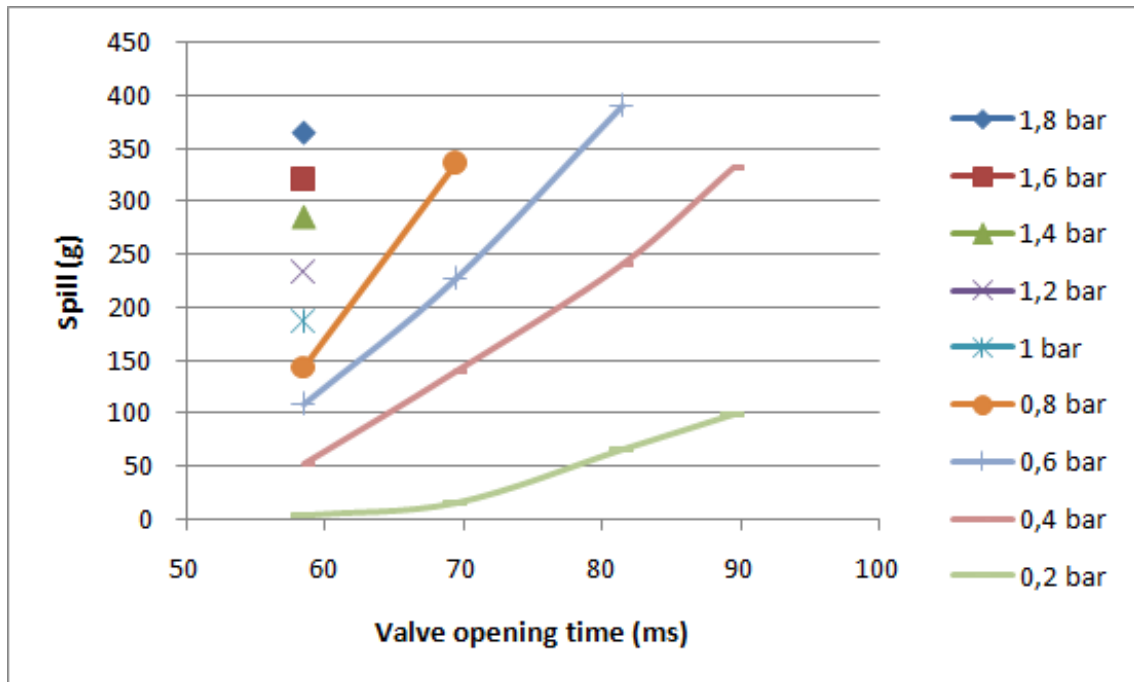
Figure 4.10: Puff-back spill calibration of the L10-56 filter.

Puff-back pulse calibration

An example of registered pulse is shown in figure 4.11 it was photographed during a puff of 90 ms and a tank pressure of 0,2 bar over pressure. This figure also explains the different graphs and how to read them. The lowest pressure drop needed to create spill Δp_{min} is found by finding the pressure drop Δp_{peak} at the lowest possible spill. Figure 4.12 shows that the tendency of Δp_{min} at approximately 600 Pa. The figure shows an unstable reading from the oscilloscope but the overall tendency of the tests is here taken into account. This is therefore set as minimum pressure drop to obtain any spill at all. Active time is then read as the time any pulse reaches beyond this value. The blue line in figure 4.11 show the active time obtained by the valve in open position 90 ms and 0,2 bar tank over pressure.

The graph in figure 4.13 is produces by reading all the active time values. It shows the relation between active time and the amount of spill. Ideally, according to the active time theory, the figure should only show a single line describing the relation between the active time and the spill. The results have the resemblance to a straight line, but have a lot of deviations. The variations are probably a result of unreliable measurements and uncertain reading. More accurate measurements and reading would decrease uncertainties and create easier and more accurate reading. A computer based accusation system could be a better solution in this case. The results could also suggest that the amount of spill is dependent on other variables as well, such as Risnes suggests in his specific impulse theory [18].

51
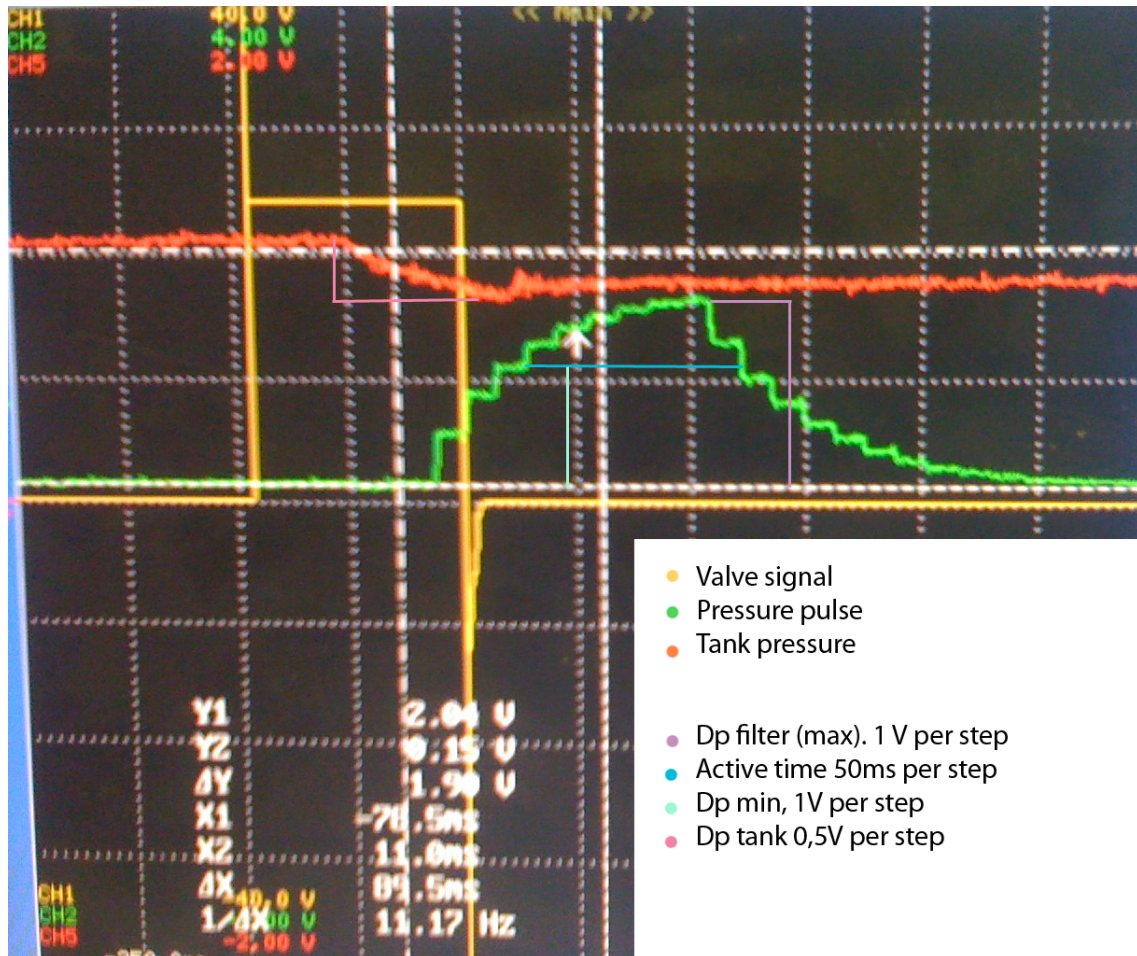
Figure 4.11: Picture from ociliscope at 90 ms and 0,2 bar.

4.2.3 Heating test

Test #1

The first test showed that the instrumentation was functioning well. The filter was heated and the logging showed a consistent heat rise in the different parts of the filter. However, as shown in figure 4.14 the different areas of the filter was not increasing simultaneously, therefore did not reach the desired end temperature at the same time. The figure shows that after about two and a half to three hours the front and back cone reached the desired temperature and was able to stabilize. Regulation area two, controlling the louver part, increased its temperature at a lower rate, which can be explained by the greater mass to heat at the louver and feeder of granular media. Also the total length of heating cables connected to the regulator would reduce the effect and less heat are conducted in the heating cables. More details are given in appendix A.2. A table of the temperatures at the different temperature measurement points and the maximum effect $A_\%$ are given in table 4.3. The temperatures were extracted from LabView after 3 hours, when most of the temperatures were stabilized. This table shows that the regulator two temperature stops at 300 °C when the front cone and the back cone reached the desired temperature of 350 °C. Although regulator two used maximum allowed
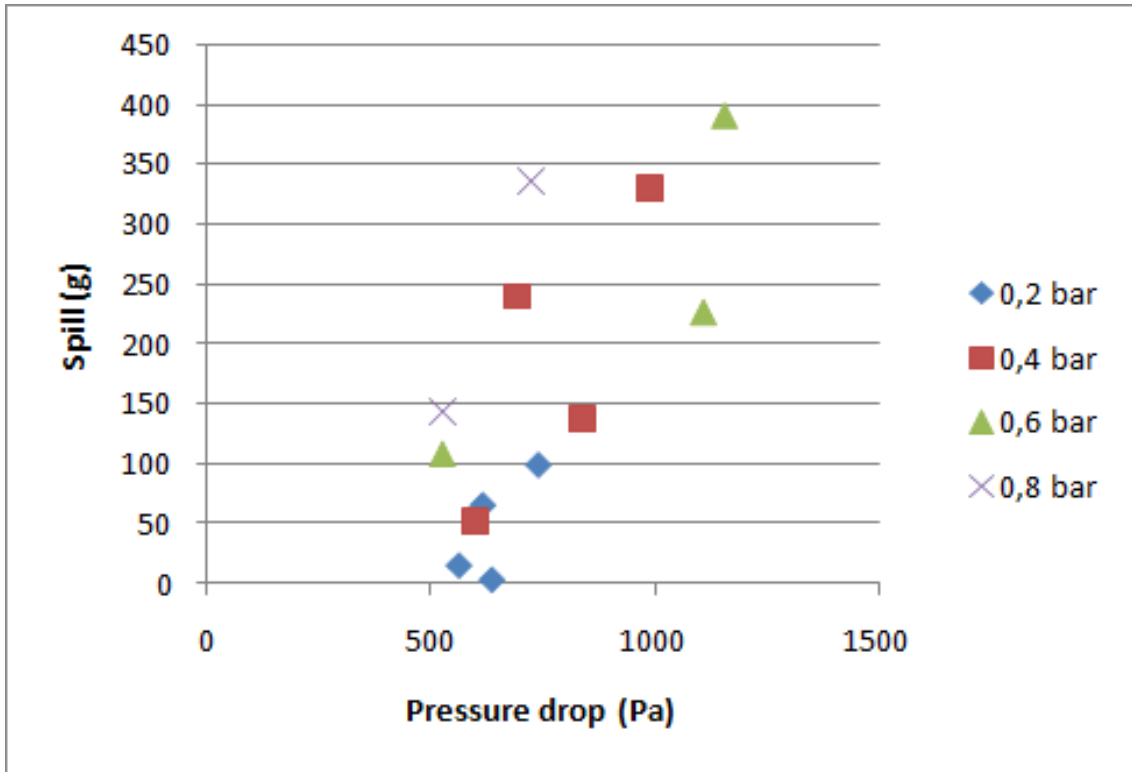
Figure 4.12: Δp_{min} for L10-56 test rig.
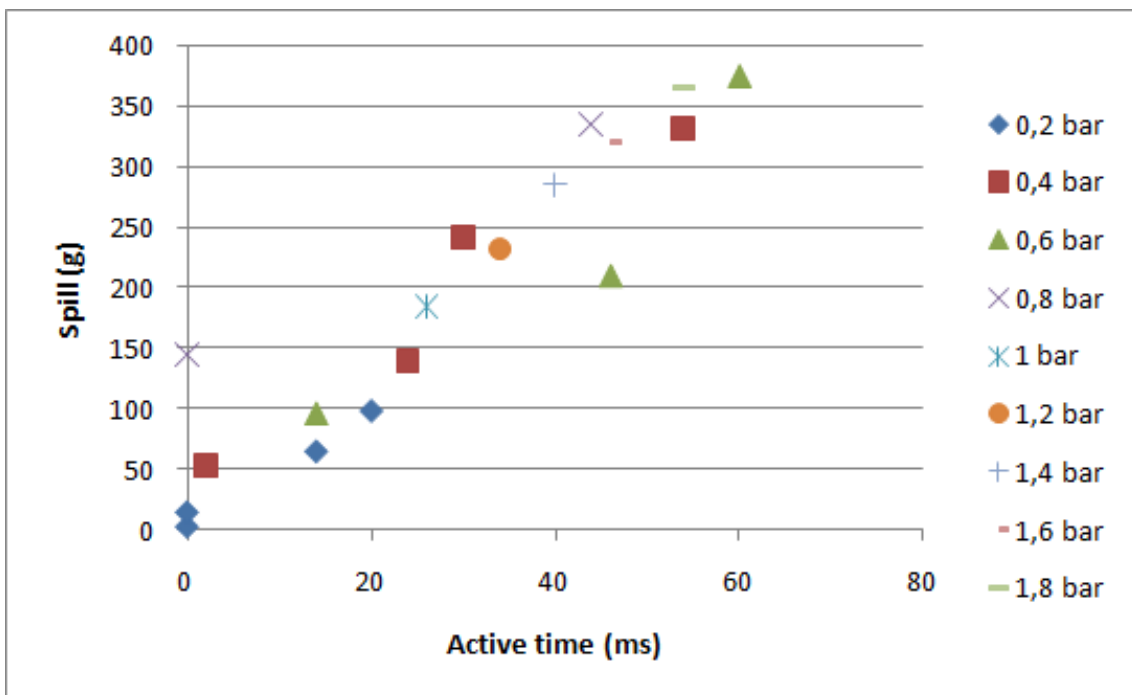
Figure 4.13: Active time for the L10-56 test rig.
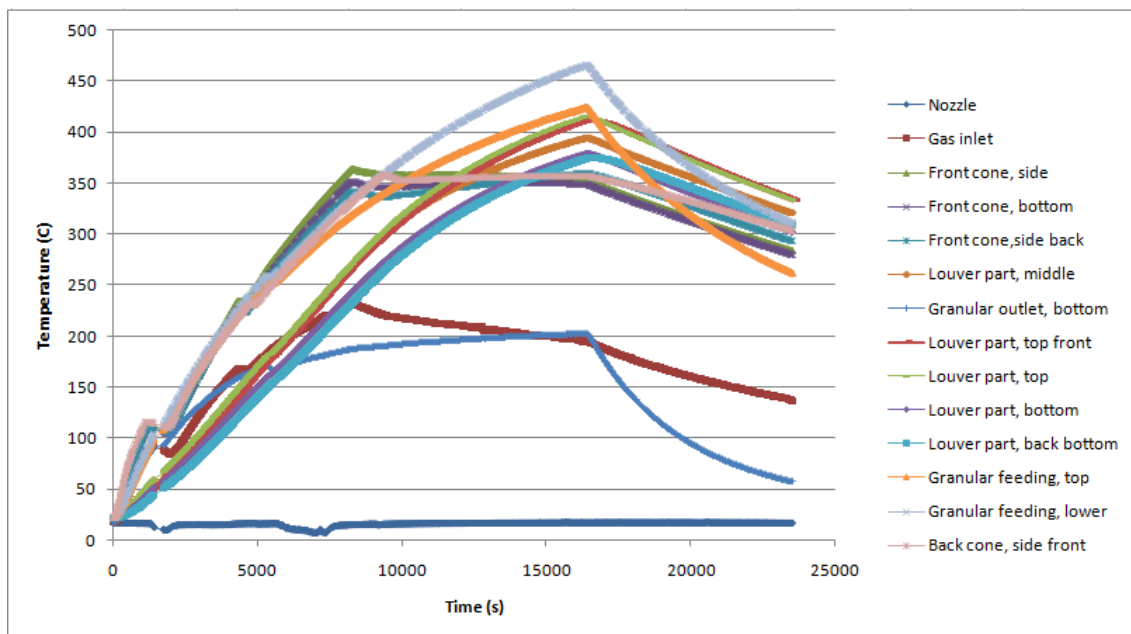
Figure 4.14: Temperatures from heating test #1.

Thermocouples										Regulators			A%
T1	Noz	18,5		T7	A4	350		T13	B6	320	R1	A5	350	18
T2	A1	210		T8	B3	350		T14	D2	382	R2	E2	300	30
T3	Lab	18		T9	E1	197		T15	D1	413	R3	C3	350	10
T4	Lab	18		T10	B5	362		T16	C1	356	R4	N/A	N/A	N/A
T5	A3	359		T11	B4	364							
T6	A6	348		T12	B2	327							

Table 4.3: Results from heating test #1 after 3 hours.

power, it was not able to reach more than 300 °C, however, figure 4.14 shows that the temperatures in this area kept rising through the entire test. This means that the regulator temperature was measured on a point that was not representative for the area. The solution might be to move the temperature measuring point to a more representative point. T8, in table 4.3, is closest to the median temperature of the heating area. This point could therefore be chosen to give the regulator a representative regulation temperature. In further tests the temperature in the middle of the filter area (T8) will be used instead of the one used for regulator two during this test.

Test #2

Figure 4.15 shows a more simultaneous rise of all the temperatures including the middle section in the second test. This indicates that the ramping set point regulation is better and easier to use than the manual set point regulation. However, there are still some problems with regulator two. This regulator is still not able to give enough effect to keep up with the other regulators. Regulator two was working

Thermocouples										Regulators			A%
T1	Noz	18		T7	A4	349		T13	B6	333		R1	A5	350	18
T2	A1	224		T8	E2	185		T14	D2	298		R2	B3	350	40
T3	Lab	19		T9	E1	100		T15	D1	349		R3	C3	350	10
T4	Lab	19		T10	B5	359		T16	C1	359		R4	N/A	N/A	N/A
T5	A3	356		T11	B4	361									
T6	A6	349		T12	B2	330									

Table 4.4: Results from heating test #2 after 6 hours.

constantly at the maximum $A_\%$ allowed effect while the other two regulators were working up and down within their limits. This means that the middle regulator needs more effect to keep up with the ramping temperature rise. The $A_\%$ for regulator two was therefore increased in the middle of the test from 30% to 40%. The power output calculations for each regulator are shown in appendix A.2.

There were still some problems during the settling of the temperature of regulator two. The regulator parameters were not optimal. It was discovered that the regulator was set to rise well above the set point and then reduce temperature to desired settling point. This resulted in a high temperature in the middle of the filter. After a while the temperature settled at the desired temperature. Adjusting the regulation parameters for regulator two should solve the problem before the third test.

Figure 4.15 shows the temperature rise in the filter rig. The two highest temperatures are the temperatures on the granular feeding (top and lower) which are settling below desired temperature when the regulation becomes stable. The two lowest temperatures are the granular outlet (up and bottom). The reason for this is most likely that they are located at the bottom of the filter, while the heat rises to the top. This means that the granular feeding get the two highest temperatures because it is on top of the filter and the outlet get the lowest temperatures because they are at the bottom of the filter. In addition, a minimum of insulation is added for easy access to fit the outlet valve and the collecting tank at a later stage.

As seen in figure 4.15 the gas inlet temperature is also low. This is probably due to poor insulation at the inlet and direct contact with the air from the laboratory. The cold air and draft from the laboratory seem to have an effect on the temperature measured in the inlet area. When the inlet of the filter is connected to the inlet pipe before the full test, more sufficient insulation will be provided and the hot air inlet will most likely sustain a satisfactory temperature.

A table of the temperatures at the different temperature measurement points and the maximum effect $A_\%$ is given in table 4.4. The data was extracted from a LabView program after 6 hours and 8 minutes, when the temperatures were stabilized.

Test #3

The third test showed that the regulators finally were adjusted to good parameters. Figure 4.16 shows that the temperature is rising steadily and simultaneously towards 350 °C. Only the top temperatures are rising more rapid and higher. They finally
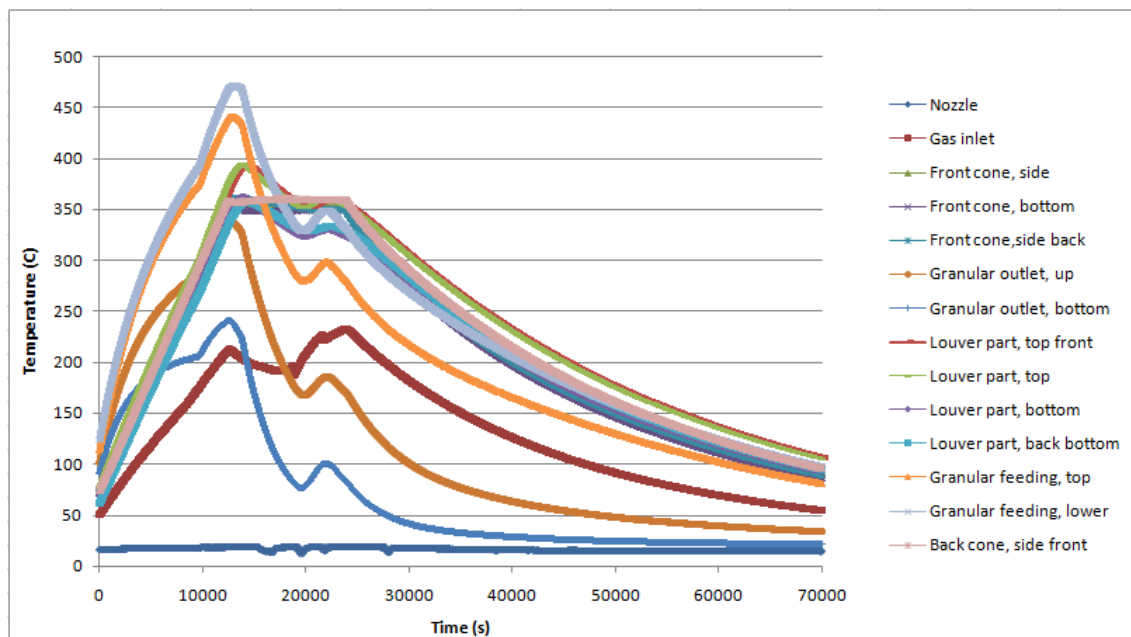
Figure 4.15: Temperatures from heating test #2.

Thermocouples										Regulators			$A_\%$
T1	Noz	18		T7	A4	349		T13	B6	330	R1	A5	350	18
T2	A1	257		T8	E2	180		T14	D2	291	R2	B3	300	30
T3	Lab	20		T9	E1	94		T15	D1	341	R3	C3	350	10
T4	Lab	20		T10	B5	356		T16	C1	359	R4	N/A	N/A	N/A
T5	A3	358		T11	B4	357								
T6	A6	350		T12	B2	327								

Table 4.5: Results from heating test #3 after 7 hours.

reach about 450 °C before they start to decrease and settle at an acceptable level. All of the important temperatures eventually settles around 350 °C and are stable during the rest of the test which lasts 8 hours and 26 minutes. The two highest temperatures need to be taken into account during full filtration tests, because it is believed that adding the granular media can affect the heating test. The third heating test finalizes the preheating tests with good results. Further work with the regulation to reach a more uniform temperature will enquire changes in the layout of the heating pads or increasing the number of regulators.

Table 4.5 shows the temperatures at the different temperature measurement points and the maximum effect allowed for each regulator. The data was extracted from a LabView program after 7 hours of the test and the same reasons for the lack of heating at certain points on the filter as in the second test apply here.

The new method of regulating the temperature automatically and stepwise all in all showed good results. This setup for the rig will be used in the further filtration tests performed on the L10-56 test rig.

Figure 4.16: Temperatures from heating test #3.

Chapter 5

Conclusion

Three tests were performed on the filter tray test rig: puff-back calibration, heat testing and filtration tests.

The puff-back calibration of the Filter tray test rig resulted in proving an even spill from the three filter trays. The tests also resulted in a tool created to easily obtain the right input values to the puff-back system to generate a given amount of spill.

The pulse calibration showed that the lowest pressure drop over the filter to create any spill at all, was between 80 and 120 Pa. It also highl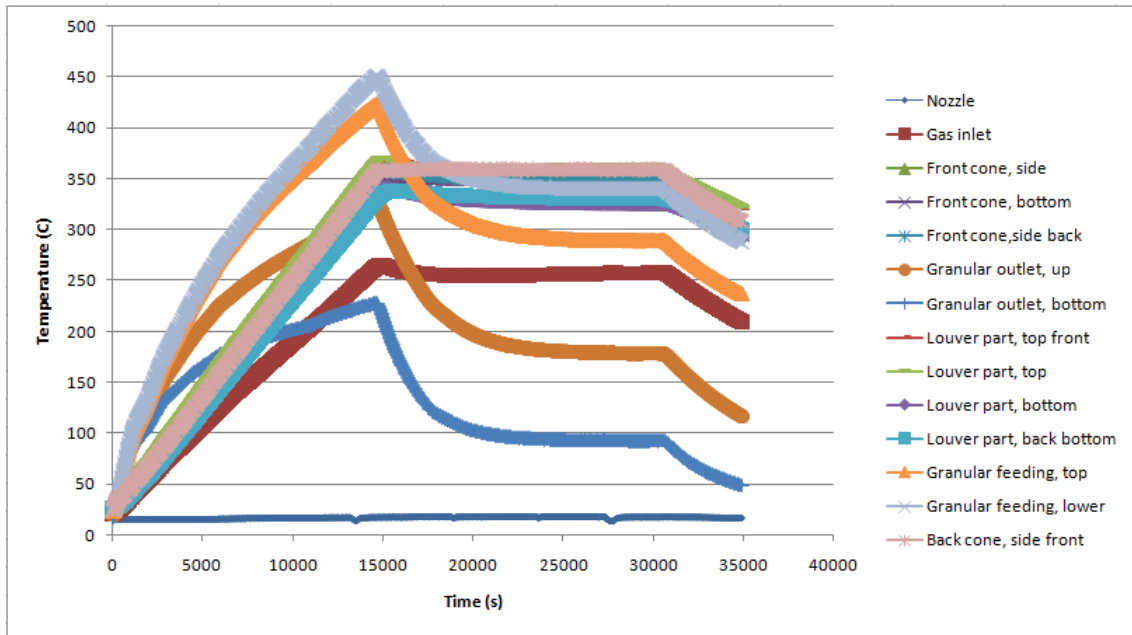ighted a certain dependency between the spill and the active time theory. It was discovered that a spill of 200 g of alumina spheres required a usage of 3,2 l of air.

The heating tests performed showed, after some modifications, that the rig was able to reach and sustain a stable temperature at the design temperature of 120 °C. The rig was able to obtain this temperature after 50 minutes of heating.

The filtration tests performed on the filter tray test rig showed that the filter performed well. However, the spill was much more dependent on the cake formation on the filter, and the temperature than expected. This resulted in nearly twice the amount of spill than during puff-back calibration at ambient temperature without cake formation on the filter. Despite the large amounts of spill the residual pressure seemed to settle at about 330 Pa in the tests performed. A filtration efficiency above 99,5% was obtained. The calculated emissions from these tests are 0,9 to 15,1 mg/Nm^3.

Two tests, puff-back calibration and heat testing, were performed on the L10-56 test rig, and a HBU was constructed.

The HBU test rig was completed and ready to be used. All the necessary instrumentation and programs were in place for a test on the exhaust gas from the oil sand extraction pilot plant.

The puff-back calibration tests on the L10-56 test rig created a tool to easily obtain the right input values needed for the puff-back system to create the desired amount of spill. The spill was shown to be repeatable from test to test.

The Δp_{min} at 600 Pa obtained from the puff-back pulse calibration showed the same value obtained from earlier tests on this rig. This shows that more force is required for the L10-56 test rig than in the filter tray test rig, to create any spill. The pulse was also found to be dependant on the active time theory.

The heating tests performed showed an acceptable, uniform temperature

distribution over the filter rig. The instrumentation identified only a few areas on the rig which were not in the right temperature level. These areas are believed to be affected by the inclusion of sand and the hot gas flowing through the filter during filtration tests and were therefore approved despite the deviation. The filter was able to reach the operating temperature of 350 °C within a heating period of 4 hours.

Chapter 6

Proposal for future work

The work that has been completed with the panel bed filters can be developed further. An overview of potential future work is therefore included below.

6.1   General future work

Puff-back system

Improving the puff back system by improving the opening and closing times of the valve, could have great effect on the puff-back performance. Secondly altering the design of the puff-back system, i.e. shorten the pulse length and optimize the pressure within the tank could increase the efficiency and accuracy of the puff-back.

Flow measurement system

There is a large potential for improving the flow measurement system, which would enable easier and much more accurate flow measurements.

6.2   Filter tray design

Temperature

The filter tray test rig was only tested at 120 °C. The next step would be to increase the filtration temperature to 350 °C to meet industrial application needs.

Velocity

Higher velocities enable higher flow rates, or reduce the filtration area. The velocity also influences the filtration efficiency.

Pressure drop

The maximum allowed pressure drop tested was only 2000 Pa. Increasing the maximum allowed pressure drop over the filter could have positive effects on the filtration efficiency and filtration costs.

Filtration length

Increase the length of the filtration tests to define the behavior of the residual pressure.

Puff-back material

Analysis of the puff-backed materials could help determine how many layers of granular media to remove. It can therefore assist in improving the puff-back calibration.

6.3 L10-56 test rig

Particle Size Distributions

The particle size distribution of the input and the output dust is important to know the filter capability.

Bibliography

[1] C. Benestad, G. Braastad, and H. H. Normann et.al. Combustion plants - guidelines for environmental inspectors, 1995. veileder 95:13.

[2] R. C. Brown. *Air Filtration - An integrated approach to the theory and applications of fibrous filters*. Pergamon Press, ISBN 0-08-041274-2, 1993.

[3] W. L. Chiou. Us patent 7445123 - ceramic filter with a ceramic filter core cleaning device, 2007.

[4] J. Ødegaard. Gas cleaning with panel bed filter (PBF). Project thesis, Norwegian University of Science and Technology, EPT-P-2008-73, 2008.

[5] Statens forurensningstilsyn. Forskrift om begrensning av forurensning (forurensningsforskriften), Miljøverndepartementet, FOR 2004-06-01 nr. 931, 2004.

[6] G. Krammer. Compendium in environmental and cleaning technologies, Norwegian University of Science and Technology, 2006/2007.

[7] C. S. Lee and A. K. Li. Us patent 5382396 - method of making a porous ceramic filter, 1995.

[8] K. C. Lee. *Filtration of redispersed power-station fly ash by panel bed filter with puffback*. PhD thesis, The City University of New York, 1975.

[9] K. C. Lee, I. Rodon, M. S. Wu, R. Pfeffer, and A. M. Squires. The panel bed filter. Technical report, Electric Power Institute, Palo Alto, California, 1977. EPRI AF-560, Final report, May 1977.

[10] F. Löfler, H. Dietrich, and W. Flatt. *Dust collection with bag filters and envelope filters*. Friedrich Vieweg und Sohn Verlagsgesellschaft mbh, ISBN 3-528-08933-4, 1988.

[11] R. Mai, H. Leibold, H. Seifert, and S. Heidenreich. Operation behavior of a multi-candle filter with coupled pressure pulse recleaning during normal operation and in the case of a filter candle failure. Technical report, Department of Energy, Office of Scientific and Technical Information, DOE 835772, 2002.

[12] M. J. Matteson and C. Orr. *Filtration principle and practices*. Marcel Dekker, Inc. ISBN 0-8247-7582-1, 2. edition, 1987.

[13] The European Parliament and the Council of the EU. On the limitation of emissions of certain pollutants into the air from large combustion plants, Directive 2001/80/EC, 2001.

[14] W. Peukert. High temperature filtration in the process industry. *Filtration and separation, Vol 35, pp 461-464*, 1998.

[15] W. Peukert and F. Löffler. Influence of temperature on particle separation in granular bed filters. *Powder technology, Vol 68, pp 263-270*, 1991.

[16] D. B. Purchas and K. Sutherland. *Handbook of filter media.* Elsevier Advanced Technology, ISBN 978-1856172783, 3rd edition, 2002.

[17] D. B. Purchas and K. Sutherland. *Handbook of filter media, p. 1.* Elsevier Advanced Technology, ISBN 978-1856172783, 3rd edition, 2002.

[18] H. Risnes. *High temperature filtration in biomass combustion and gassification processes.* PhD thesis, Norwegian University of Science and Technology, ISBN 82-471-5463-3, 2002.

[19] I. Rodon, K-C Lee, R. Pfeffer, A.M Squires, and O.K. Sønju. Granular-bed filtration assisted by filter-cake formation 2. The panel bed gas filter with puffback renewal of gas-entry surfaces. *Powder Technology Vol 155, pp 52-61*, 2005.

[20] Ø. Saanum. Videreutvikling av panelbedfilter for rensing av høytemperatur røykgass. Master's thesis, Norwegian University of Science and Technology, Project number 95:43, 1996.

[21] A. M. Squires. Us patent 7033556 - method and apparatus for treating fluids and non-fluid materials, 1967.

[22] A.M Squires. Granular-bed filtration assisted by filter-cake formation: 4. Advanced designs for panel-bed filtration and gas treating. *Powder technology, Vol 155, pp 74-84*, 2005.

[23] D. Stanghelle. Gassrensing med granulært filter for høytemperatur anvendelser. Master's thesis, Norwegian University of Science and Technology, EPT-H-2004-62, 2004.

[24] D. Stanghelle. *High temperature filtration of biomass combustion and gasification processes.* PhD thesis, Norwegian University of Science and Technology, ISBN 978-82-471-1085-0, 2008.

[25] D. Stanghelle, A. Norheim, J. Hustad, and O. K. Sønju. High temperature granular bed filtration of biomass gasification gas. Presented and published in proceedings of the 10th world filtration congress Leipzig, Germany, April 14-18, 2008.

[26] M.S. Wu, K.-C. Lee, R. Pfeffer, and A.M Squires. Granular-bed filtration assisted by filter-cake formation: 3. Penetration of filter cakes by a monodisperse aerosol. *Powder technology, Vol 155, pp 62-73*, 2005.

Appendix

Appendix A

L10-56 test rig

A.1   Panel Bed Filter
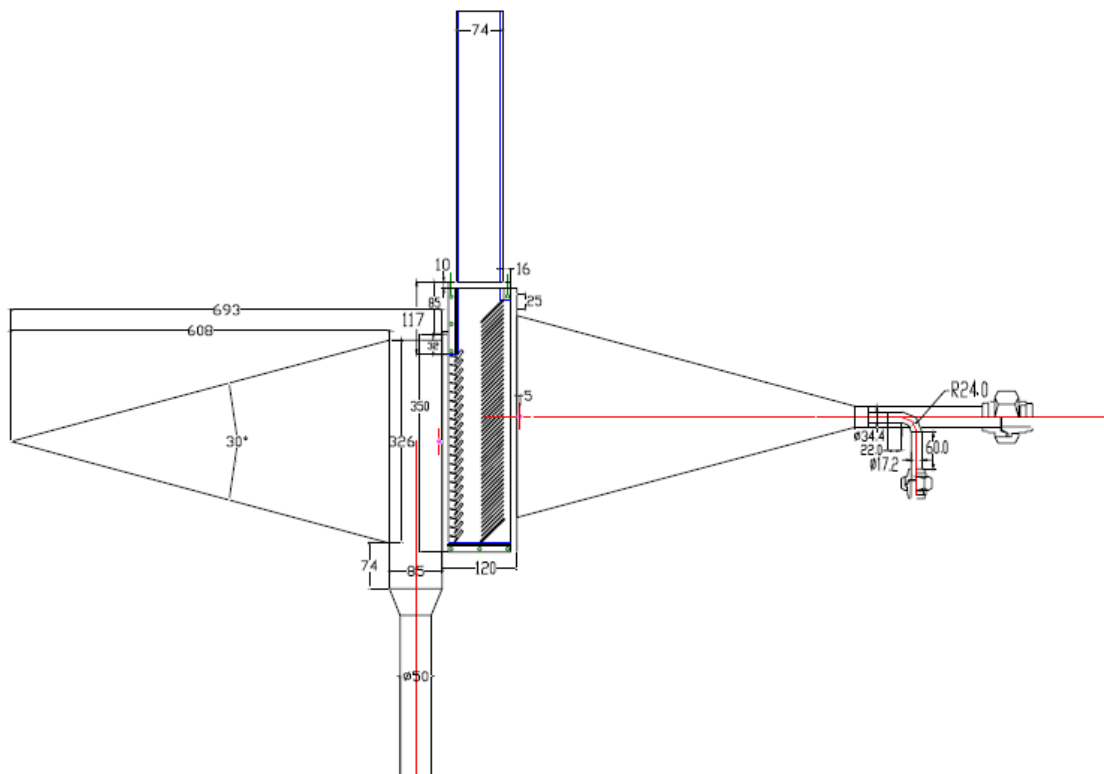
Figure A.1: Panel bed with dimensions.
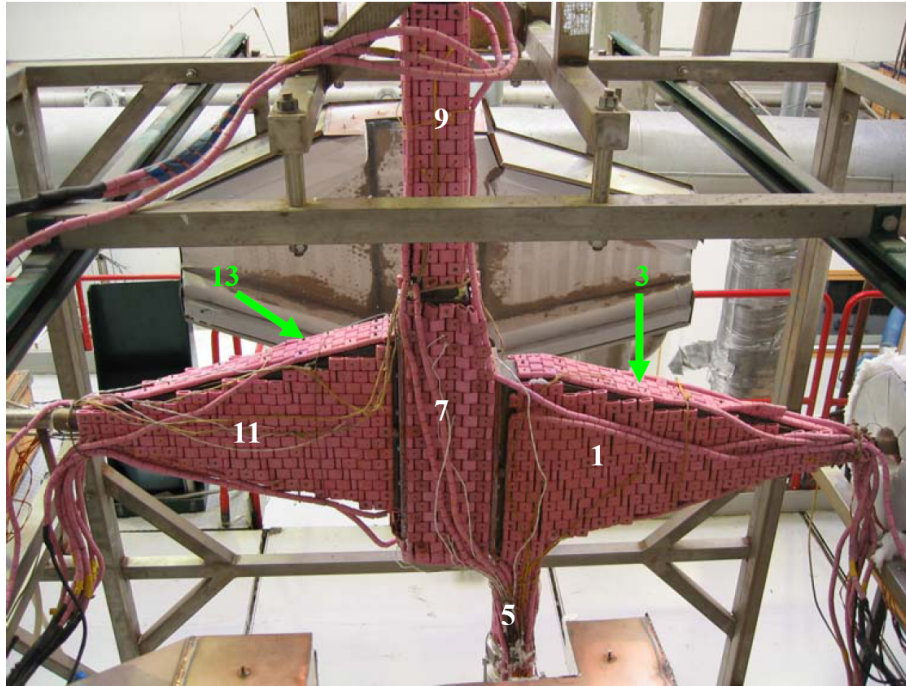
Figure A.2: Heating cables, right side seen from the outlet.

A.2 Heating cables

Three regulators are regulating the power input to the heating cables. Therefore the heating cables are divided into three areas which where each area have a designated coupling box. The coupling is done according to table A.1. The heating cables are coupled in series to increase the resistance. Length, resistance and cable effect are also shown in table A.1.
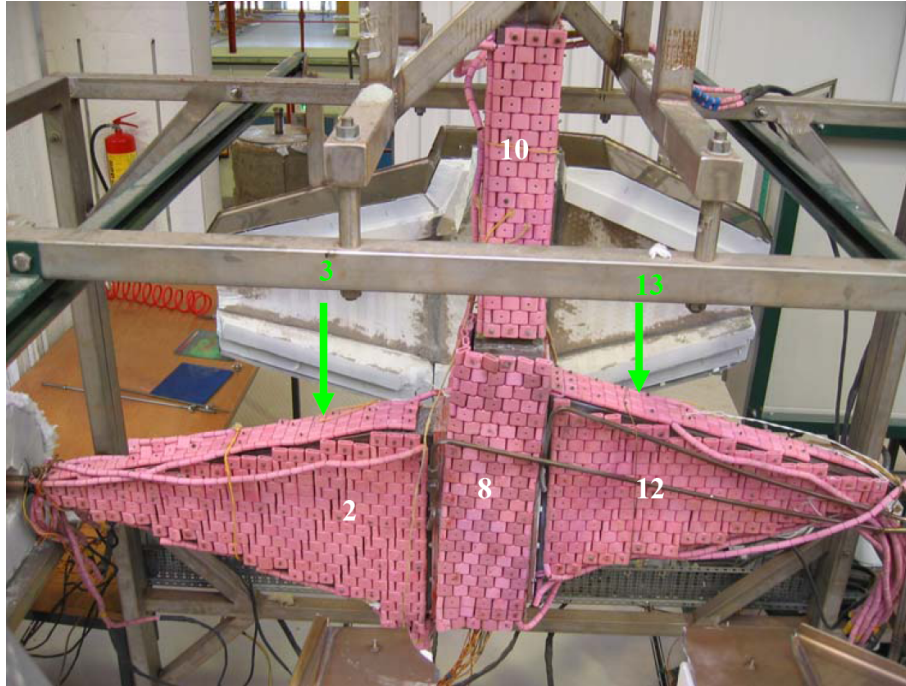
Figure A.3: Heating cables, left side.
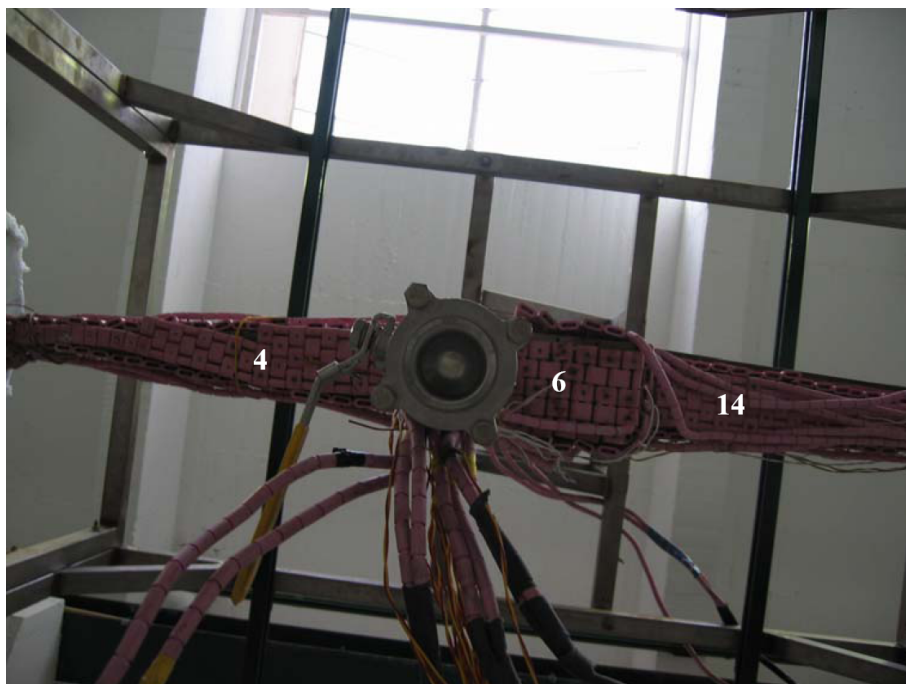
Figure A.4: Heating cables, from below.

Cable	Resistance [ohm]	Effect [W]	Effect per box [W]	Lengh [m]	Box
1	4,7	1556,1784		9,4	1
2	4,76	1576,0445		9,52	1
3	1,71	566,18406		3,42	1
4	1,47	486,71963		2,94	1
Total	12,64		4185,126582	25,28	
5	1,9	407,76502		3,8	2
6	0,86	184,56733		1,72	2
7	3,23	693,20054		6,46	2
8	3,6	772,60741		7,2	2
9	2,9	622,37819		5,8	2
10	3,21	688,90827		6,42	2
Total	15,7		3369,426752	31,4	
11	3,62	1942,0739		7,24	3
12	3,65	1958,1684		7,3	3
13	1,3	697,42984		2,6	3
14	1,36	729,61891		2,72	3
Total	9,93		5327,291037	19,86	

Table A.1: Heating cables overview.
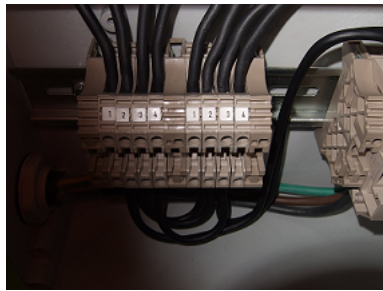
(a) Box 1.
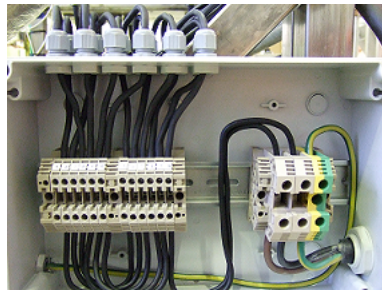
(b) Box 2.
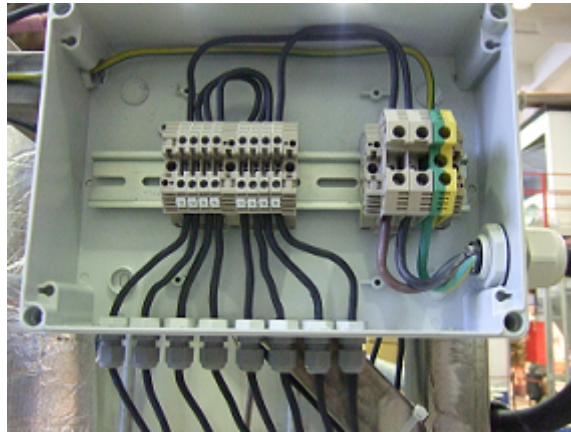
(c) Box 3.

Figure A.5: Coupling boxes.
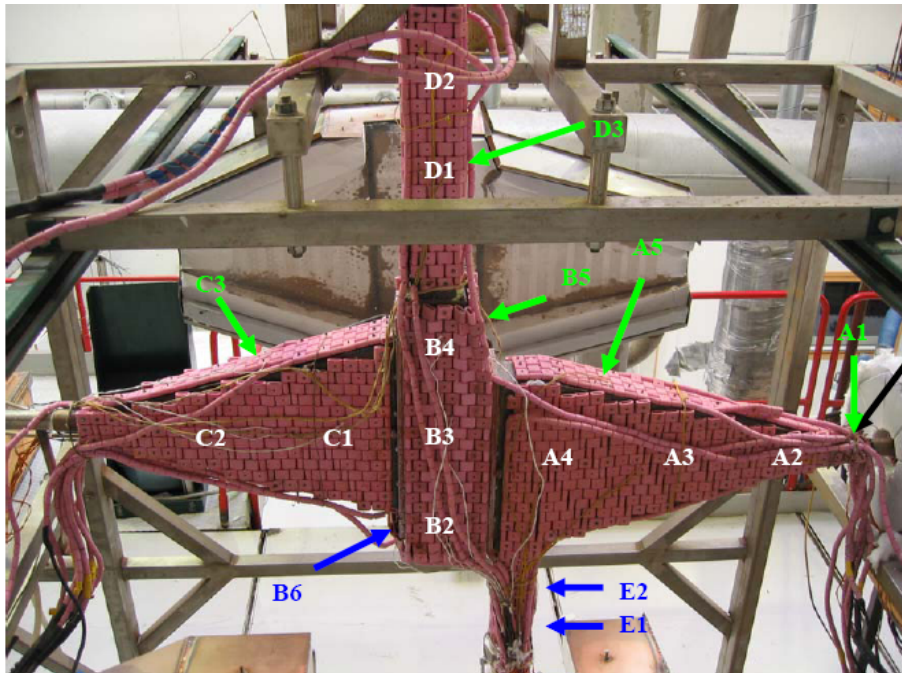
Figure A.6: Thermocouples, left side from absolute filter.

A.3 Placing of thermocouples
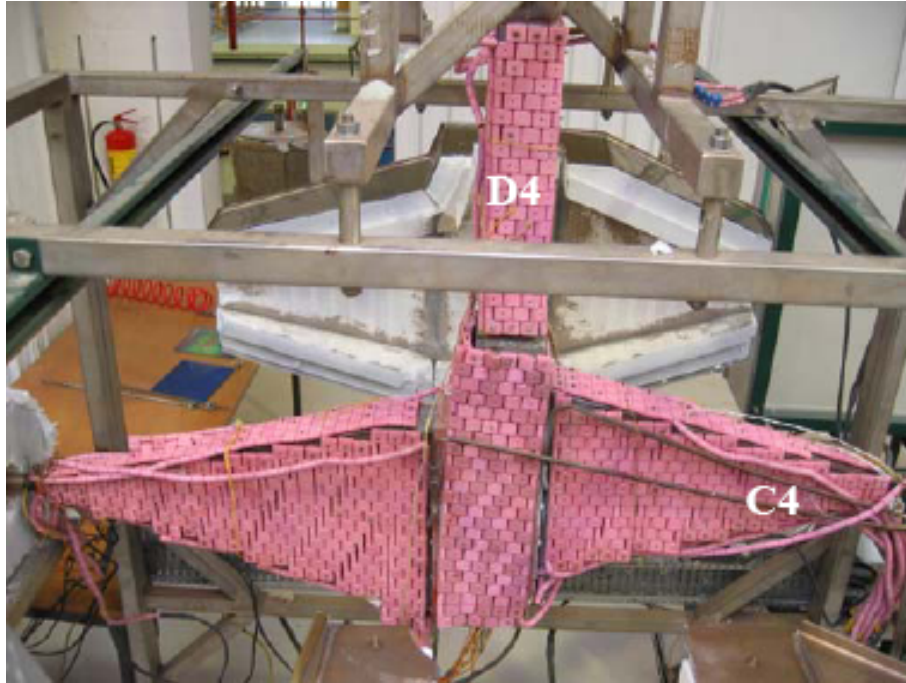
Figure A.7: Thermocouples, right side.
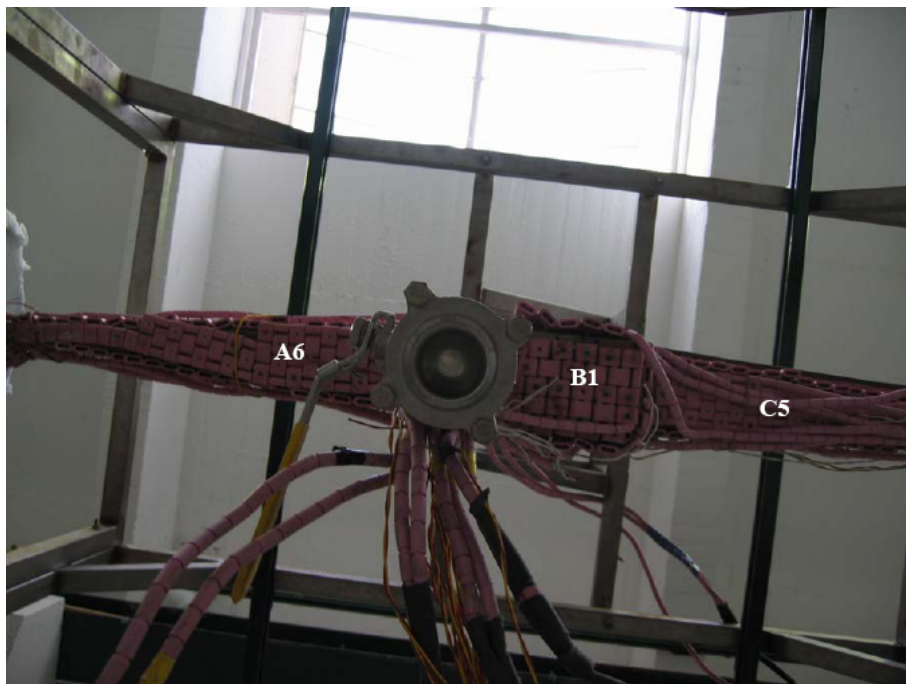
Figure A.8: Thermocouples, from below.

Appendix B

Filter tray design

This appendix include the instrumentation settup of the filter tray rig as well as the operating manual for the test rig. The manual is provided on norwegian only.
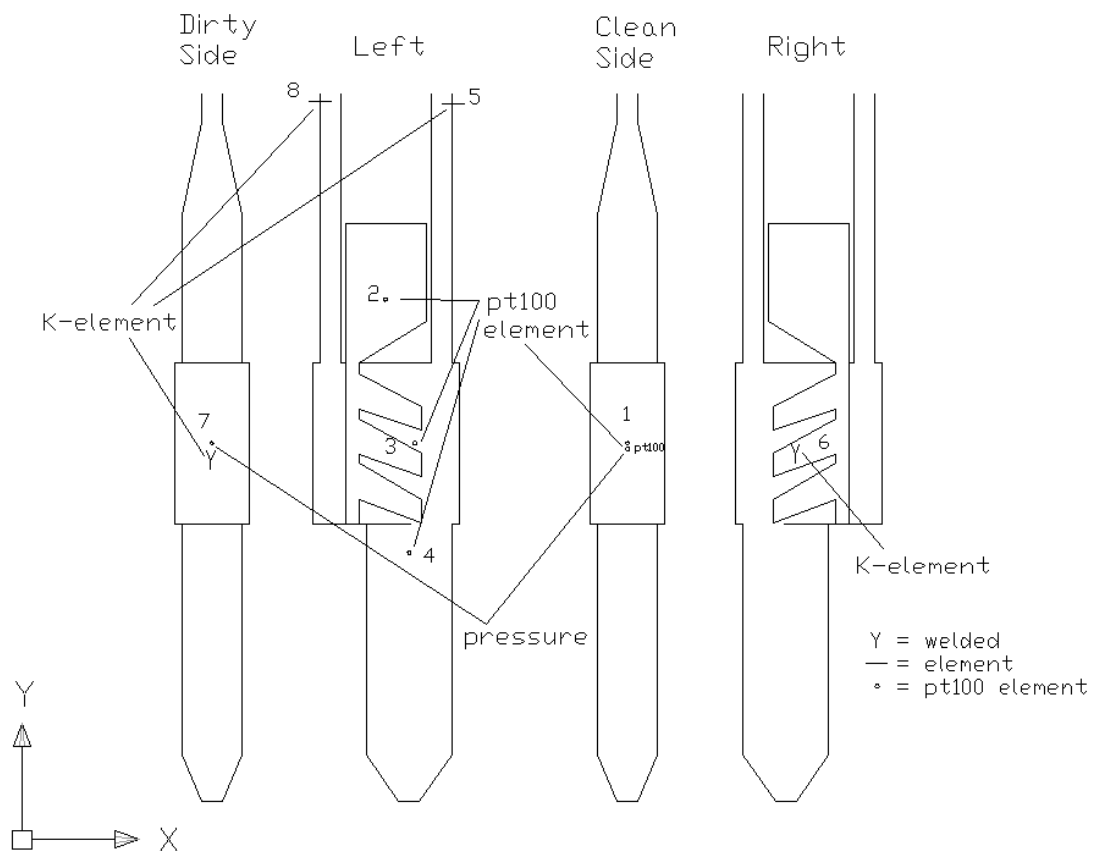
Figure B.1: Filter tray instrumentation.

Panel Bed Filter Ny labrigg (Kavita)

Hovedstrømsskjema skap1 Panel Bed filter (Kavita)

Dato	12.06.2009		Oppr. tegn.	Erst. for	Erst. av
Utført	Marius Døllner				
Godkj.	Marius Døllner				
Norm	NEK400				

Prosjekt nr.		Utg.	
Målestokk	Tegn.nr.		
1:1 A3		Blad 1	
	nr.1	N.bl.	

L1
L2
L3
N
PE

-F1   Merket A

-F2   -F3   -Q1

-F4   -Q2

-X1   -X2
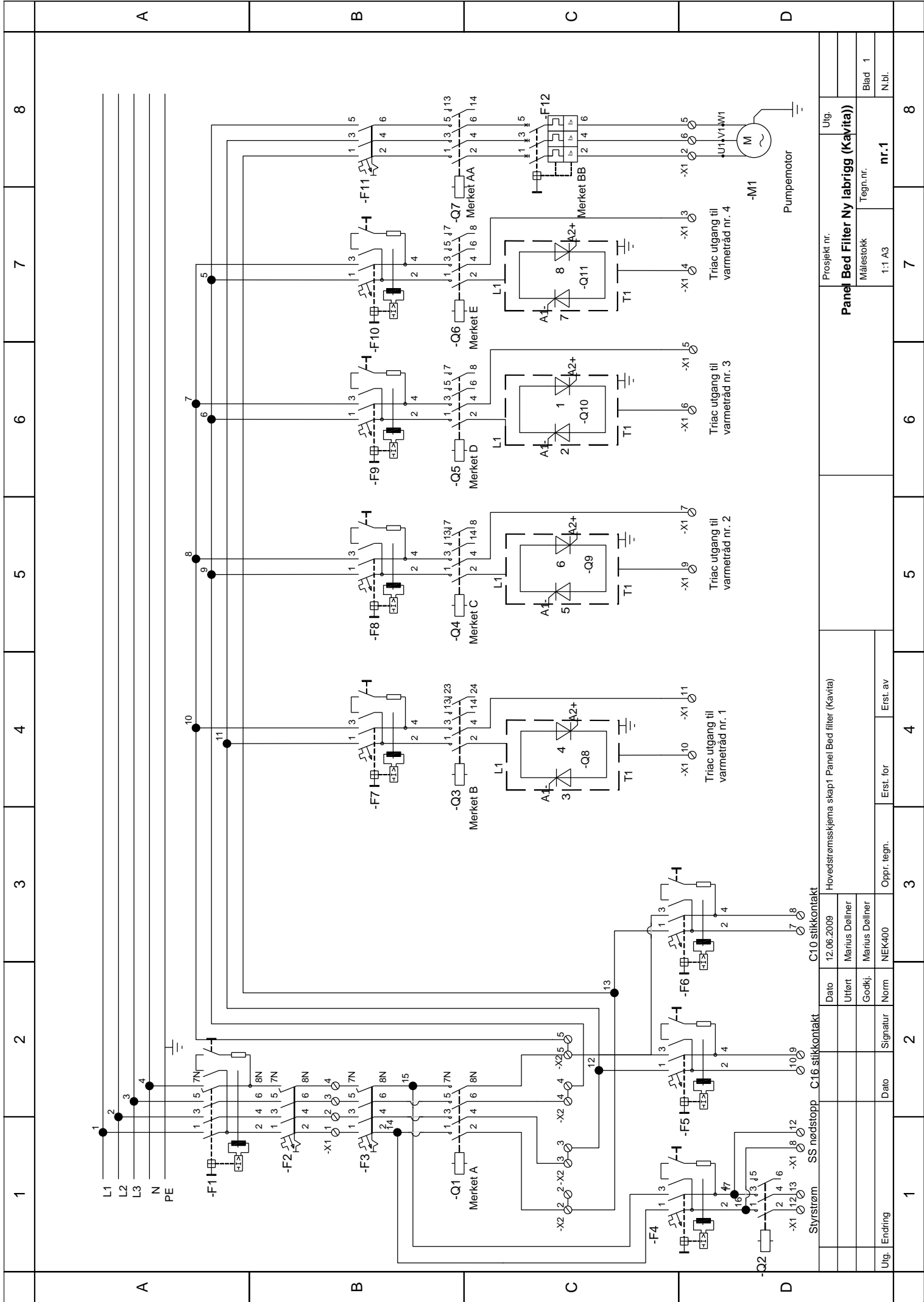
C16 stikkontakt

C10 stikkontakt

SS nødstopp

Styrstrøm

-F5   -F6

-F7   -F8   -F9   -F10   -F11

-Q3   Merket B
-Q4   Merket C
-Q5   Merket D
-Q6   Merket E
-Q7   Merket AA

-Q8
-Q9
-Q10
-Q11

-F12   Merket BB

Triac utgang til varmetråd nr. 1
Triac utgang til varmetråd nr. 2
Triac utgang til varmetråd nr. 3
Triac utgang til varmetråd nr. 4

-M1   Pumpemotor
M
U1,V1,W1

Merkes CC

Tilkoblet L1
bane 1D ved 12

Alle 54 merkes
bare med 5

Tilkoblet N
bane 1D ved 11

N Merkes DD

-S3
-S2
-S1
-Q2
-Q1

-S13
-S12
-S14
-Q1 (1.1)
-Q3 (1.2)

-S4
-S5
-Q4
-Q4 (1.3)
Merket B
Merket A-Q3
Merket C

-S7
-S6
-Q5
-Q5 (1.4)
Merket D

-S9
-S8
-Q6
-Q6 (1.5)
Merket E

-S11
-S10
-F
-Q7
-Q7 (1.6)
Merket BB
BB1
Merket AA

13
14
53
54
A1
A2

Merket CC

Tilkoblet L1
bane 6A
tegning nr.2
ved 3

-Q1 63 64 Merket A

-Q3 63 64 Merket B

-Q4 63 64 Merket C

-Q5 63 64 Merket D

-Q6 63 64 Merket E

-Q7 63 64 Merket AA

-F12 21 22 Merket BB

Alle 64 merkes 65

-H1 -H2 -H3 -H4 -H5 -H6 -H7

Tilkoblet N
bane 6D
tegning nr. 2
ved 4

Merket DD

			Date	15.06.09		Styrestrømskjema for Panel Bed filter skap 1			Prosjekt nr.		Utg.
			Utført	Marius Døllner					**Panel Bed Filter Ny lab rigg (kavita)**		
			Godkj.	Marius Døllner		Ark 2			Målestokk	Tegn.nr.	Blad 1
			Norm	NEK400		Oppr. tegn.	Erst. for	Erst. av	1:1 A3	**nr.3**	N.bl.
	Dato	Signatur									
Utg.	Endring		Dato	Signatur							
			2			3	4		7		8
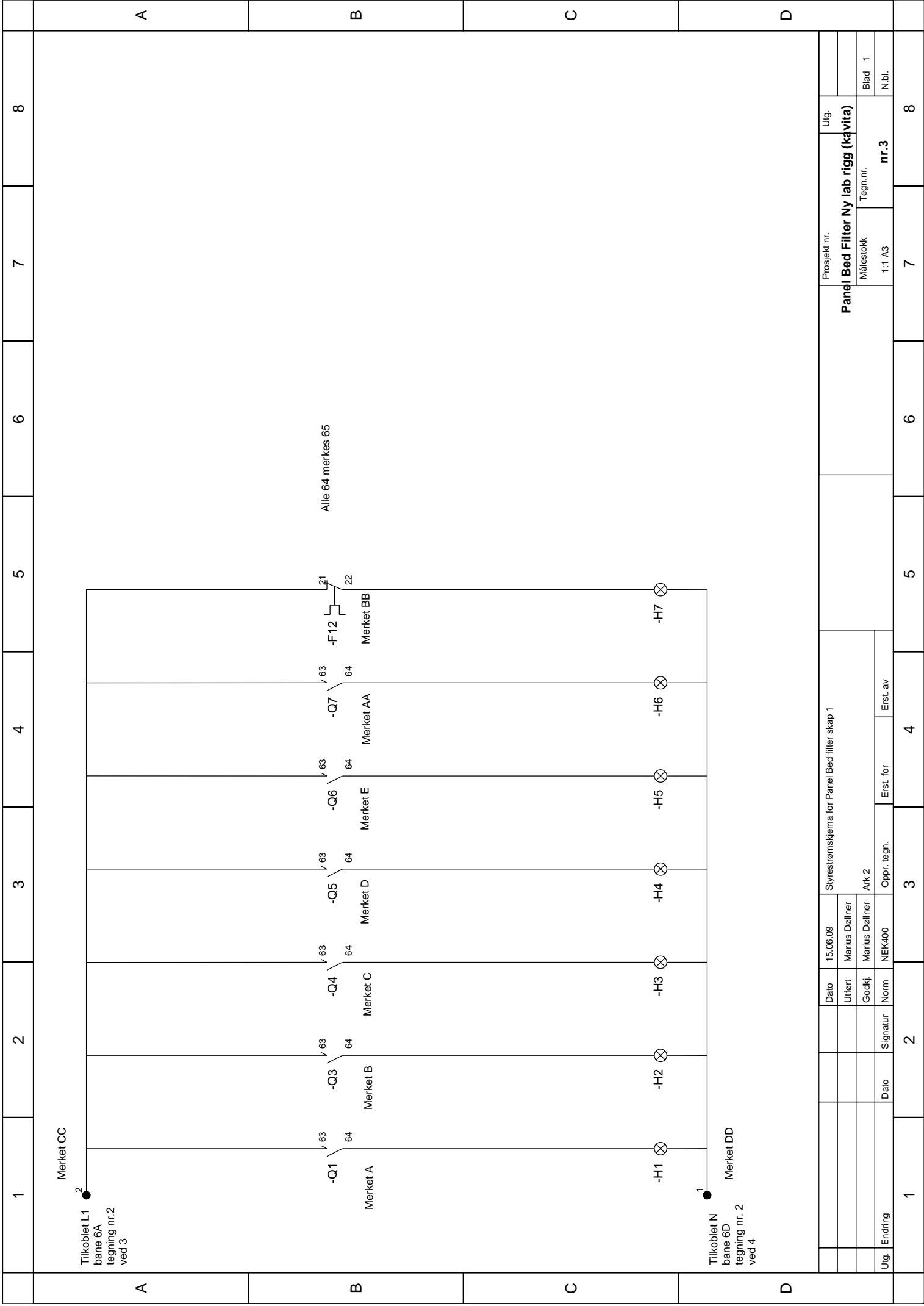
8 | 7 | 6 | 5 | 4 | 3 | 2 | 1

A | B | C | D

L1
L2
L3
N
PE

-F1
-F2
-F3
-Q1
-F4
-K1
-X1
-X2

230Vac

L1 tilkobling bane 1A tegning
nr.5

N tilkobling bane 1D tegning
nr.5

Logger

Omf. 230Vac til 24Vdc

Omf. 230Vac til 12Vdc

PN

Skap 1

Skap 2

TIC 1
9: L1 power
10: N power
Utgang til Triac -Q8
1: + 5V SSR (10+)
3: - SSR   (9-)
utg. fra NI9265 inp.AQ0
Inngang:
4: + 0-20mA
6: - 0-20mA

TIC 2
9: L1 power
10: N power
Utgang til Triac -Q9
1: + 5V SSR (10+)
3: - SSR   (9-)
utg. fra NI9265 inp.AQ1
Inngang:
4: + 0-20mA
6: - 0-20mA

TIC 3
9: L1 power
10: N power
Utgang til Triac -Q10
1: + 5V SSR (10+)
3: - SSR   (9-)
utg. fra NI9265 inp.AQ2
Inngang:
4: + 0-20mA
6: - 0-20mA

TIC 4
9: L1 power
10: N power
Utgang til Triac -Q11
1: + 5V SSR (10+)
3: - SSR   (9-)
utg. fra NI9265 inp.AQ3
Inngang:
4: + 0-20mA
6: - 0-20mA

Tilkoblet L1
bane 6 ved
punkt 5

Tilkoblet N
bane 6 ved
punkt 6

-S2
-S1
-K1 (1.1) 53 54
-K1 (1.1) 63 64
-H1
-K1 A1 A2

		Prepared by	Number	Date
EPT **HMS** **handbok**	**4.5.1.1 Preparations for Running Experiments**	E.L		03.08.2009
		Approved by	page	replaces
			1 of 3	

Må fylles ut før hvert forsøk.

Eksperiment, navn, nummer:	Dato/ Sign
Panel bed filter, new filter tray 2009	
Prosjekt leder:	
Otto K. Sønju / Kavitha Pathmanathan	
Eksperiment leder:	
Kavitha Pathmanathan	
Operatører:	
Jonas Hustad og Johnny Ødegård.	

	Utgangspunkt for forsøket:	Utført
	Eksperimenter gjennomføres mellom 08:00 og 15:00 (sommertid) 16:00 (vintertid)	
	Dersom eksperimentene kan påføre andre i nærheten konsekvenser skal de gis beskjed til de som blir berørt. Også bruk av felles utstyr eller ventilasjon etc. må koordineres med andre i laboratoriet.	
	To personer skal alltid være tilstede i laboratoriet hvor en av dem må være opplært som operatør.	
	Sjekk at det er gitt beskjed til lab-ansvarlig (Morten Grønli) angående eksperimentet. - Dersom det er gitt beskjed skal det stå på tv-skjermen ved inngangen at riggen kjøres i dag.	
	Ha tilgang på det rette sikkerhetsutstyret. - Vernesko, vernebriller og støvmaske skal være tilgjengelig.	
	Klargjøring	**Utført**
	Sett opp ¨Forsøk pågår¨ skilt.	
	Kontroll før start: 1. Fyll beholderen på toppen av riggen med kuler. Hus å lukke ventilen helt etterpå. 2. Sjekk at samletanken på bunn er tom og at ventilen er lukket 3. Fyll støv i støvmateren. Vei støvet du tilsetter.	
	Skru på strøm og start LabView 1. Slå inn sikringer og skru på main power knappen. 2. Skru på instrument strøm. 3. Programmet ligger på C:\Documents and Settings\biorigg\Desktop\labrig v2009\Novel rig\ Novel filter tray rig.vi 4. Det ligger et eksempel på oppsett på pulten, se over at ting stemmer.	

		Prepared by	Number	Date
EPT **HMS** **handbok**	**4.5.1.1 Preparations for Running Experiments**	E.L		03.08.2009
		Approved by	page	replaces
			2 of 3	

Oppstartsprosedyre:	**Utført**

Oppvarming av rigg:
   1. Sjekk at regulatorene mottar riktig rom temp og regulerings temp.
   2. Sjekk at ingenting ligger inntil varme flater.
   3. Oppvarming startes med å skru på heating cable 1-4 på skapet.
   4. Kontroller med jevne mellomrom at temperaturen er korrekt. Dersom temperaturen blir alt for høy (170° C) må nødbryteren slås inn.	

Oppvarming av innløpsluft, start av varmebatteri:
   1. Lukk innløpsventilen (galleri).
   2. Se til at effektbryter er inne og at "start effectbr. Q2 varmebatt" er på (i kjelleren).
   3. Åpne spjeld i LabView.
   4. Start "regulering via varmebatteri-rigg" (Øverste svarte bryter, vris til høyre). Sjekk at regulatoren (tredje fra venstre) står på 170 °C.
   5. Start vifte 2.
   6. Når "varmebatteri klar til start" lyser, trykk på start knappen under.
   7. Sjekk at temperaturen stiger.	

Trykksetting:
   1. Se over trykkslange.
   2. Sett i hurtigkobling.
   3. Åpne sikkerhetsventilen.	

Skru på vann til varmeveksleren:
   1. Vannet skrus på ved sikkerhetsbryteren ved rekkverket.
   2. Det er også en hovedbryter under taket nedenfor. Denne bør også være stengt når riggen ikke brukes.	

Test:	

Ved oppstart:
   1. Kjør ett puff eller to før oppstart.
   2. Åpne innløpsventilen.
   3. Start pumpen med "motor power".
   4. Start logging i LabView
   5. Skru på støvmater.
   6. Start integreringen av massestrøm i LabView.	

Under testing:
   1. Hold øye med utviklingen av trykk differansen.
   2. Hold øye med trykk og temperatur.
   3. Etterfyll kuler etter 10 puff.	

Puffing:
   1. Puffing skal gjennomføres når testens maksimum differansetrykk er nådd.
   2. Skru av integreringen av massestrøm i LabView.
   3. Skru av motoren.
   4. Skru av støvmater.	

			Prepared by	Number	Date
EPT **HMS** **handbok**		**4.5.1.1 Preparations for Running Experiments**	E.L		03.08.2009
			Approved by	page	replaces
				3 of 3	

5. Lukk innløpsventilen	
6. Trykk på puffknappen.	
7. Ta ut og vei kuler og støv fra bunnen, hus å stenge ventilen. Ta vare på de brukte kulene i merket beholder.	
8. For oppstart se punkt ved oppstart.	
Avslutning:	
1. Følg punkt 2 til 5 i puffing.	
2. Skru av "heating cable 1-4"	
3. Trykk på stopp knappen under varmebatteri klar til start(1. etg.). La viften gå i noen minutter, skru så av viften og regulatoren, samt lukk spjeldet.	
4. Skru av vannbryteren, sikkerhetsventilen og hovedbryter.	
5. Stopp LabVew og send loggefiler til johnnyod@gmail.com.	
6. Skru av "main power når du ikke lenger trenger strøm	
Før du går:	
Ta bort skilt og bariærer som ble satt opp før forsøket, kontroller at riggen er kald.	
Rydd opp etter deg og lever tilbake verktøy og utstyr.	
Rydd pulten klar til neste forsøk.	
Refleksjon:	
Var eksperimentet vellykket?	
Hadde du tilstrekkelig tilgang på kompetanse fra tilgjengelige medarbeidere, vedrørende sikkerhet og andre spørsmål?	
Skriv ned andre ting medarbeidere eller etterkommere burde vite til senere eksperimenter.	
Siling av kuler:	
Dersom du går tom for kuler, eller har litt tid til overs kan du sile de brukte kulene som du har samlet inn. Disse kan brukes igjen i senere forsøk, bare du husker å skrive en kommentar i testrapporten om at det ble brukt silte kuler, ikke nye rene.	

Must be filled out for each experiment!

Appendix C

Data sheets

Olivine AFS 30

CHEMICAL COMPOSITION

MgO	49,9	%
SiO_2	41,5	%
Fe_2O_3	7,2	%
Cr_2O_3	0,32	%
Al_2O_3	0,44	%
NiO	0,32	%
MnO	0,09	%
CaO	0,09	%
Na_2O	0,01	%
K_2O	0,02	%

PHYSICAL PROPERTIES

Bulk density	1700 - 1900 kg/m³
Specific gravity	3200 - 3300 kg/m³
Hardness	6,5 - 7,0 Moh's scale
Colour	Greenish grey
Melting point	Approx. 1760 °C
Initial sintering	Approx. 1450 °C
Angle of repose	Approx. 45 °
Stowage factor	0,54 m³/t (19 ft³/t)

MINERALOGICAL COMPOSITION

Forsterite	Mg_2SiO_4	93 %
Fayalite	Fe_2SiO_4	7 %

The chemical and physical data are expected average figures at loading at the company port. They are given in good faith but without guarantee. All chemical analyses are in dry state. Oxides are not indication of the phases present, only conventional representation of elements.
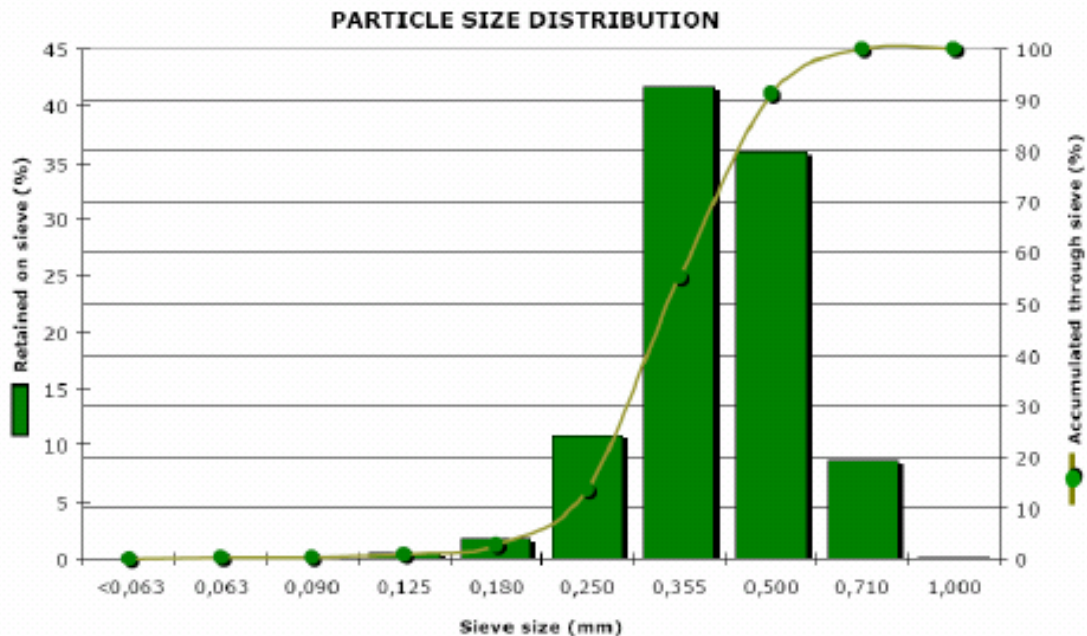
Figure C.1: Data sheet for Olivine AFS30/GL70 sand.

Saint-Gobain Proppants 20/40 Sintered Bauxite

Typical Properties

Size and Shape

Sieve No.	% Retained
20	5
30	75
40	20
<40	TR

TR = Trace

Median Particle Diameter = 0.662 mm
= 0.026 inches

Shape/Sphericity 0.9
(Krumbein & Sloss)

Physical Properties

Property	Value	
Bulk Density	2.04 g/cc	
	127 lbs/ft³	
Specific Gravity	3.5 g/cc	
Absolute Volume	0.0347 gal/lb	
Acid Solubility, %	1.9	
Crush Resistance @ Stress %	7,500 psi	0.5
	10,000 psi	1.2
	12,500 psi	2.2
	15,000 psi	4.0

20/40 Sintered Bauxite Conductivity (@ 300° F)

md-ft

	2,000 psi	4,000 psi	6,000 psi	8,000 psi	10,000 psi	12,000 psi	14,000 psi
Conductivity (md-ft)	7,065	5,980	5,030	4,140	2,800	2,030	1,595

Closure Stress

20/40 Sintered Bauxite Permeability (@ 300° F)

Darcies

	2,000 psi	4,000 psi	6,000 psi	8,000 psi	10,000 psi	12,000 psi	14,000 psi
Permeability (Darcies)	424	334	299	240	178	132	130

Closure Stress

Figure C.2: Alumina spheres, Sintered Bauxite 20/40.

ELLIS COMPONENTS

Stonebroom Industrial Estate
Stonebroom
Alfreton
Derbyshire DE55 6LQ
England
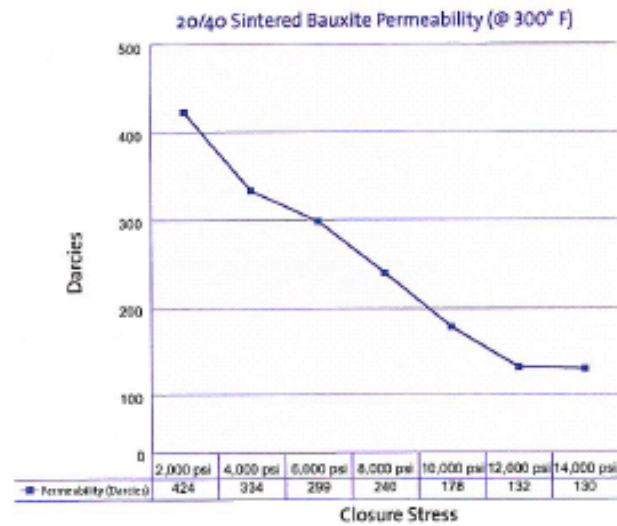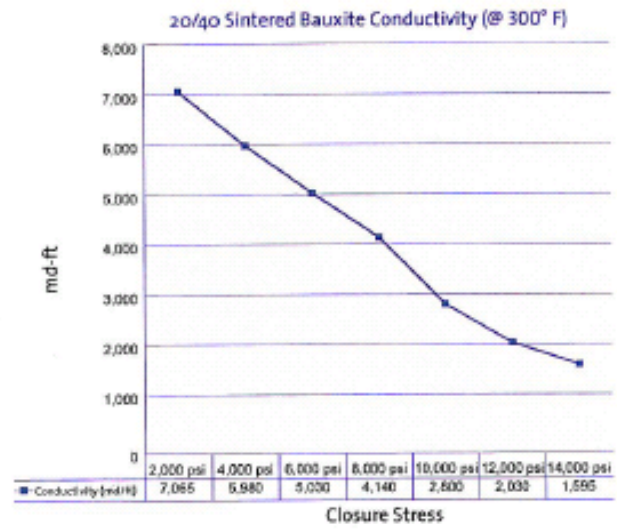Tel: 01773 873151
Fax: 01773 874645
E-mail: sales@ellis-components.co.uk

Standardized Arizona Test Dust Contaminant

ISO12103-1 Fine Grade (A2)
(SAE J726/ISO 5011 Fine Grade)

Prepared by Powder Technology Incorporated, Minnesota, USA

Typical Chemical Analysis

% By weight		% By Weight	
SiO_2	68 - 76	K_2O	2 - 5
AL_2O_3	10 - 15	MgO	1 - 2
Fe_2O_3	2 - 5	TiO_2	0.5 - 1.0
Na_2O	2 - 4	Loss On Ignition 2 - 5	
CaO	2 - 5		

Particle Size Distribution by Volume %

Size in Micrometres	% Smaller Than
1	2.5 - 3.5
2	10.5 - 12.5
3	18.5 - 22.0
4	25.5 - 29.5
5	31.0 - 36.0
7	41.0 - 46.0
10	50.0 - 54.0
20	70.0 - 74.0
40	88.0 - 91.0
80	99.5 - 100
120	100

Packaging & Price Information

Number of Jars Per Order (3.5kg per jar)	GBP Each per Jar
1 - 3	70
4 - 11	60
12 - 20	54
24 +	48

Quantities of 12 or more jars are only available in multiples of 4 jars.
Particle size distribution as analysed with a Coulter Multisizer IIe is provided with each shipment.
Prices are ex-works, subject to VAT for UK customers and may be changed without notice.
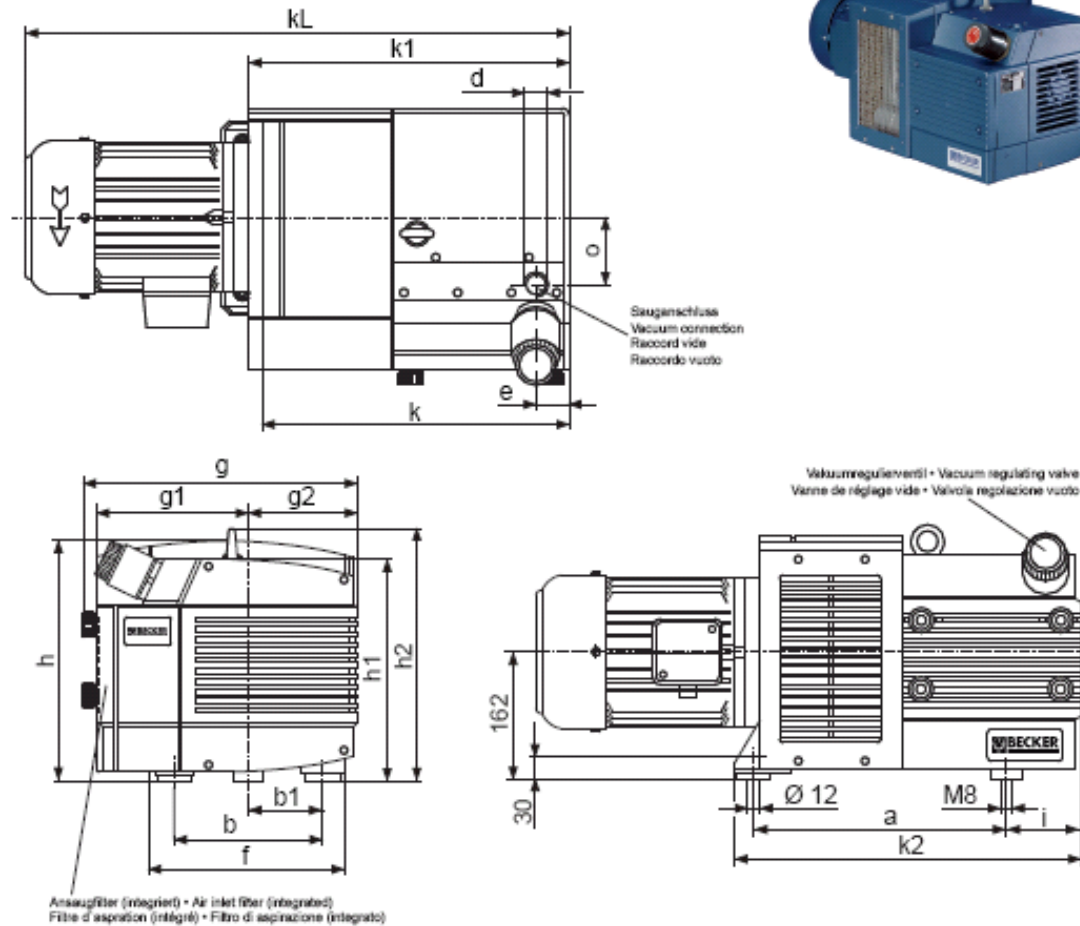
Ref: 0109

Ken Ellis & Son Ltd T/A Ellis Components Registered in England No.933 859
Registered Office: Stonebroom Industrial Estate, Stonebroom, Alfreton, Derbyshire DE55 6LQ, England

Figure C.3: Dust data sheet.

BECKER

Drehschieber-Vakuumpumpen
Rotary vane vacuum pumps
Pompes à vide à palettes
Pompe per vuoto a palette

trockenlaufend, luftgekühlt, für x-tra Betriebsstunden
oil-free, air-cooled, for x-tra operating hours
fonctionnant à sec, refroidies par air, pour les heures de travail x-tra
funzionanti a secco, raffreddate ad aia, per x-tra ore operative

Sauganschluss
Vacuum connection
Raccord vide
Raccordo vuoto

Vakuumregulierventil · Vacuum regulating valve
Vanne de réglage vide · Valvola regolazione vuoto

Ansaugfilter (integriert) · Air inlet filter (integrated)
Filtre d'aspiration (intégré) · Filtro di aspirazione (integrato)

X	m³/h		mbar (abs.[1])		kW 3~			dB(A)[2]		kg
	50 Hz	60 Hz	50 Hz	60 Hz	50 Hz	60 Hz	(M)	50 Hz	60 Hz	
KVX 3.60	55	68	100	100	2,4	3,0	1	71	73	69
KVX 3.80	67	78,5	100	100	2,4	3,0	1	72	75	69
KVX 3.100	98	112	100	100	3,0	3,5	2	75	77	101
KVX 3.140	129	154	100	200	4,0	4,8	3	78	79	111

(M)		kW		V[b]		min^-1		A		IP	ISO	
		50 Hz	60 Hz	50 Hz	60 Hz	50 Hz	60 Hz	50 Hz	60 Hz			
1	3~	2,4	3,0	190-254 / 330-440	190-288 / 330-500	1440	1733	10,6-11,4 / 6,1-6,6	12,6-10,6 / 7,3-6,1	55	F	86 / Ø 250
2	3~	3,0	3,5	190-254 / 330-440	190-288 / 330-500	1465	1780	13,0-13,6 / 7,5-7,9	15,5-12,4 / 8,9-7,2	55	F	86 / Ø 250
3	3~	4,0	4,8	190-254 / 330-440	190-288 / 330-500	1430	1765	17,2-21,9 / 9,9-12,7	20,5-19,0 / 11,8-11,0	55	F	86 / Ø 250

← mm →	a	b	b1	d	e	f	g	g1	g2	h	h1	h2	i	k	k1	k2	kL	o
KVX 3.60	328	190	95	G 1	48	250	363	195	141	312	289	328	96	397	415	448	709	85
KVX 3.80	328	190	95	G 1	48	250	363	195	141	312	289	328	96	397	415	448	709	85
KVX 3.100	398	245	122,5	G 1¼	60	295	470	223	230	390	297	336	140	501	539	583	835	95
KVX 3.140	398	245	122,5	G 1¼	60	295	470	223	230	390	297	336	140	501	539	583	873	95

1) mbar absolut · mbar absolute · mbar absolu · mbar assoluto → mbar relativ (relative · relatif · relativo) = (x mbar abs.) – 1000
2) bei mittlerer Belastung, beide Seiten abgeleitet · at medium load, both sides derived · à régime moyen, les deux côtés dérivés · a medio regime, entrambi i lati derivati : DIN EN ISO 2151 + DIN EN ISO 3744 (KpA = 3 dB(A))
3) andere Spannungen auf Anfrage · other voltages on request · autres tensions sur demande · altre tensioni su richiesta
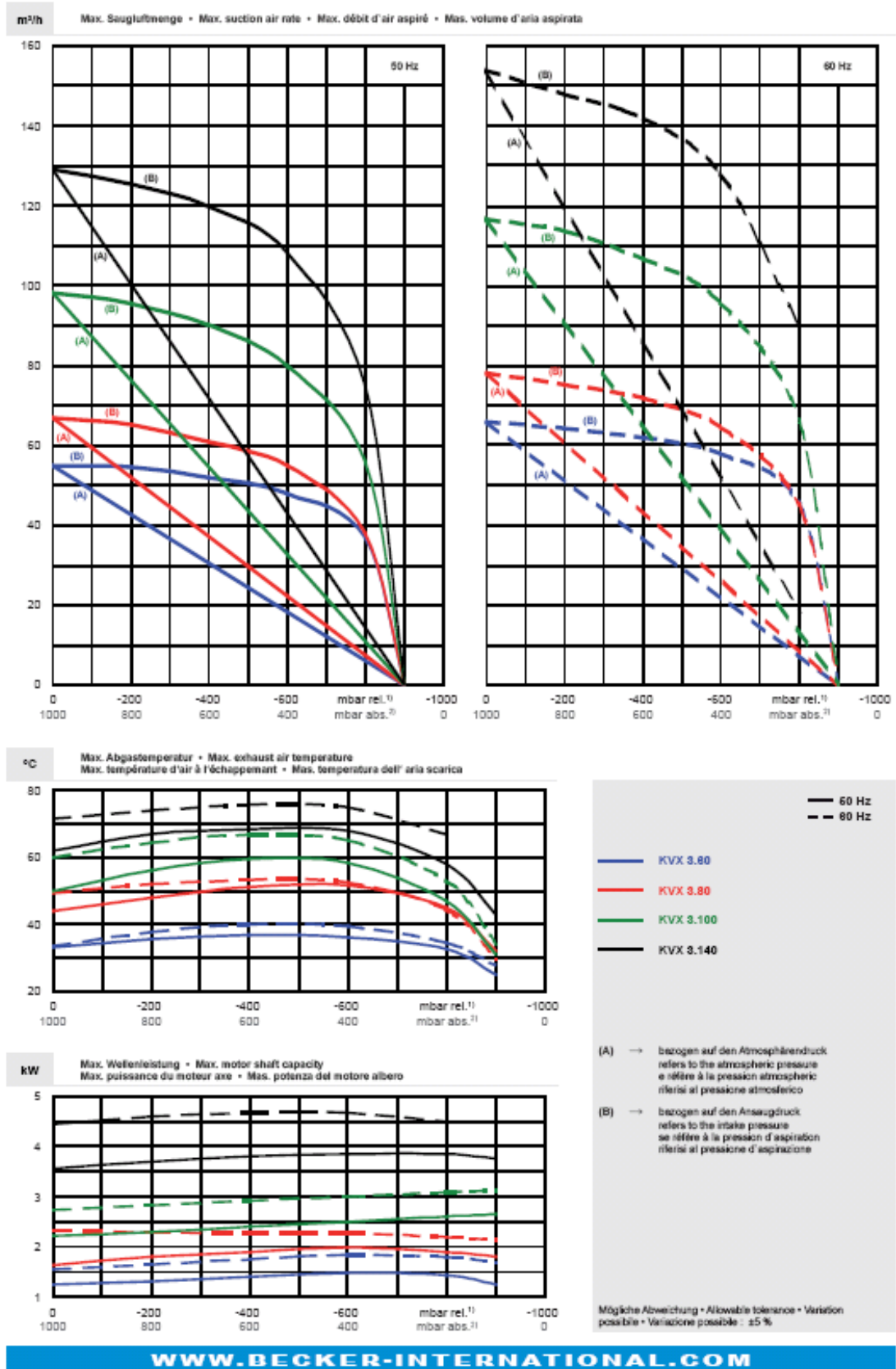
WWW.BECKER-INTERNATIONAL.COM

Figure C.4: Data sheet Becker KVT 3.80.

85

Figure C.5: Data sheet Becker KVT 3.80 (page 2).